Chemosensory navigation in disease vector mosquito larvae

Eleanor Kaori Lutz

a dissertation
submitted in partial fulfillment of the
requirements for the degree of

Doctor of Philosophy
University of Washington
2020

reading committee
Jeffrey Riffell, Chair
Bingni Brunton
Thomas Daniel

program authorized to offer degree:
biology

© COPYRIGHT 2020
ELEANOR KAORI LUTZ

UNIVERSITY OF WASHINGTON

ABSTRACT

Chemosensory navigation in disease vector mosquito larvae

Eleanor Kaori Lutz

CHAIR OF THE SUPERVISORY COMMITTEE:
JEFFREY RIFFELL
DEPARTMENT OF BIOLOGY

Mosquitoes spread deadly diseases that kill millions of people every year. Understanding mosquito physiology and behavior at all life stages is vital for public health and disease prevention. In these series of chapters for my dissertation, I investigated the exploration behavior and chemosensory navigation of six species of disease vector mosquito larvae. I found striking differences in exploration behavior among all six disease vector species, suggesting that mosquito larvae may experience strong selection on navigation behavior correlated with environmental or evolutionary history. To gain a deeper understanding of the mechanism of larval navigation in one species, I further explored important characteristics of navigation behavior in *Aedes aegypti* larvae, and how they responded to chemical stimuli. Using experimental methods and computational simulations, we demonstrate that *Aedes aegypti* larvae use an unusual search strategy to navigate chemical gradients, and respond to starvation by optimizing exploration behavior. Taken together, our findings establish mosquito larvae as a promising model for understanding phylogenetic differences in chemosensory behavior and navigation.

Table of Contents

Acknowledgements

This dissertation would not have been possible without the guidance of colleagues, friends, and the scientific community. It is my pleasure and honor to acknowledge their support.

Funding Agencies

I gratefully acknowledge the research funding I received from the National Science Foundation Graduate Research Fellowship, Robin Mariko Harris Award, and the Margo and Tom Wyckoff Fellowship. Additionally, thank you to the University of Washington Natural Sciences Dean's Scholarship, SICB Conference Charlotte Mangum Award, the Harvard ComSciCon Travel Award, the NACIS Conference Travel Award, and the NASA Data Visualization and Storytelling Award for making my graduate school experience more enriching and exciting.

My Advisor

I am grateful to my advisor, Jeff Riffell, for his continued mentorship and support throughout the past five years. In addition to his guidance of my research projects, I greatly appreciate his encouragement of my personal career goals and my participation in the Data Science program.

My Thesis Committee Members

I would like to thank my thesis committee members for the generous gift of their time and expertise. Thank you to Bing Brunton for her invaluable advice on computational methods, and for mentoring me as a teaching assistant in her Data Science for Biologists course. Thank you to Jay Parrish for mentoring me throughout my first-year rotation, and for teaching me many useful methods in microscopy and insect behavior. Thank you to Tom Daniel for inviting me to many insightful discussions with his lab group, and for working with me as a TA in his Introduction to Neuroscience course. Finally, thank you to Sheri Mizumori for offering helpful advice and kind guidance during all of my committee meetings and my General Exam.

My Colleagues

A sincere thank you to my labmates, who made my time in the Riffell Lab more fun and exciting - Jeremy Chan, Ryo Okubo, Claire Rusch, Yasmeen Hussain, Marie Clifford, Diego Alonso san Alberto, Tjinder Grewal, Kim Ha, Chloé Lahondère, Clément Vinauger, Gabriella Wolff, and Floris van Breugel. Additionally, thank you to Binh Nguyen, Kara Kiyokawa, Wai Pang Chan, the Biology Department Facilities, and the Biostatistics Consulting Group for supporting my research experiments. Finally, thank you to the many anonymous scientists who provided thoughtful peer reviews of my submitted manuscripts.

My Family and Friends

Last but not least, I owe a heartfelt thank you to my family and friends. Thank you for enjoying the past five years with me.

Mosquitoes spread deadly diseases that kill millions of people every year [1]. Understanding mosquito physiology and behavior is vital for public health and disease prevention, and many important questions remain unanswered in the field of mosquito neuroethology.

Particularly little is known about the behavior of disease vector mosquito larvae. Nevertheless, larval based mosquito control strategies are extremely effective [2], and larval fitness affects adult survival, fecundity, and biting behavior [3]. There are several specific research endeavors that could add insight into this gap in knowledge. First, a comprehensive review of the existing state of larval mosquito chemosensation is needed to pinpoint promising areas of future research and summarize our current understanding of larval mosquito behavior. Next, modern behavioral tools are needed to better understand larval search and avoidance strategies. Genetic tools are also needed to explore the neurobiology and physiology of mosquito larvae, and such tools could also be used to explore important aspects of adult behavior. Finally, a comparative analysis of larval behaviors across disease vector species is needed. Adults of disease vector species exhibit a wide range of behaviors across species, even among those that all selectively feed from humans, and larvae may exhibit similar heterogeneity.

The experiments in this dissertation address many of these important research questions. First, I collaborated on a comprehensive literature review of the current state of the field in mosquito chemosensory behavior [4]. Our literature review highlighted the gap in research into the larval stage of the mosquito life cycle. In particular, there is sparse information available about the chemosensory behaviors of many larval mosquito species, and most research studies rely on coarse experimenter observations rather than video recordings or other measurements taken over smaller timescales.

To address this gap, I worked alongside collaborators from the University of Washington and the University of California San Diego to develop novel genetic and behavioral tools to analyze chemosensory behavior in *Aedes aegypti* disease vector mosquito larvae [5]. By combining behavioral techniques with live calcium imaging, we were able to establish several new lines of GCaMP6 genetically modified mosquitoes as a tractable model for future mosquito neuroethology research. In addition, our comparative behavioral assays on olfactory-receptor-deficient and wildtype larvae showed that larvae do not require *orco* olfactory receptors to detect food cues.

We next used these new behavioral tools to explore the detailed mechanism of *Ae. aegypti* foraging behavior. We found that this species uses an unusual search strategy - orthokinesis - to forage and avoid repellents. We also discovered that *Ae. aegypti* larvae are attracted to microbial RNA, a previously unknown foraging attractant, while not responding to several olfactory cues known to attract adult *Ae aegypti* for oviposition [6].

Finally, we compared the behavior of six different species of mosquito larvae to better understand species-specific navigation and foraging behaviors [7]. Surprisingly, we found significant differences across species in navigation behavior in the absence of chemosensory cues. However, when an attractive or aversive chemosensory cue was added, all species appeared to gather near preferred cues through passive aggregation rather than directed navigation.

This work explores only a small subset of mosquito behaviors in a very limited set of environmental conditions. Nevertheless, they highlight unusual patterns in mosquito larval search behavior that appear consistent across disease vector species. Our work also reveals striking behavioral differences across even closely related species of mosquito larvae. These results highlight the need for future research exploring the extent of species-specific behavior, and cautions against generalizing experimental results across multiple disease vector mosquito species.

References

[1] WHO, "Mosquito-borne diseases," 2019.

[2] T. G. Floore, "Mosquito larval control practices: Past and present," *J. Am. Mosq. Control Assoc.*, vol. 22, pp. 527–533, Sept. 2006.

[3] H. Briegel, "Metabolic relationship between female body size, reserves, and fecundity of *Aedes aegypti*," *J. Insect Physiol.*, vol. 36, pp. 165–172, Jan. 1990.

[4] E. K. Lutz, C. Lahondère, C. Vinauger, and J. A. Riffell, "Olfactory learning and chemical ecology of olfaction in disease vector mosquitoes: A life history perspective," *Curr. Opin. Insect Sci.*, vol. 20, pp. 75–83, Apr. 2017.

[5] M. Bui, J. Shyong, E. K. Lutz, T. Yang, M. Li, K. Truong, R. Arvidson, A. Buchman, J. A. Riffell, and O. S. Akbari, "Live calcium imaging of *Aedes aegypti* neuronal tissues reveals differential importance of chemosensory systems for life-history-specific foraging strategies," *BMC Neurosci.*, vol. 20, June 2019.

[6] E. K. Lutz, T. S. Grewal, and J. A. Riffell, "Computational and experimental insights into the chemosensory navigation of *Aedes aegypti* mosquito larvae," *Proc. Biol. Sci*, 2019.

[7] E. K. Lutz, K. T. Ha, and J. A. Riffell, "Chemosensory navigation in six species of disease vector mosquito larvae," *BioRxiv*, 2020.

Olfactory learning and chemical ecology of olfaction in disease vector mosquitoes: A life history perspective

Eleanor K. Lutz, Chloé Lahondère, Clément Vinauger and Jeffrey A. Riffell

Published in: Current Opinion in Insect Science. 2017

Abstract

Mosquitoes transmit many debilitating diseases including malaria, dengue and Zika. Odors mediate behaviors that directly impact disease transmission (blood-feeding) as well as life history events that contribute to mosquito survival and fitness (mating and oviposition, nectar foraging, larval foraging and predator avoidance). In addition to innate olfaction-mediated behaviors, mosquitoes rely on olfactory experience throughout their life to inform advantageous choices in many of these important behaviors. Previous reviews have addressed either the chemical ecology of mosquitoes, or olfactory-driven behaviors including host-feeding or oviposition. Adding to this literature, we use a holistic life history perspective to integrate and compare innate and learned olfactory behavior at various stages of mosquito development.

Introduction

Many mosquito control strategies target the mosquito olfactory system at both the larval and adult stages. Larval control strategies can target chemosensory mediated behaviors with techniques such as predator introduction and ingestible microbial larvicides [1]. Predators emit chemosensory cues[1] which larvae can sense and avoid [2], and larvae may use chemosensory cues to recognize ingestible larvicides as food. Although microbial larvicides are highly effective [1,3] and harmless to nontarget organisms [1], increased larval resistance [3] highlights the possible need for additional control options. A better understanding of larval olfactory deterrents may help identify new microbial larvicides. At the adult stage, mosquito control methods include olfactory attractants (e.g. Carbon dioxide, 1-octen-3-ol, Attractive Toxic Sugar Baits [4–8] and repellents (e.g. DEET, picaridin [9]). Olfaction thus represents a major target in effective control of mosquito populations.

Here we discuss mosquito olfactory experience during both the larval and adult stage. We begin by addressing the behavioral role of olfaction throughout the mosquito life cycle. These behaviors include larval foraging, larval predator avoidance, adult nectar foraging, host selection, mating, and oviposition (Figure 1) [10]. Associative and non-associative olfactory learning can also increase individual fitness by refining behavioral choices throughout a mosquito's life [10]. Next we give a brief overview of the comparative olfactory neuroanatomy of mosquito larvae and adults. Finally we examine promising areas of future research in the field of mosquito chemical ecology, and argue that the similar neurobiological processes mediating experience-dependent behavioral plasticity at the adult and larval stages may provide suitable targets for mosquito control.

[1]In many papers describing mosquito chemosensory ecology, the mechanism of mosquito behavior is not examined directly. Therefore, we cannot preclude the possibility that some semiochemicals may be processed by other sensory systems such as the gustatory system. Throughout this review we use the term "chemosensory" to describe findings in which this is particularly unclear.

Olfactory Learning and Behavior in Mosquito Larvae

Unlike adults, many disease vector mosquito larvae inhabit small aquatic environments including flower vases and water pots [13]. Due to spatial restrictions in these habitats, larvae may be particularly vulnerable to predation and lack of food. Chemosensory indicators of these dangers are thus ecologically relevant to both adult and larval mosquitoes. It is advantageous for gravid adult females to recognize and choose oviposition sites with ample food and few predators [13–15] (See detailed discussion in "Olfactory cues involved in mating and oviposition"). In addition, there is likely a fitness advantage to larvae using chemosensory cues to avoid predator kairomones [2] and seek out olfactory indicators of food [13,16]. Deorphanization of the limited number of olfactory receptors (ORs) expressed in both larvae and adult females may help identify key olfactory signals shared in oviposition and larval fitness.

Spatial restriction may also threaten larvae with extreme changes in the physical-chemical environment (temperature, acidity, plant-derived compounds, and salinity), as smaller volumes of water are susceptible to rapid temperature change and chemical pollutants.

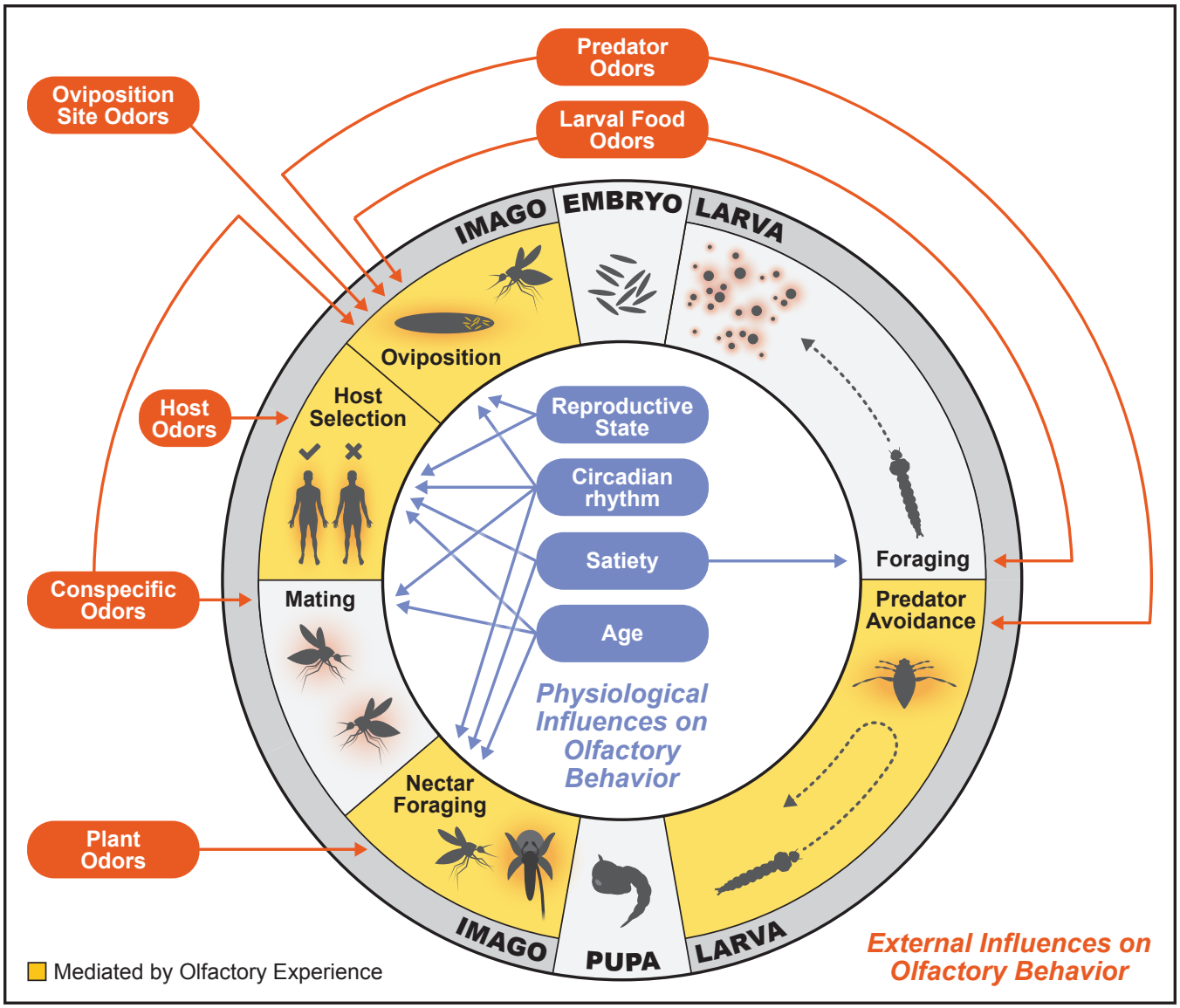

Figure 1: Known physiological and external influences on mosquito olfactory behavior [10]. Behaviors marked in yellow have been shown to be mediated by olfactory experience. These behaviors can also be modulated by physiological factors (blue), which are reviewed elsewhere [11, 12].

In fact, *Aedes aegypti* larvae exhibit many physiological adaptations to these conditions: They can survive freezing for 8 hours, eclose when reared in pH ranging from 4.4 to 9.5, or in water containing 0.9% salt [13]. Many insects learn and respond to cues associated with the physicochemical environment [17], making these stimuli suitable candidates to test in aversive learning assays.

Larval olfactory responses to food resources

Larval attraction to food is robust and mediated by olfaction [16, 18]. The three major disease vector mosquito genera (*Aedes*, *Anopheles*, *Culex*) are larval detritivores, and products of organic decay such as cresol derivatives (indole, 2-methylphenol, 4-methylcyclohexanol) are innately attractive to *Anopheles gambiae* larvae [18]. In *Ae. aegypti*, the axon guidance gene semaphorin-1*a* has been identified as an important component of larval olfactory development and attraction to yeast [19]. Nonetheless, microbes produce more than 1000 different volatile compounds [20], and it is unclear which semiochemicals are involved in larval attraction to food. In adult *Ae. aegypti*, many bacterial kairomones affect oviposition in a concentration-dependent manner: Some bacterial species deter oviposition while others stimulate egg-laying, and many kairomone isolates (nonanoic acid, tetradecanoic acid, methyl tetradecanoate) stimulate oviposition only at a narrow concentration range [21]. It remains unknown whether larvae also use this large dimensional chemical space [20] to modulate their behavior, or can be learned by the larvae in an asso-

ciative manner. However, the sensitivity of ovipositing females to bacterial kairomones [21] suggests that the composition of the microbial community is important to larval fitness. Further, several microbes (*Bacillus sphaericus*, *Bacillus thuringiensis* var. *israelensis*) cause larval death within 48 hours [1]. As such, chemosensory indicators of dangerous bacterial communities may be innately aversive to larvae, or readily learned as aversive when encountered alongside toxic bacterial byproducts.

Olfactory experience in larval predator avoidance

An important fitness-related effect is for mosquito larvae to avoid predation in small, spatially restrictive, pools [2, 13], and indeed, mosquito larvae have been shown to display species-specific avoidance of chemosensory cues from predators [2]. For example, *Culex pipiens* larvae can detect chemosensory cues from *Notonecta undulata*, a natural predator of this larval species [2]. *Cx. pipiens* show significant refuge-seeking behavior and movement reduction in water containing *N. undulata* chemical cues [2]. However, *Ae. aegypti* larvae (a species with no evolutionary history of *Notonecta* predation) do not respond to *N. undulata* odor [2], suggesting that there may be species-specific olfactory tuning to predator cues. Given the extremely limited number of larval ORs (see detailed discussion in "The Neurophysiological Bases of Mosquito Olfactory Learning"), it is possible that larvae simply do not express ORs tuned to ecologically irrelevant predators. Comparative studies examining inter-species differences in chemosensory responses to predator-related cues could reveal whether these behavioral differences are caused by differences in sensory detection or innate responses.

In addition to innate predator avoidance [2], mosquito larvae can learn new associations between predator odors and perceived danger [22]. In *Cx. restuans*, larvae exhibit movement reduction in the presence of injured conspecific alarm cues [22]. Although naive *Cx. restuans* larvae do not change their behavior in the presence of salamander odor, larvae conditioned with salamander odor and crushed conspecifics demonstrated significant movement reduction in salamander odor alone [22]. This paper did not establish the chemical composition of salamander odor, but *Notonecta maculata* — another predator of larval mosquitoes — release cuticular hydrocarbons (*n*-heneicosane, *n*-tricosane) that repel ovipositing *Culiseta longiareoleta* [23]. Larvae may use similar cues, but the mechanism of chemosensory predator detection is still unknown. Further, the *An. gambiae* larval olfactory system includes both ORs and ionotropic receptors [16], raising the possibility that multiple chemosensory channels may be involved in predator detection.

Olfactory Learning and Behavior in Adult Disease Vector Mosquitoes

Olfactory cues involved in food-seeking behaviors

Sugar meal: While female disease-vector mosquitoes require a blood-meal to produce and mature their oocytes, both females and males also seek carbohydrates (sugars) as a source of energy to sustain their metabolism and behavior [13]. Energetically, sugar and blood are interchangeable [24], and sugars represent the sole food for males and, in some non-blood-feeding species, for both males and females (e.g. *Toxorhynchites* spp. mosquitoes). Mosquitoes find carbohydrates by visiting plants that provide floral and extrafloral nectar, ripe fruits, honeydew, and tree sap [24] which also contain other nutrients such as amino acids. A wide range of volatile compounds are emitted by these sugar sources, including aldehydes, alcohols, ketones, phenols and terpenes [25], which are detected by the mosquito olfactory system (Figure 2). Despite their potential importance, the chemical identities and blends that mediate responses by mosquitoes to nectar resources remains largely uncharacterized. Combined fieldwork and laboratory assays have shown that male *An. gambiae* mosquitoes exhibit a preference for specific plant species (e.g. *Mangifera indica* (*Anacardiaceae*), *Thevetia neriifolia* (*Apocynaceae*), and *Dolonix regia*, *Senna siamea*, and *Cassia sieberiana* (all *Fabaceae*)) [26]. Females are equally attracted to specific plant odor bouquets and to synthetic blends based on the plants' scent composition [27]. Interestingly, several plant species that attract *An. gambiae* produce both floral and extrafloral nectar, and all emit terpenoids [28], including monoterpenes such as α-pinene, D-limonene and β-myrcene, that are common constituents of essential oils described in the literature as presenting mosquito repellent activity [29].

This olfactory mediated attraction to plants is not limited to *Anopheles* mosquitoes. Both male and female *Cx. pipiens* are attracted to plant extract and artificial chemical blends [39, 40]. In addition, a successful nectar meal can constitute a positive reinforcement for mosquitoes and modulate their behavior based on past experience [41]. For example, the attraction to floral scent increased for both male and female *Cx. pipiens pipiens* when the floral scent was paired with a 5% sucrose solution [41]. In *Cx. quinquefasciatus* both males and females could learn the association between odors and a sugar meal [42]. It is worth noting that not only do mosquitoes respond to plant scents [26,27], but some species of mosquitoes (e.g. *Ae. Oc. communis*, *Ae. Oc. canadensis*) also pollinate these plants

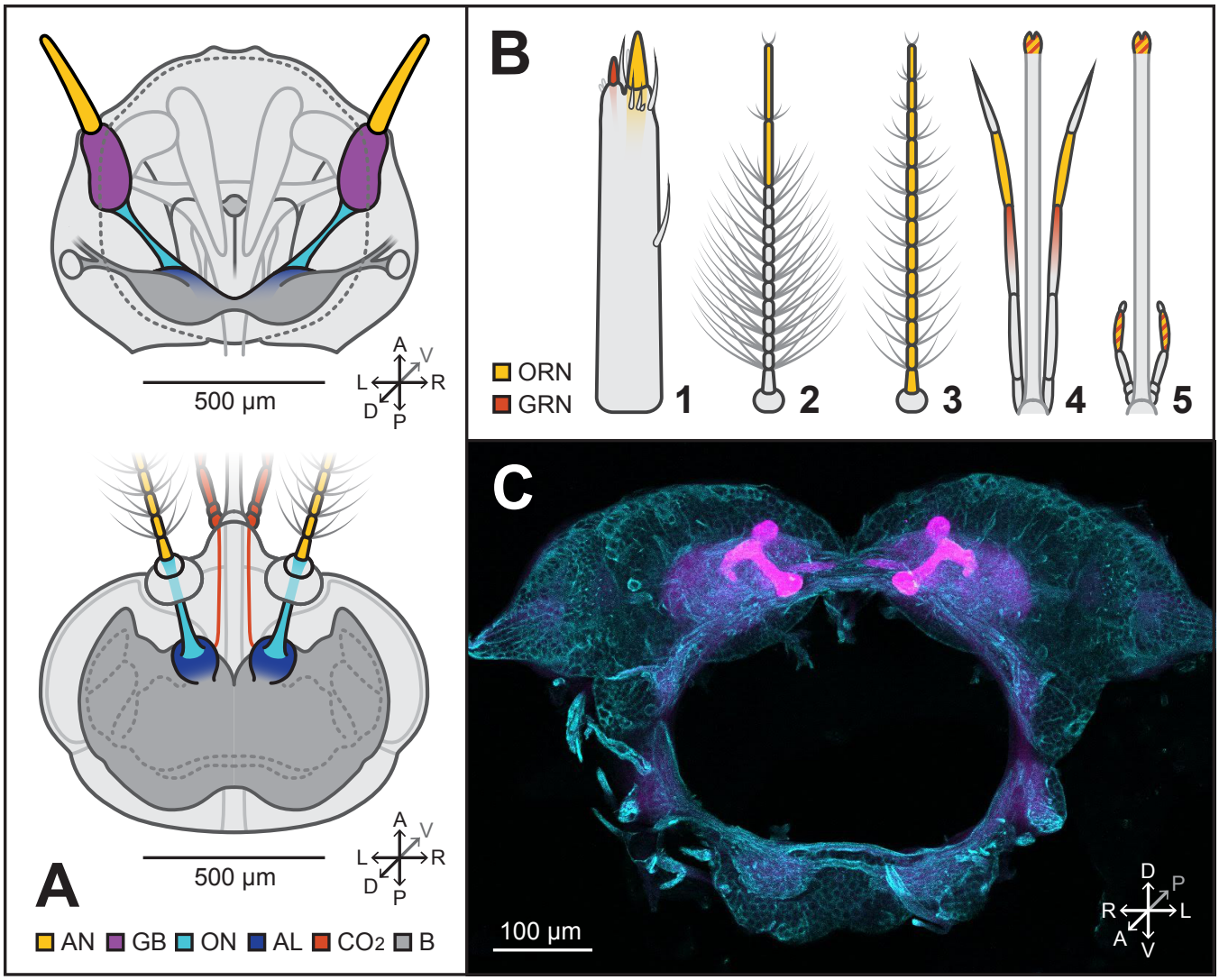

Figure 2: **A**: Neuroanatomy of the *Ae. aegypti* olfactory system. Top: larva [13]. Bottom: adult female [13, 30]. AN: antennae, GB: germinal bud of adult antennae, ON: olfactory nerve, AL: antennal lobe, CO_2: CO_2-sensitive receptor neurons and afferents, B: other regions of the brain. **B**: Distribution of chemosensory sensilla in the *Ae. aegypti* antennae and maxillary palps. **B1**: larval antennae [31], **B2**: adult male antennae [13, 32], **B3**: adult female antennae [13, 33], **B4**: adult male maxillary palps and proboscis [13, 34–36], **B5**: adult female maxillary palps and proboscis [13, 30, 36, 37]. ORN: olfactory receptor neurons. GRN: gustatory receptor neurons, including CO_2-sensitive receptor neurons. **C**: Confocal scan of the mushroom bodies of *Ae. aegypti* L4 stage larvae. Anti-DC0 (magenta, used here at a concentration of 1:250) recognizes the catalytic subunit of cAMP dependent protein kinase A in all arthropods investigated thus far [38]. This anti-DC0 was a generous gift from Dr. Daniel Kalderon, Columbia University. A monoclonal antiserum against α-tubulin (cyan, 12G10) was also used at a 1:100 concentration (developed by Drs. J. Frankel and E. M. Nelsen at NICHD, obtained from the Developmental Studies Hybridoma Bank).

when nectar feeding [43]. Finally, sugar-feeding and blood-feeding are not completely independent. Blood and sugar feeding activities are often observed in the same activity period and have been described as antagonistic and mutually exclusive [24]. Although sugar intake increases the mosquito lifespan, biting rates are usually reduced when sugar is available [44], suggesting a potential epidemiological impact of the blood-feeding versus sugar-feeding conflict as the absence of sugar sources would increases vectorial capacity [44]. However, whether sugar-feeding experience, by increasing attraction to floral scents, affects host biting frequency is still to be determined.

Blood-meal: Female mosquitoes have been shown to exhibit preferences for a given host species (including humans for anthropophilic mosquitoes such as *An. gambiae* [45] and *Ae. aegypti* [13]), yet other species (e.g. *Cx. nigripalpus*) [46] change their host preference in response to seasonal variations in host availability or changes in host defensive behaviors such as antiparasitic and grooming behaviors [47]. In this context, olfactory signals may be particularly valuable as they allow mosquitoes to identify preferred hosts from a safe distance. Furthermore, mosquitoes can learn from previous encounters with host olfactory cues and use this learned information to select hosts that are the

least defensive and easiest to feed on [48–50]. By modulating responses to host-related olfactory cues such as L-(+)-lactic acid and 1-octen-3-ol [51–53], as well as impacting the efficiency of popular insect repellents such as DEET [53], individual experience certainly plays an important role in mosquito host choice and preference. As learning abilities might affect mosquitoes biting behavior patterns amongst host populations, and consequently the rate of parasite transmission, it is thus important to consider them in epidemiological models and to develop efficient control strategies [48, 49, 53–55].

Olfactory cues involved in mating and oviposition

Chemosensory cues play an important role in mosquito social interactions and mating behavior, and these responses can be modulated by the prior experience and physiological state of the haematophagous insect. For instance, evidence for aggregation pheromones has been found in *Cs. inornata* [56] and more recently in *Ae. aegypti* mosquitoes [57]. Interestingly, when the odors of male mosquitoes and the odor of a potential host (i.e. a rat) were presented together, *Ae. aegypti* females showed a typical flight response towards the male odors but did not respond to the host signal [58]. This highlights how the reproductive state can modulate the response to host odors and affect host-seeking behaviors, although the volatiles mediating this attraction have yet to be identified. Several other studies support the hypothesis of the presence of a contact sex pheromone that could be used for sex and conspecific recognition [59], but the chemical composition of these substances has yet to be determined, and whether these behaviors can be modulated by previous experience remains an open question in mosquitoes. However, in other haematophagous insects such as the gregarious species *Triatoma infestans*, the attraction to aggregation pheromones is modulated by previous experience [60]. Their innate attraction to this latter could even be switched to a learned aversion after associative conditioning [60].

Mated female mosquitoes use various signals (visual, humidity, olfactory etc.) to locate a place to oviposit, and evidence exists that this behavior can be modulated by the mosquitoes prior experience. For example, *An. coluzzii* can detect deterrent chemicals associated with overcrowded pools of water, and avoid these specific areas as they would not be suitable for the optimal development of progeny [61]. In *Cs. longiareolata*, females are able to detect the presence and density of predators such as *Notonecta* and avoid laying eggs in these specific water pools [62]. Similarly, *Culex* mosquitoes avoid ovipositing in water that previously contained larval predators, suggesting the use of predator-released kairomones [63]. While some *Notonecta* kairomones have been identified (*n*-heneicosane, *n*-tricosane) [23], less is known about similar cues from other predator species. In malaria vectors, it has been shown that olfactory cues not only from conspecifics [64, 65] and microorganisms [66] but also from the soil (e.g. the sesquiterpene alcohol cedrol) [67] or the surrounding environment [68, 69] are used by gravid females for oviposition site selection. In Zika, dengue and yellow fever vectors, bacteria present in the water have been shown to increase the oviposition rate [70] as well as the presence of conspecifics [71–73] and chemicals resulting from decaying vegetation (e.g. *p*-cresol) [74]. Like nectar and host seeking, oviposition site preference can also be modulated by individual experience in *Cx. quinquefasciatus* [75] and *Ae. aegypti* [76], although the cues mediating these responses, and the nature of the learned response (i.e. associative or non-associative) remains unknown. It thus seems that, in addition to innate olfactory behaviors, individual experience plays a role in various steps of the adult mosquitoes' life [77, 78].

The Neurophysiological Bases of Mosquito Olfactory Learning

Several articles describe the beginning stages of olfactory information processing in adult mosquitoes [79–81], but detailed understanding of the neural substrates of olfactory plasticity remains an open question. In adults, information flows from ORs and CO_2-sensitive receptors located on the antennae and the palps, through the antennal lobes (AL), to higher order brain areas such as the lateral horns and mushroom bodies, thought to be involved in learning and memory (Figure 2A,B). Compared to the adults, the larval olfactory neuroanatomy is numerically simpler. Adult female *Ae. aegypti* have 3800 putative antennal olfactory receptor neurons (ORNs) [33], while larvae of the same species only have 24 [31]. Interestingly, there are 21 putative OR genes expressed in *Ae. aegypti* larval antennae [34] [2]- far more than the 12-13 ORNs found in each antenna [31]. This comparatively large number of expressed OR genes is unusual for the 1OR:1ORN relationship typical of insects [34]. *Ae. aegypti* larvae might express multiple ORs on the antennal gustatory receptor neurons, or express different ORs based on developmental stage, sex, or nutritional state. Electrophysiology and deorphanization studies have thus far focused primarily on adults [79, 82]. Similar work would be of interest in larvae, as 14 of 21 *Ae. aegypti* larval ORs are larvae-specific [34], as well as 4 of 12 in *An. gambiae* larvae [18].

While understanding how odor information is processed in higher-order brain centers remains an

[2] not including two pseudogenes and the obligate olfactory coreceptor *orco*

open question in both adults and larvae, a handful of neuroanatomical studies have been conducted in adult mosquitoes [80, 83]. While the structure and function of larval mushroom bodies (Figure 2C) is not well studied, our work has shown there is remarkable similarity in the physical neuroanatomy of the mushroom body between the larval and adult stages (Figure 2C). In *Drosophila melanogaster* [84] and *Ae. aegypti* [19] the larval olfactory system has many fewer neurons than adults, but exhibits strong similarities in overall architecture. Although more work is necessary to characterize comparative adult and larval olfactory neuroanatomy in other mosquito species, the relatively simple larval system may be a useful model for investigating key aspects of mosquito olfaction conserved across life stages.

What are possible neural mechanisms that permit behavioral flexibility by larvae and adult mosquitoes, and how is the odor information coupled with the appetitive "reward", or aversive "punishment", to form the learned association? Work in many insects, including our own work with *Ae. aegypti* mosquitoes, has shown the importance of neurons that release amine neuromodulators (eg, serotonin, dopamine or octopamine), and their cognate receptors, for olfactory learning [17, 50, 85]. For example, a large serotonin-immunoreactive neuron innervates all glomeruli in the *Ae. aegypti* AL, and sends axon branches to the mushroom body calyces, the central complex — both brain regions thought to operate in memory-related behaviors — and the lateral horn, and receptors are expressed in these brain regions as well as on the mosquito antennae and maxillary palps [37, 86]. Similarly, large dopamine-immunoreactive neurons innervate the AL and superior medial protocerebrum, and dopamine receptors are expressed at high levels in these brain regions [50]. Pharmacological interventions and genetic manipulations of dopamine receptors selectively suppress olfactory learning in *Ae. aegypti*, suggesting the dopamine pathway is critical for learning and memory [50]. Thus, these amines may provide the reinforcement system to increase olfactory responses from the AL and mediate the formation of memory in the mushroom bodies [50, 85]. Work from diverse insects, including *Drosophila* and honeybees, supports this general hypothesis: when stimulated by the unconditioned stimulus (US) neuromodulatory neurons are activated leading to neurotransmitter release in the AL and mushroom bodies. The coincident input from the AL (via the odor stimulus, or conditioned stimulus: CS) with dopamine release causes synaptic growth in mushroom body neurons and memory formation.

How neuromodulators like dopamine influence olfactory circuits and odor representations in mosquitoes remains an open question. In specific brain regions, innervation by large neuromodulatory neurons can be global, or confined to specific sub-regions and possibly sub-circuits. For instance, in the *Ae. aegypti* AL the serotonin-immunoreactive neuron has a similar innervation pattern across glomeruli [86], whereas the dopamine-immunoreactive neuron selectively innervates some glomeruli more than others (eg, the MD glomeruli, which respond to host volatiles) [50]. Serotonin and tyrosine hydroxylase, a dopamine precursor, are also expressed in the *Ae. aegypti* larval AL and lateral protocerebrum (Personal communication, Gabriella H. Wolff), possibly suggesting conserved functions between life-history phases. While the relative function of dopamine, serotonin and octopamine is unclear, partly due to their overlapping and cooperative interactions [87], nonetheless, studies have shown they are critical for diverse processes, including circadian activity state, arousal, and learning [17, 85], suggesting that these neuromodulators serve as "control knobs" for specific olfactory channels, thereby allowing certain odors to be processed under different environmental and physiological conditions.

Conclusions and Prospects for Future Research

We have provided an overview of studies investigating the role of olfaction during the mosquito life and its role in ecologically and epidemiologically important behaviors. Individual experience, historically neglected in epidemiological models and control strategies, plays a role in the majority of olfactory behaviors of both larvae and adults. Some olfactory cues, such as larval predator odors and larval food odors, are used by both adults and larvae. These odors also play a critical role for adult female mosquitoes when choosing an oviposition site. However, how these odors are used by mosquitoes in an experience-dependent manner remains an open question. Given the importance of olfactory learning throughout mosquito life history and its interaction with commonly used pesticides [53], a better understanding of the mechanism and limitations of learning may help improve the application of existing olfactory control techniques. Thus far, behavioral experiments, single-sensillum electrophysiological recordings, and ORN staining studies have contributed to a better understanding of neural mechanisms behind these behaviors [79–82]. However, several urgent questions remain in the field of mosquito olfaction.

First, there is a dearth of information on the neuroanatomy of higher order brain structures in mosquito larvae. Due to the numerical simplicity of larval neuroanatomy, mosquito larvae are an attractive model for understanding the neural encoding of mosquito olfactory behavior. Analyzing the physical structure and interconnectivity of higher order larval brain areas is a key step in studying functional changes that occur during mosquito learning and memory, as well as providing

the basis for comparing learning and memory between the different life-history stages.

Secondly, the breadth of chemosensory ligands and their cognate receptors that mediate mosquito behavior is still unknown, particularly in larvae. Although *Xenopus* receptor expression studies have characterized the tuning properties of many *An. gambiae* larval ORs [18], similar information is lacking for other species. Importantly, the mosquito olfactory subgenome exhibits significant divergence between genera [34, 88]. A cross-species study of the full range of behaviorally relevant semiochemicals is crucial to understanding adult and larval chemical ecology, deorphanizing olfactory receptors, identifying associated neurobiological functions, and inter-species differences in mosquito behavior.

In addition, the mechanism of discrimination between complex odors is not well understood. As discussed, mosquitoes respond to olfactory information from a wide variety of sources including plants, animal hosts, conspecifics and oviposition sites. These odors often consist of several hundred different chemical compounds [89, 90], many of which are shared amongst unrelated odor sources [82, 91]. Decoding the key compounds in mosquito mixture processing may help explain some of the differences in intra- and inter-species host attractiveness.

Last, determining how neuromodulatory systems influence the processing of olfactory information remains an important gap in mosquitoes. Amines like dopamine — critical for aversive and appetitive learning — may influence local and regional brain areas, but such determinations remain untested. An outstanding question in olfactory neurobiology is thus identifying how aminergic neuromodulators selectively modulate specific olfactory circuits, and how that modulation transforms information processing in downstream areas of the brain. Given the importance of learning and associated neuromodulatory systems in diverse life-history processes, future studies on these topics could facilitate our understanding of mosquito-host interactions and potentially identify genetic targets for vector control.

Acknowledgements

We are grateful to Gabriella H. Wolff for her contribution of confocal scan images for Figure 2. We thank the three anonymous reviewers for their thoughtful comments, which helped us improve the manuscript. We acknowledge the support of the Air Force Office of Sponsored Research under grants FA9550-14-1-0398 (JAR) and FA9550-14-1-0398 (TLD and JAR); National Science Foundation under grants DGE-1256082 (EKL) and IOS-1354159 (JAR); the National Institute of Health under grant R01DC013693 (JAR); an Endowed Professorship for Excellence in Biology (JAR); The Washington Research Foundation; and the Human Frontiers in Science Program under grant HFSP-RGP0022 (JAR and CV).

References

[1] T. G. Floore, "Mosquito larval control practices: Past and present," *J. Am. Mosquito Contr.*, vol. 22, no. 3, pp. 527–533, 2006.

[2] A. Sih, "Antipredator responses and the perception of danger by mosquito larvae," *Ecology*, vol. 67, no. 2, pp. 434–441, 1986.

[3] N. S. Zahiri and M. S. Mulla, "Susceptibility profile of *Culex quinquefasciatus* (diptera: *Culicidae*) to *Bacillus sphaericuson* selection with rotation and mixture of *B. sphaericus* and *B. thuringiensis israelensis*," *J. Med. Entomol.*, vol. 40, no. 5, pp. 672–677, 2003.

[4] D. L. Kline, "Traps and trapping techniques for adult mosquito control," *J. Am. Mosquito Contr.*, vol. 22, no. 3, pp. 490–496, 2006.

[5] J. C. Beier, G. C. Müller, W. Gu, K. L. Arheart, and Y. Schlein, "Attractive toxic sugar bait (ATSB) methods decimate populations of *Anopheles* malaria vectors in arid environments regardless of the local availability of favoured sugar-source blossoms," *Malar. J.*, vol. 11, no. 1, 2012.

[6] G. C. Müller, J. C. Beier, S. F. Traore, M. B. Toure, M. M. Traore, S. Bah, S. Doumbia, and Y. Schlein, "Successful field trial of attractive toxic sugar bait (ATSB) plant-spraying methods against malaria vectors in the *Anopheles gambiae* complex in Mali, West Africa," *Malar. J.*, vol. 9, no. 1, 2010.

[7] D. P. Tchouassi, R. Sang, C. L. Sole, A. D. S. Bastos, P. E. A. Teal, C. Borgemeister, and B. Torto, "Common host-derived chemicals increase catches of disease-transmitting mosquitoes and can improve early warning systems for Rift Valley Fever virus," *PLoS Negl. Trop. Dis.*, vol. 7, no. 1, p. e2007, 2013.

[8] W. A. Qualls, G. C. Müller, S. F. Traore, M. M. Traore, K. L. Arheart, S. Doumbia, Y. Schlein, V. D. Kravchenko, R.-D. Xue, and J. C. Beier, "Indoor use of attractive toxic sugar bait (ATSB) to effectively control malaria vectors in Mali, West Africa," *Malar. J.*, vol. 14, p. 301, Aug. 2015.

[9] J. D. Bohbot, L. Fu, T. C. Le, K. R. Chauhan, C. L. Cantrell, and J. C. Dickens, "Multiple activities of insect repellents on odorant receptors in mosquitoes," *Med. Vet. Entomol.*, vol. 25, no. 4, pp. 436–444, 2011.

[10] C. Montell and L. J. Zwiebel, "Mosquito sensory systems," *Adv. Insect Physiol.*, pp. 293–328, 2016.

[11] M. R. Brown, M. J. Klowden, J. W. Crim, L. Young, L. A. Shrouder, and A. O. Lea, "Endogenous regulation of mosquito host-seeking behavior by a neuropeptide," *J. Insect Physiol.*, vol. 40, no. 5, pp. 399–406, 1994.

[12] K. P. Siju, S. R. Hill, B. S. Hansson, and R. Ignell, "Influence of blood meal on the responsiveness of olfactory receptor neurons in antennal sensilla trichodea of the yellow fever mosquito, *Aedes aegypti*," *J. Insect Physiol.*, vol. 56, no. 6, pp. 659–665, 2010.

[13] S. Rickard Christophers, *Aedes aegypti (L.) the yellow fever mosquito: Its life history, bionomics and structure*. Cambridge University Press, 1960.

[14] J. Chesson, "Effect of notonectids (hemiptera: *Notonectidae*) on mosquitoes (diptera: *Culicidae*): Predation or selective oviposition?," *Environ. Entomol.*, vol. 13, pp. 531–538, Apr. 1984.

[15] J. W. Petranka and K. Fakhoury, "Evidence of a chemically-mediated avoidance response of ovipositing insects to bluegills and green frog tadpoles," *Copeia*, vol. 1991, no. 1, pp. 234–239, 1991.

[16] C. Liu, R. J. Pitts, J. D. Bohbot, P. L. Jones, G. Wang, and L. J. Zwiebel, "Distinct olfactory signaling mechanisms in the malaria vector mosquito *Anopheles gambiae*," *PLoS Biol.*, vol. 8, Aug. 2010.

[17] D. S. Galili, K. V. Dylla, A. Lüdke, A. B. Friedrich, N. Yamagata, J. Y. H. Wong, C. H. Ho, P. Szyszka, and H. Tanimoto, "Converging circuits mediate temperature and shock aversive olfactory conditioning in *Drosophila*," *Curr. Biol.*, vol. 24, pp. 1712–1722, Aug. 2014.

[18] Y. Xia, G. Wang, D. Buscariollo, R. J. Pitts, H. Wenger, and L. J. Zwiebel, "The molecular and cellular basis of olfactory-driven behavior in *Anopheles gambiae* larvae," *Proc. Natl. Acad. Sci.*, vol. 105, no. 17, pp. 6433–6438, 2008.

[19] K. Mysore, E. M. Flannery, M. Tomchaney, D. W. Severson, and M. Duman-Scheel, "Disruption of *Aedes aegypti* olfactory system development through chitosan/siRNA nanoparticle targeting of semaphorin-1a," *PLoS Negl. Trop. Dis.*, vol. 7, p. e2215, May 2013.

[20] B. Audrain, M. A. Farag, C.-M. Ryu, and J.-M. Ghigo, "Role of bacterial volatile compounds in bacterial biology," *FEMS Microbiol. Rev.*, vol. 39, pp. 222–233, Mar. 2015.

[21] L. Ponnusamy, N. Xu, S. Nojima, D. M. Wesson, C. Schal, and C. S. Apperson, "Identification of bacteria and bacteria-associated chemical cues that mediate oviposition site preferences by *Aedes aegypti*," *Proc. Natl. Acad. Sci.*, vol. 105, pp. 9262–9267, July 2008.

[22] M. C. O. Ferrari, F. Messier, and D. P. Chivers, "Threat-sensitive learning of predators by larval mosquitoes *Culex restuans*," *Behav. Ecol. Sociobiol.*, no. 7, pp. 1079–1083, 2008.

[23] A. Silberbush, S. Markman, E. Lewinsohn, E. Bar, J. E. Cohen, and L. Blaustein, "Predator-released hydrocarbons repel oviposition by a mosquito," *Ecol. Lett.*, vol. 13, pp. 1129–1138, Sept. 2010.

[24] W. A. Foster, "Mosquito sugar feeding and reproductive energetics," *Annu. Rev. Entomol.*, vol. 40, no. 1, pp. 443–474, 1995.

[25] V. O. Nyasembe and B. Torto, "Volatile phytochemicals as mosquito semiochemicals," *Phytochem. Lett.*, vol. 8, pp. 196–201, 2014.

[26] L.-C. Gouagna, R. S. Poueme, K. R. Dabiré, J.-B. Ouédraogo, D. Fontenille, and F. Simard, "Patterns of sugar feeding and host plant preferences in adult males of *An. gambiae* (diptera: *Culicidae*)," *J. Vector Ecol.*, vol. 35, no. 2, pp. 267–276, 2010.

[27] V. O. Nyasembe, P. E. A. Teal, W. R. Mukabana, J. H. Tumlinson, and B. Torto, "Behavioural response of the malaria vector *Anopheles gambiae* to host plant volatiles and synthetic blends," *Parasit. Vectors*, vol. 5, p. 234, Oct. 2012.

[28] M. R. Nikbakhtzadeh, J. W. Terbot, P. E. Otienoburu, and W. A. Foster, "Olfactory basis of floral preference of the malaria vector *Anopheles gambiae* (diptera: *Culicidae*) among common African plants," *J. Vector Ecol.*, vol. 39, no. 2, pp. 372–383, 2014.

[29] Y. G. Gillij, R. M. Gleiser, and J. A. Zygadlo, "Mosquito repellent activity of essential oils of aromatic plants growing in Argentina," *Bioresour. Technol.*, vol. 99, pp. 2507–2515, May 2008.

[30] P. Distler and J. Boeckh, "Central projections of the maxillary and antennal nerves in the mosquito *Aedes aegypti*," *J. Exp. Biol.*, vol. 200, no. Pt 13, pp. 1873–1879, 1997.

[31] R. Y. Zacharuk, L. R.-S. Yin, and S. G. Blue, "Fine structure of the antenna and its sensory cone in larvae of *Aedes aegypti* (L.)," *J. Morphol.*, vol. 135, no. 3, pp. 273–297, 1971.

[32] S. McIver and R. Siemicki, "Fine structure of antennal sensilla of male *Aedes aegypti* (l.)," *J. Insect Physiol.*, vol. 25, no. 1, pp. 21–28, 1979.

[33] S. McIver, "Structure of sensilla trichodea of female *Aedes aegypti* with comments on innervation of antennal sensilla," *J. Insect Physiol.*, vol. 24, no. 5, pp. 383–390, 1978.

[34] J. Bohbot, R. J. Pitts, H. W. Kwon, M. Rützler, H. M. Robertson, and L. J. Zwiebel, "Molecular characterization of the *Aedes aegypti* odorant receptor gene family," *Insect Mol. Biol.*, vol. 16, no. 5, pp. 525–537, 2007.

[35] A. J. Grant, J. G. Aghajanian, R. J. O'Connell, and B. E. Wigton, "Electrophysiological responses of receptor neurons in mosquito maxillary palp sensilla to carbon dioxide," *J. Comp. Physiol.*, vol. 177, no. 4, 1995.

[36] J. T. Sparks, B. T. Vinyard, and J. C. Dickens, "Gustatory receptor expression in the labella and tarsi of *Aedes aegypti*," *Insect Biochem. Molec.*, vol. 43, no. 12, pp. 1161–1171, 2013.

[37] J. D. Bohbot, J. T. Sparks, and J. C. Dickens, "The maxillary palp of *Aedes aegypti*, a model of multisensory integration," *Insect Biochem. Molec.*, vol. 48, pp. 29–39, 2014.

[38] G. H. Wolff and N. J. Strausfeld, "Genealogical correspondence of mushroom bodies across invertebrate phyla," *Curr. Biol.*, vol. 25, no. 1, pp. 38–44, 2015.

[39] U. S. Jhumur, S. Dötterl, and A. Jürgens, "Floral odors of *Silene otites*: Their variability and attractiveness to mosquitoes," *J. Chem. Ecol.*, vol. 34, no. 1, pp. 14–25, 2008.

[40] P. E. Otienoburu, B. Ebrahimi, P. Larry Phelan, and W. A. Foster, "Analysis and optimization of a synthetic milkweed floral attractant for mosquitoes," *J. Chem. Ecol.*, vol. 38, no. 7, pp. 873–881, 2012.

[41] U. S. Jhumur, S. Dötterl, and A. Jürgens, "Naïve and conditioned responses of *Culex pipiens pipiens* biotype *molestus* (diptera: *Culicidae*) to flower odors," *J. Med. Entomol.*, vol. 43, no. 6, pp. 1164–1170, 2006.

[42] M. R. Sanford, J. K. Olson, W. J. Lewis, and J. K. Tomberlin, "The effect of sucrose concentration on olfactory-based associative learning in *Culex quinquefasciatus* say (diptera: *Culicidae*)," *J. Insect Behav.*, vol. 26, no. 4, pp. 494–513, 2013.

[43] L. B. Thien and F. Utech, "The mode of pollination in *Habenaria obtusata* (*Orchidaceae*)," *Am. J. Bot.*, vol. 57, no. 9, p. 1031, 1970.

[44] C. M. Stone and W. A. Foster, *Plant-sugar feeding and vectorial capacity*. Wageningen Academic Publishers, 2013.

[45] N. J. Besansky, C. A. Hill, and C. Costantini, "No accounting for taste: Host preference in malaria vectors," *Trends Parasitol.*, vol. 20, pp. 249–251, June 2004.

[46] J. D. Edman and D. J. Taylor, "*Culex nigripalpus*: Seasonal shift in the bird-mammal feeding ratio in a mosquito vector of human encephalitis," *Science*, vol. 161, no. 3836, pp. 67–68, 1968.

[47] J. D. Edman, L. A. Webber, and A. A. Schmid, "Effect of host defenses on the feeding pattern of *Culex nigripalpus* when offered a choice of blood sources," *J. Parasitol.*, vol. 60, no. 5, p. 874, 1974.

[48] P. J. McCall and D. W. Kelly, "Learning and memory in disease vectors," *Trends Parasitol.*, vol. 18, no. 10, pp. 429–433, 2002.

[49] C. Vinauger, C. Lahondère, A. Cohuet, C. R. Lazzari, and J. A. Riffell, "Learning and memory in disease vector insects," *Trends Parasitol.*, vol. 32, no. 10, pp. 761–771, 2016.

[50] C. Vinauger, C. Lahondère, G. H. Wolff, L. T. Locke, J. E. Liaw, J. Z. Parrish, O. S. Akbari, M. H. Dickinson, and J. A. Riffell, "Modulation of host learning in *Aedes aegypti* mosquitoes," *Curr. Biol.*, vol. 28, pp. 333–344.e8, Feb. 2018.

[51] N. Chilaka, E. Perkins, and F. Tripet, "Visual and olfactory associative learning in the malaria vector *Anopheles gambiae* sensu stricto," *Malar. J.*, vol. 11, no. 1, 2012.

[52] G. Menda, J. H. Uhr, R. A. Wyttenbach, F. M. Vermeylen, D. M. Smith, L. C. Harrington, and R. R. Hoy, "Associative learning in the dengue vector mosquito, *Aedes aegypti*: Avoidance of a previously attractive odor or surface color that is paired with an aversive stimulus," *J. Exp. Biol.*, vol. 216, pp. 218–223, Jan. 2013.

[53] C. Vinauger, E. K. Lutz, and J. A. Riffell, "Olfactory learning and memory in the disease vector mosquito *Aedes aegypti*," *J. Exp. Biol.*, vol. 217, no. 13, pp. 2321–2330, 2014.

[54] G. Hasibeder and C. Dye, "Population dynamics of mosquito-borne disease: Persistence in a completely heterogeneous environment," *Theor. Popul. Biol.*, vol. 33, no. 1, pp. 31–53, 1988.

[55] D. W. Kelly and C. E. Thompson, "Epidemiology and optimal foraging: Modelling the ideal free distribution of insect vectors," *Parasitology*, vol. 120, no. 3, pp. 319–327, 2000.

[56] J. T. Lang, "Contact sex pheromone in the mosquito *Culiseta Inornata* (diptera: *Culicidae*)," *J. Med. Entomol.*, vol. 14, no. 4, pp. 448–454, 1977.

[57] E. Y. Fawaz, S. A. Allan, U. R. Bernier, P. J. Obenauer, and J. W. Diclaro, "Swarming mechanisms in the yellow fever mosquito: Aggregation pheromones are involved in the mating behavior of *Aedes aegypti*," *J. Vector Ecol.*, vol. 39, no. 2, pp. 347–354, 2014.

[58] M. Cabrera and K. Jaffe, "An aggregation pheromone modulates lekking behavior in the vector mosquito *Aedes aegypti* (diptera: *Culicidae*)," *J. Am. Mosq. Control Assoc.*, vol. 23, pp. 1–10, Mar. 2007.

[59] H. F. Nijhout, H. Frederik Nijhout, and G. B. Craig, "Reproductive isolation in *Stegomyia* mosquitoes. evidence for a sexual pheromone," *Entomol. Exp. Appl.*, vol. 14, no. 4, pp. 399–412, 1971.

[60] S. L. Mengoni, A. N. Lorenzo-Figueiras, and S. A. Minoli, "Experience-dependent modulation of the attraction to faeces in the kissing bug *Triatoma infestans*," *J. Insect Physiol.*, vol. 98, pp. 23–28, 2017.

[61] E. Suh, D.-H. Choe, A. M. Saveer, and L. J. Zwiebel, "Suboptimal larval habitats modulate oviposition of the malaria vector mosquito *Anopheles coluzzii*," *PLoS One*, vol. 11, p. e0149800, Feb. 2016.

[62] A. Silberbush and L. Blaustein, "Mosquito females quantify risk of predation to their progeny when selecting an oviposition site," *Funct. Ecol.*, vol. 25, no. 5, pp. 1091–1095, 2011.

[63] L. Blaustein, J. Blaustein, and J. Chase, "Chemical detection of the predator *Notonecta irrorata* by ovipositing *Culex* mosquitoes," *J. Vector Ecol.*, vol. 30, pp. 299–301, Dec. 2005.

[64] C. B. Ogbunugafor, C. Brandon Ogbunugafor, and L. Sumba, "Behavioral evidence for the existence of a region-specific oviposition cue in *Anopheles gambiae* s.s," *J. Vector Ecol.*, vol. 33, no. 2, pp. 321–324, 2008.

[65] E. Rejmánková, R. Higashi, J. Grieco, N. Achee, and D. Roberts, "Volatile substances from larval habitats mediate species-specific oviposition in *Anopheles* mosquitoes," *J. Med. Entomol.*, vol. 42, pp. 95–103, Mar. 2005.

[66] J. M. Lindh, M. N. Okal, M. Herrera-Varela, A.-K. Borg-Karlson, B. Torto, S. W. Lindsay, and U. Fillinger, "Discovery of an oviposition attractant for gravid malaria vectors of the *Anopheles gambiae* species complex," *Malar. J.*, vol. 14, p. 119, Mar. 2015.

[67] L. A. Sumba, T. O. Guda, A. L. Deng, A. Hassanali, J. C. Beier, and B. G. J. Knols, "Mediation of oviposition site selection in the African malaria mosquito *Anopheles gambiae* (diptera: *Culicidae*) by semiochemicals of microbial origin," *Int. J. Trop. Insect Sci.*, vol. 24, no. 03, 2004.

[68] B. Wondwosen, G. Birgersson, E. Seyoum, H. Tekie, B. Torto, U. Fillinger, S. R. Hill, and R. Ignell, "Rice volatiles lure gravid malaria mosquitoes, *Anopheles arabiensis*," *Sci. Rep.*, vol. 6, p. 37930, Nov. 2016.

[69] B. Wondwosen, S. R. Hill, G. Birgersson, E. Seyoum, H. Tekie, and R. Ignell, "A(maize)ing attraction: gravid *Anopheles arabiensis* are attracted and oviposit in response to maize pollen odours," *Malar. J.*, vol. 16, p. 39, Jan. 2017.

[70] G. L. Benzon and C. S. Apperson, "Reexamination of chemically mediated oviposition behavior in *Aedes aegypti* (l.) (diptera: *Culicidae*)," *J. Med. Entomol.*, vol. 25, pp. 158–164, May 1988.

[71] "Studies of *Aedes triseriatus* oviposition attractants produced by larvae of *Aedes triseriatus* and *Aedes atropalpus* (diptera: *Culicidae*)," *J. Med. Entomol.*, vol. 13, no. 1, pp. 112–115, 1976.

[72] K. Ganesan, M. J. Mendki, M. V. S. Suryanarayana, S. Prakash, and R. C. Malhotra, "Studies of *Aedes aegypti* (diptera: *Culicidae*) ovipositional responses to newly identified semiochemicals from conspecific eggs," *Aust. J. Entomol.*, vol. 45, no. 1, pp. 75–80, 2006.

[73] T. Seenivasagan, K. R. Sharma, K. Sekhar, K. Ganesan, S. Prakash, and R. Vijayaraghavan, "Electroantennogram, flight orientation, and oviposition responses of *Aedes aegypti* to the oviposition pheromone *n*-heneicosane," *Parasitol. Res.*, vol. 104, pp. 827–833, Mar. 2009.

[74] M. D. Bentley, I. N. McDaniel, M. Yatagai, H.-P. Lee, and R. Maynard, "*p*-cresol: an oviposition attractant of *Aedes triseriatus*," *Environ. Entomol.*, vol. 8, no. 2, pp. 206–209, 1979.

[75] P. J. Mccall and G. Eaton, "Olfactory memory in the mosquito *Culex quinquefasciatus*," *Med. Vet. Entomol.*, vol. 15, no. 2, pp. 197–203, 2001.

[76] J. S. Kaur, Y. L. Lai, and A. D. Giger, "Learning and memory in the mosquito *Aedes aegypti* shown by conditioning against oviposition deterrence," *Med. Vet. Entomol.*, vol. 17, no. 4, pp. 457–460, 2003.

[77] C. R. Lazzari, "Chapter 1: Orientation towards hosts in haematophagous insects," *Adv. Insect Physiol.*, pp. 1–58, 2009.

[78] M. R. Sanford and J. K. Tomberlin, "Conditioning individual mosquitoes to an odor: Sex, source, and time," *PLoS ONE*, vol. 6, no. 8, p. e24218, 2011.

[79] S. Anton and J.-P. Rospars, "Quantitative analysis of olfactory receptor neuron projections in the antennal lobe of the malaria mosquito, *Anopheles gambiae*," *J. Comp. Neurol.*, vol. 475, no. 3, pp. 315–326, 2004.

[80] R. Ignell, T. Dekker, M. Ghaninia, and B. S. Hansson, "Neuronal architecture of the mosquito deutocerebrum," *J. Comp. Neurol.*, no. 2, pp. 207–240, 2005.

[81] O. Riabinina, D. Task, E. Marr, C.-C. Lin, R. Alford, D. A. O'Brochta, and C. J. Potter, "Organization of olfactory centres in the malaria mosquito *Anopheles gambiae*," *Nat. Commun.*, vol. 7, no. 1, 2016.

[82] M. Ghaninia, M. Larsson, B. S. Hansson, and R. Ignell, "Natural odor ligands for olfactory receptor neurons of the female mosquito *Aedes aegypti*: Use of gas chromatography-linked single sensillum recordings," *J. Exp. Biol.*, vol. 211, no. 18, pp. 3020–3027, 2008.

[83] K. Mysore, S. Flister, P. Müller, V. Rodrigues, and H. Reichert, "Brain development in the yellow fever mosquito *Aedes aegypti*: a comparative immunocytochemical analysis using cross-reacting antibodies from *Drosophila melanogaster*," *Dev. Genes Evol.*, vol. 221, no. 5-6, pp. 281–296, 2011.

[84] A. Ramaekers, E. Magnenat, E. C. Marin, N. Gendre, G. S. X. E. Jefferis, L. Luo, and R. F. Stocker, "Glomerular maps without cellular redundancy at successive levels of the *Drosophila* larval olfactory circuit," *Curr. Biol.*, vol. 15, pp. 982–992, June 2005.

[85] S. Waddell, "Reinforcement signalling in *Drosophila*; dopamine does it all after all," *Curr. Opin. Neurobiol.*, vol. 23, no. 3, pp. 324–329, 2013.

[86] K. P. Siju, B. S. Hansson, and R. Ignell, "Immunocytochemical localization of serotonin in the central and peripheral chemosensory system of mosquitoes," *Arthropod Struct. Dev.*, vol. 37, no. 4, pp. 248–259, 2008.

[87] A. Chen, F. Ng, T. Lebestky, A. Grygoruk, C. Djapri, H. O. Lawal, H. A. Zaveri, F. Mehanzel, R. Najibi, G. Seidman, N. P. Murphy, R. L. Kelly, L. C. Ackerson, N. T. Maidment, F. Rob Jackson, and D. E. Krantz, "Dispensable, redundant, complementary, and cooperative roles of dopamine, octopamine, and serotonin in *Drosophila melanogaster*," *Genetics*, vol. 193, no. 1, pp. 159–176, 2013.

[88] Z. Syed, "Chemical ecology and olfaction in arthropod vectors of diseases," *Curr. Opin. Insect Sci.*, vol. 10, pp. 83–89, 2015.

[89] A. Cork and K. C. Park, "Identification of electrophysiologically-active compounds for the malaria mosquito, *Anopheles gambiae*, in human sweat extracts," *Med. Vet. Entomol.*, vol. 10, no. 3, pp. 269–276, 1996.

[90] U. R. Bernier, D. L. Kline, D. R. Barnard, C. E. Schreck, and R. A. Yost, "Analysis of human skin emanations by gas chromatography / mass spectrometry. 2. Identification of volatile compounds that are candidate attractants for the yellow fever mosquito (*Aedes aegypti*)," *Anal. Chem.*, vol. 72, no. 4, pp. 747–756, 2000.

[91] J. A. Riffell, "Olfactory ecology and the processing of complex mixtures," *Curr. Opin. Neurobiol.*, vol. 22, no. 2, pp. 236–242, 2012.

Chapter 1

Live calcium imaging of *Aedes aegypti* neuronal tissues reveals differential importance of chemosensory systems for life-history-specific foraging strategies

Michelle Bui, Jennifer Shyong, Eleanor K. Lutz, Ting Yang, Ming Li, Kenneth Truong, Ryan Arvidson, Anna Buchman, Jeffrey A. Riffell and Omar S. Akbari

Published in: BMC Neuroscience. 2019

Abstract

The mosquito *Aedes aegypti* has a wide variety of sensory pathways that have supported its success as a species as well as a highly competent vector of numerous debilitating infectious pathogens. Investigations into mosquito sensory systems and their effects on behavior are valuable resources for the advancement of mosquito control strategies. Numerous studies have elucidated key aspects of mosquito sensory systems, however there remains critical gaps within the field. In particular, compared to that of the adult form, there has been a lack of studies directed towards the immature life stages. Additionally, although numerous studies have pinpointed specific sensory receptors as well as responding motor outputs, there has been a lack of studies able to monitor both concurrently. To begin filling aforementioned gaps, here we engineered *Ae. aegypti* to ubiquitously express a genetically encoded calcium indicator, GCaMP6s. Using this strain, combined with advanced microscopy, we simultaneously measured live stimulus-evoked calcium responses in both neuronal and muscle cells with a wide spatial range and resolution. By coupling *in vivo* live calcium imaging with behavioral assays we were able to gain functional insights into how stimulus-evoked neural and muscle activities are represented, modulated, and transformed in mosquito larvae enabling us to elucidate mosquito sensorimotor properties important for life-history-specific foraging strategies.

Background

The yellow fever mosquito, *Aedes aegypti*, is a global vector of numerous debilitating arboviruses including Chikungunya, Dengue, Yellow Fever, and Zika [1]. Due to its ability to transmit copious pathogens, adaptability to diverse climates, flexibility in oviposition sites, and desiccation-tolerant eggs, *Ae. aegypti* are significant worldwide epidemiological burdens, leading to hundreds of millions of infections annually resulting in over 50,000 deaths [2–5]. To decrease the imposed global burden, many vector control methodologies have been developed and implemented, including a number of innovative genetic-based technologies such as the release of insects carrying dominant lethal (RIDL) [6] and the infection and introduction of mosquitoes harboring the intracellular bacterium, *Wolbachia* either spread into populations to reduce viral transmission [7, 8], or used for population suppression through *Wolbachia* induced cytoplasmic incompatibility (IIT) [9]. Moreover, there are also a number of innovative "gene drive" based technologies that are rapidly being developed in *Ae. aegypti* with the hope of making an impact in the future, in addition to innovative methods of generating sterile males using CRISPR [10–14]. Nonetheless, the most prevalent form of mosquito control used in the field today is the traditional use of chemical insecticides [15]. Although insecticides can have an impact on mosquito populations, due to their high costs, environmental impacts, requirements for continuous application, and rapid susceptibility to resistance [16], they are not sustainable long-term solutions. Therefore, significant efforts are necessary to discern the underlying molecular, genetic and physiological mechanisms important for arboviral vector competence with the overall aim of developing additional novel, insecticide-free methods to disrupt viral disease cycles [17].

At both larval and adult stages, mosquito sensory systems play pivotal roles in mediating a variety of behaviors, including locating food resources, habitat selection, and predator avoidance (reviewed in [18–20]). As such, sensory systems provide attractive targets for suppressing vector behaviors at both the larval and adult stages. Over the years there have been numerous studies on adult mosquito sensory systems that have greatly advanced the field, such as the discovery of key olfactory and gustatory receptors [21, 22] as well as behavioral responses to host cues [23–25]. Notwithstanding, there remains critical gaps in understanding the direct relationships between sensorimotor and behavioral responses, specifically important for behaviors linked to vector competence such as host seeking and chemical avoidance. Additionally, only a handful of studies have focused on larval chemosensory systems result-

ing in significant gaps in a holistic understanding of mosquito sensory systems [26]. For example, olfaction is important for detecting long-range host cues in adult mosquitoes. However in an aquatic environment, either gustation, olfaction, or both, could detect long-range food indicators [27]. Food scarcity is an important ecological constraint on mosquito larvae [28], but little is known about the chemosensory mechanism of foraging in larval mosquitoes. Given the relative simplicity of the larval nervous systems, understanding chemosensory signal transduction, coding, and behavior in larvae could lead to novel control interventions and enable a more holistic understanding of mosquito behavior in areas such as food seeking and chemotaxis [19, 26].

Notwithstanding, as of recently, we have lacked effective genetic tools to study mosquito larval sensory systems as they process environmental information. Current tools used in mosquitoes to monitor neural activity include extracellular recording from sensilla and antennal lobe cells [29], as well as using synthetic calcium-sensitive dyes (e.g. FURA-2) *in vivo*, or in heterologous systems [30, 31]. To overcome the challenges of these existing approaches, here we have engineered *Ae. aegypti* to ubiquitously express a Genetically Encoded Calcium Indicator (GECI), termed GCaMP6s. GCaMP6s enables imaging of sensory-evoked calcium transients through changes in relative fluorescence [32]. Using this tool we gained the unprecedented ability to concurrently measure *in vivo* sensory responses and motor responses with high spatial and temporal resolution in regions of neuropil and muscles of live responding mosquitoes. This enabled us to generate functional insights into the importance of chemosensory channels in mediating behavior (e.g. foraging) by inactivating distinct olfactory and gustatory channels and measuring larval neural responses to diverse chemosensory stimuli in various genetic backgrounds such as those harboring mutations in important olfactory and gustatory receptors [21, 22]. Taken together, our results demonstrate the utility of GCaMP6s to link the sensory processing of specific stimuli to behavior responses of swimming larvae, thereby gaining a deeper functional understanding of mosquito multisensory integration.

Results

Development of an optogenetic-reporter of neuronal activity in *Ae. aegypti*

To visualize live calcium activity, we engineered a transgenic *Ae. aegypti* strain harboring genomic sources of a genetically-encoded calcium indicator, GCaMP6s [32]. To express GCaMP6s, we utilized the *polyubiquitin* promoter (AAEL003877, henceforth *PUb*), chosen for its generally high expression during nearly all developmental life stages and tissues as shown by previous promoter characterization experiments and developmental transcriptional profiling (Figure 1A) [33, 34]. We inserted the *PUb* promoter upstream of the coding sequence for GCaMP6s within a randomly inserting *piggyBac* transposable element. Downstream to the *PUb* promoter driven GCaMP6s, we included an OpIE-2 promoter driving dsRed expression to serve as a robust transgenesis marker (Figure 1B). To obtain a transgenic strain, the engineered *piggyBac* transgene was injected into the germ cells of 200 pre-blastoderm stage *Ae. aegypti* embryos (0-1hr old). Transgenic G1 mosquitoes harboring the transgene were readily identified by a bright expression of OpIE-2 driven dsRed in the abdomen, in addition to a robust calcium signaled activation of GCaMP6s in muscle and neural cells (Figure 1C). To ensure that this strain represented a single chromosomal insertion, we backcrossed isolated individuals for four generations to wild-type (+/+) and measured Mendelian transmission ratios each generation and observed 50% of offspring inheriting the transgene, indicating that this strain likely represents a single chromosomal insertion. To precisely determine its genomic insertion location, we used inverse PCR and found the location of insertion to be on the 2nd chromosome with flanking 5' and 3' *piggyBac* regions positioned at AaegL5.0 reference (genomic loci 285,175,805-285,176,289 and 285,175,275-285,175,803, respectively). The location of the insertion site was mapped to a intronic region of an uncharacterized locus. To determine the fitness cost of our inserted transgene, we performed experiments comparing fertility, fecundity, egg hatching rate, and larval development time of our GCaMP6s inserted line to +/+. These experiments indicated that the transgene insertion did not significantly affect fertility ($p=0.4376$), egg hatching rate ($p=0.1536$), or larval development time ($p=0.2034$), however fecundity was slightly increased ($p<0.05$) (Supplementary Table 1).

Temporal and Spatial Odor-Evoked GCaMP6s Responses in Adults

To assess GCaMP6s functionality in a +/+ genetic background (termed GCaMP6s/+/+ from hereon), and to visualize sensorimotor activity elicited by specific sensory channels, we initially recorded and quantified calcium transients in adult mosquitoes that were stimulated with CO_2. Distinct regions-of-interest (ROIs) were imaged across various sensory organs of adult mosquitoes using laser-scanning confocal microscopy. Calcium-evoked changes in fluorescence varied between sensory organs tested. For example, the tip of the maxillary palp displayed significant changes in fluorescence intensity across 4 replicates presumably related to the location of olfactory sensory neurons (OSNs) within capitate peg sensilla on the maxillary palp [21] (mean $\Delta F/F0$ is 1.24 ± 0.13, p-value = 0.0323,

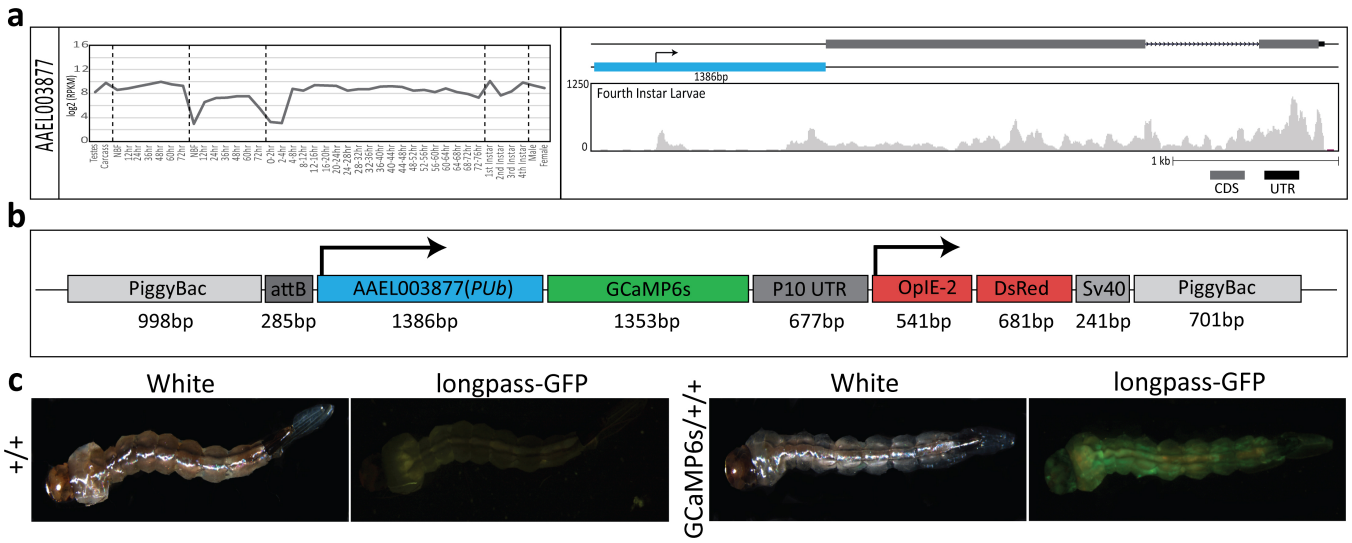

Figure 1: RNAseq expression, schematic representation of the GCaMP6s construct and larval fluorescence. Log_2 (RPKM) expression values for the promoter, AAEL003877 (*PUb*) was plotted across development. Samples include, from left to right: testes; male carcasses (lacking testes); carcasses of females prior to blood feeding (NBF); female carcasses 12 hr, 24 hr, 36 hr, 48 hr, and 72 hrs post blood meal; ovaries from NBF females and at 12 hr, 24 hr, 36 hr, 48 hr, and 72 hr post ecdysis; embryos from 0∼2 hrs through 72∼76 hrs; whole larvae from 1st instar, 2nd instar, 3rd instar and 4th instar; male pupae; and female pupae. A genome browser snapshot was with the Y axis showing expression level based on raw read counts of fourth instar larvae (**A**). A schematic representation of the *piggyBac*-mediated GCaMP6s construct. GCaMP6s is driven by AAEL003877(*PUb*)(blue) while dsRed by OpIE-2, the latter serving as a transgenic marker (**B**). Larval bright field images (left) and corresponding fluorescent images (right) show robust GFP transients throughout the whole body and DsRed fluorescence in the abdomen. +/+ represents wild-type larva. GCaMP6s/+/+ represents transgenic GCaMP6s larvae (**C**).

replicates = 4) (Supplementary Figure 1A, Supplementary Video 1). While in the adult antennal flagellum, changes in fluorescence were recorded in the nodes between antennal segments (mean $\Delta F/F0$ is 0.04±0.31, p-value = 0.8240 and 0.01±0.12, p-value = 0.9469, for ROI 1 and 2 respectively) and the internodes (mean $\Delta F/F0$ is -0.08±0.07, p-value = 0.1467), although neither were highly significant when comparing across 6 replicates (Supplementary Figure 1B, Supplementary Video 2). Additionally, when observing clusters of ommatidia within the adult eyes, changes in calcium signaled GCaMP6s activation were highly stochastic across 4 replicates presumably due to continuous optical responses as the mosquito is sensing the environment (mean $\Delta F/F0$ is 0.02±0.01, p-value = 0.4700; -0.15±0.20, p-value = 0.4398; 0.02±0.04, p-value = 0.4949, for ROIs 1-3 respectively) (Supplementary Figure 1C, Supplementary Video 3). Although these results indicated that many regions (e.g. adult antennal flagellum and adult ommatidia) did not demonstrate significantly consistent odor-evoked responses across multiple replicates, accurate detection of subcuticular fluorescence was hindered by the adult's thick cuticle and dense setation. To overcome this limitation in adults, we performed careful dissections of the head cuticle which enabled us to investigate the labeling efficacy of our GCaMP6s strain within the adult antennal lobe by examining several major cell types of potential interest to mosquito sensory processing. We found that GCaMP6s expression is sufficiently high to morphologically characterize diverse cell types including individual glomeruli, lateral cell cluster neurons, glia, and medial cell cluster neurons which will be invaluable for future studies (Supplementary Figure 2).

Relative Odor-Evoked GCaMP6s Responses in Larvae

Compared to adults, 2nd instar larvae have relatively simplified neuroanatomical systems and a transparent cuticle making them well suited for detecting subcutaneous changes in fluorescence intensity reported by GCaMP6s without the need for dissections. These factors coupled with the limited knowledge regarding mosquito larval sensory responses motivated us to simultaneously image muscle and sensory calcium-evoked responses with the GCaMP6s/+/+ strain. Using either a 5X or 10X objective permitted us to record fluorescence in the whole body, or just the head capsule, respectively. Results from these experiments revealed significant changes in calcium transients within the longitudinal muscles within the 2nd abdominal segment across 4 replicates (mean $\Delta F/F0$ is 3.45±0.57, p-value = 0.0011) (Supplementary Figure 1D, Supplementary Video 4) in the body in addition to the lateral retractors (mean $\Delta F/F0$ is 2.04±0.77, p-value = 0.004497), the deuterocerebrum (DE) (mean $\Delta F/F0$ is 0.45±0.14, p-value = 0.002150) and medial retractors (mean $\Delta F/F0$ is 2.57±01.27, p-value =

0.013050) in the head (Supplementary Figure 1E, Supplementary Video 5). To further determine the cell type specificity of *PUb*-GCaMP6s expression within the larval brain, co-staining for GFP as well as either Glutamine Synthetase (GS) (which labels astrocyte-like glial) or alpha tubulin (which labels the nervous system) was performed [35]. Results exhibited colocalization between fixed GFP and both antibodies thus demonstrating that GCaMP6s under the *PUb* promoter expressed robosutly in a variety of cell types (Supplementary Figure 3). Taken together, these results indicate that GCaMP6s can be used to effectively visualize sensorimotor activity in neural and muscle tissues of live mosquito larvae.

Calcium Imaging of Odor-evoked Responses in the Larval brain in Response to Olfactory Stimuli

To gain a more comprehensive understanding of the links between stimulus-evoked calcium responses in the brain and muscles of the larval head, a novel, minimally invasive, tethered-swimming assay was developed. This assay consisted of adhering the dorsal side of the larval head to a chambered cover glass, thereby immobilizing the head, while the larva was submerged in enough water to enable constant imaging of calcium transients within the head capsule while the tail could freely swim and the breathing tube could siphon oxygen (Figure 2A). Importantly, the larval head capsule is strikingly transparent requiring no surgical removal of cuticle thus enabling the larva to survive for extended periods (up to 48 h) permitting multiple recordings on the same individual. Responses in the DE and lateral abductors were analyzed as representatives of neural and muscle responses, respectively with at minimum 3 biological replicates per stimuli. Stimuli tested included chemicals previously shown to be relevant to adult mosquitoes such as a known olfactory receptor agonist (2-(4-Ethyl-5-(pyridin-3-yl)-4H-1,2,4-triazol-3-ylthio)-N-(4-ethylphenyl) acetamide, henceforth VUAA1) [36], attractants (1-octen-3-ol, ethyl acetate and lactic acid) [37–40], a known exciter of multiple groove-peg OSNs (butylamine) [27], and other behaviorally relevant compounds (sucrose, lobeline, glutamate, fish food) [41, 42]. All stimulants were prepared at 6×10^{-5}M. Previous studies have demonstrated mosquito larval response to various stimuli at concentrations ranging from 10^{-5} to 10^{-2}M [43], here we used the bottom range of concentrations in order to prevent overstimulation within our small chambered cover glass. By stimulating GCaMP6s/+/+ larvae to this panel of chemicals we found that there were significant calcium responses in the DE to several stimuli including 1-octen-3-ol (max ΔF/F0 is 6.09±3.85, p-value = 0.0145), butylamine (max ΔF/F0 is 3.29±3.05, p-value = 0.0092), ethyl acetate (max ΔF/F0 is 3.14±2.61, p-value = 0.0077), lobeline (max ΔF/F0 is 2.57±2.17, p-value = 0.0224), lactic acid (max ΔF/F0 is 2.31±1.72, p-value = 0.0366), and VUAA1 (max ΔF/F0 is 2.12±1.66, p-value = 0.0458), while sucrose (max ΔF/F0 is 2.01±2.70, p-value = 0.1053), glutamate (max ΔF/F0 is 0.79±0.61, p-value = 0.1632), and fish food extract (max ΔF/F0 is 0.62±1.02, p-value = 0.6101) did not display significant changes in fluorescence intensity when compared to responses evoked by water (Figure 2D,2E, Supplementary Figure 4,5A). Interestingly, 1-octen-3-ol, a known mosquito adult attractant produced by microbes [44], displayed the greatest calcium response, followed by butylamine and ethyl acetate, with the former previously documented to induce a response in activated grooved-peg OSNs in *Anopheles gambiae*, *Anopheles quadriannulatus*, and *Culex quinquefasciatus* [27, 45]. Moreover, when observing muscle responses to the same stimuli we observed significant calcium increases in 5 of the 6 stimuli that also displayed significant responses in the DE. These stimuli included 1-octen-3-ol (max ΔF/F0 is 6.38±1.50, p-value = $2.91e^{-05}$), butylamine (max ΔF/F0 is 6.11±4.04, p-value = $4.11e^{-05}$), Ethyl Acetate (max ΔF/F0 is 3.10±2.88, p-value = 0.00096), lobeline (max ΔF/F0 is 2.41±2.45, p-value = 0.00408), and VUAA1 (max ΔF/F0 is 3.16±2.16, p-value = 0.00437). Similar to the DE, the muscles did not exhibit significant responses to sucrose (max ΔF/F0 is 1.04±1.64, p-value = 0.07634), glutamate (max ΔF/F0 is 0.68±1.07, p-value = 0.1453), or fish food (max ΔF/F0 is 0.59±0.45, p-value = 0.1534) when compared to responses evoked by water. Contrary to results from the DE, responses by muscles to lactic acid (max ΔF/F0 is 1.53±1.88, p-value = 0.07509) were not significant. Lastly, the universal expression of GCaMP provided an opportunity for temporal comparison between brain and muscle responses. When analyzing the latency in response between the DE and muscles (Figure 2 B,C), 1-octen-3-ol elicited a significant latency of 2.24±3.19 sec (p-value = 0.003036), while butylamine elicited a latency of 0.48±1.11 sec (p-value = 0.2867) (Figure 2F). Furthermore, a persistence in response to 1-octen-3-ol was seen in the DE but not in the muscle. This contrasted with the response to a majority of the other stimuli including butylamine where fluorescent expression in the muscle matched that of the DE (Supplementary Figure 8). To further explore the potential functionality of our GCaMP6s mosquito line, we used 2-photon microscopy to investigate higher spatial resolution in imaging GCaMP6s expression. Although this experimental protocol was unsuitable for imaging stimulus-evoked responses due to the substantial movement of the brain, we were able to image various regions of interest throughout the brain of live, head-fixed larvae (Figure 3), demonstrating that this technique may be useful for future studies in larval neurobiology such as larval vision or nociception.

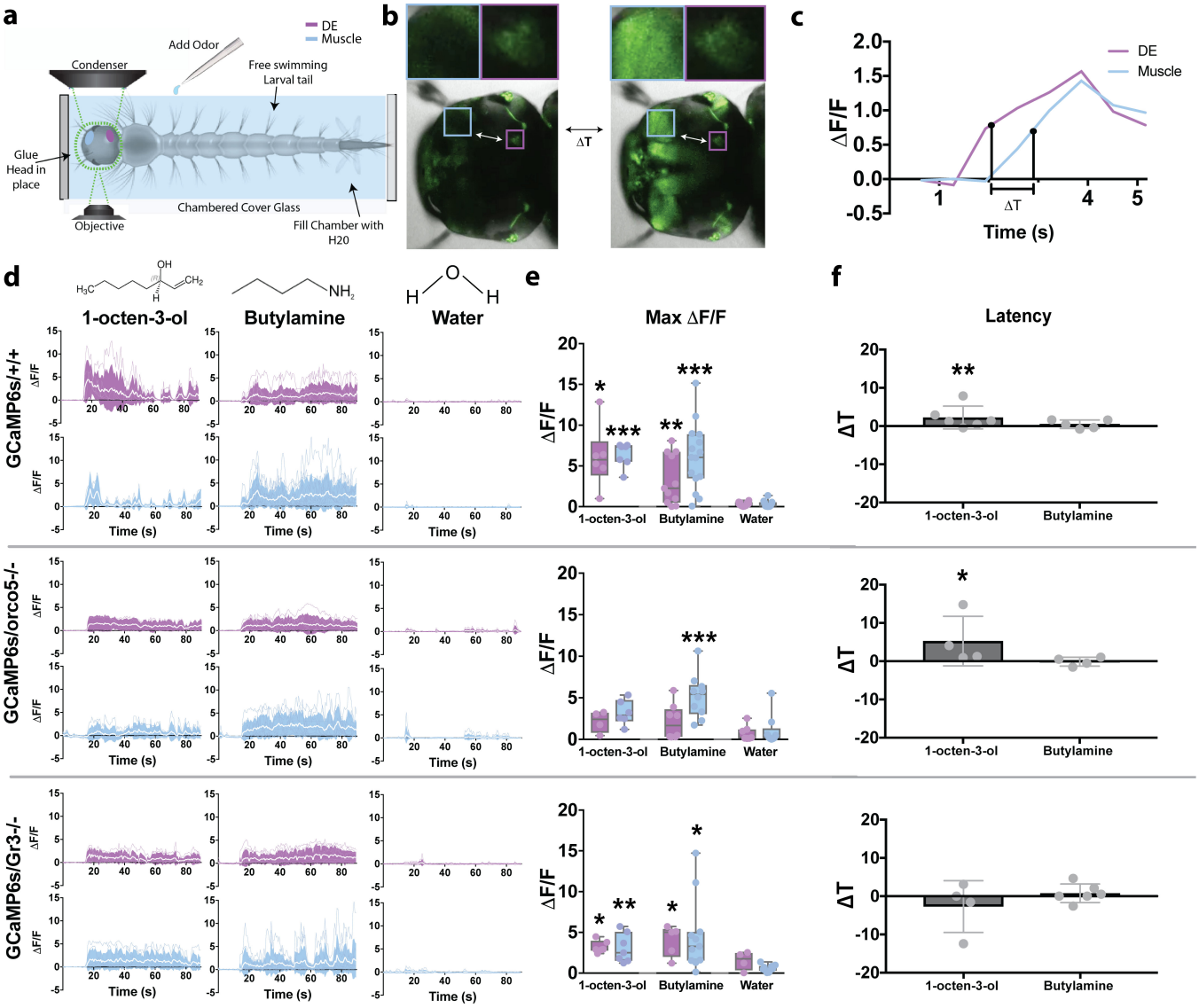

Figure 2: Live calcium imaging of stimulus-evoked responses in GCaMP6s/+/+, GCaMP6s/*orco*5-/-, and GCaMP6s/Gr3-/-. Mosquito larval calcium responses to various stimulants were recorded using a Leica SP5 Confocal microscope. To secure the larval head for imaging while allowing free movement of the larval tail, the dorsal side of the larva's head was adhered to a chambered cover glass using quick setting adhesive. The chamber was then filled with water and the larvae was allowed to rest before being introduced to stimulants (**A**). To compare temporal difference between the Deuterocerebrum (DE, purple) and muscles (blue), the difference between time points at 50% of the maximum ΔF/F of the first response peak following the addition of stimuli (**B,C**). Stimuli, including 1-octen-3-ol, butylamine, and water were introduced to GCaMP6s/+/+, GCaMP6s/*orco*5-/-, and GCaMP6s/Gr3-/- larvae 15 sec after the start of recording. Calcium responses within the Deuterocerebrum and muscles were recorded at 0.645 frames/sec (**D**) and maximum fluorescence values were plotted (**E**). The temporal difference in seconds between the DE and Muscle responses were calculated and plotted by comparing DE and muscle timepoints at 50% of maximum ΔF/F (**F**). The number of biological replicates used for each experiment were 3 or greater. Differences in ΔF/F and latency were analyzed using a Welch's T-test and a Mann-Whitney U test respectively. *: p-value < 0.05, **: p-value < 0.01, ***: p-value < 0.001. (GCaMP6s/+/+ DE: 1-octen-3-ol n=6; butylamine n=11; water n=12. GCaMP6s/+/+ Muscle: 1-octen-3-ol n=7; butylamine n=15; water n=12. GCaMP6s/*orco*5-/- DE: 1-octen-3-ol n=4; butylamine n=8; water n=7. GCaMP6s/*orco*5-/- Muscle: 1-octen-3-ol n=6; butylamine n=10; water n=9. GCaMP6s/Gr3-/-: 1-octen-3-ol n=6; butylamine n=11; water n=12. GCaMP6s/Gr3-/- DE: 1-octen-3-ol n=6; butylamine n=5; water n=4, GCaMP6s/Gr3-/- Muscle: 1-octen-3-ol n=7; butylamine n=11; water n=10. Latency of GCaMP6s+/+ response: 1-octen-3-ol n=6; butylamine n=5. Latency of GCaMP6s/*orco*5-/- response: 1-octen-3-ol n=4; butylamine n=4. Latency of GCaMP6s/Gr3-/- response: 1-octen-3-ol n=4; butylamine n=6).

Larval Brain responses to Olfactory Stimuli in Mutant Genetic Backgrounds

To gain further insight into the genetic basis for neuronal responses to various stimuli, we genetically introgressed GCaMP6s/+/+ mosquitoes into two separate genetic backgrounds that harbored homozygous viable mutations in either an important odorant coreceptor required for odor detection (*orco*; [22]) or a subunit of the heteromeric CO_2 receptor (Gr3-/-; [21])

(Supplementary Figure 6). Previous studies have demonstrated that *orco* is a highly conserved subunit of ORs that influences multiple odorant receptors and plays a role in the discrimination between different host organisms' olfactory cues. Gr3 on the other hand has been noted to play a major role in CO_2 detection, thus also affecting host detection. Using our larval tethered-swimming confocal imaging assay and stimulus panel described above to compare calcium evoked responses between GCaMP6s/+/+, GCaMP6s/*orco*5-/-, GCaMP6s/Gr3-/- enabled us to parse out receptors important for eliciting responses to various stimuli. Interestingly, we found that, compared to GCaMP6s/+/+, the DE and muscles of GCaMP6s/*orco*5-/- elicited fewer significant responses to stimuli (p-value >0.05) as well as a general reduction in calcium evoked responses to all stimuli (Supplementary Figures 2, 3B). Only butylamine elicited significant responses compared to the water control in the muscles (max ΔF/F0 is 5.20±2.60, p-value = $8.55e^{-4}$) (Figure 2E, Supplementary Figure 5B). Additionally, when comparing DE and muscle responses between GCaMP6s/*orco*5-/- and GCaMP6s+/+, only muscle responses to 1-octen-3-ol and VUAA1 within GCaMP6s/*orco*5-/- showed a significant decrease (Supplementary Figure 5E). A strong decrease in DE response to 1-octen-3-ol was also seen in GCaMP6s/*orco*5-/-, however it was not significant (max ΔF/F is 2.14±1.30, p-value = 0.0563). Examining the latency of response in GCaMP6s/*orco*5-/- demonstrated that stimulation with 1-octen-3-ol elicited responses in muscles 5.27±6.50 sec after activation of the DE (p-value = 0.04412), while butylamine showed little difference in the latency between DE and muscle response (0.13±1.14 sec; p-value = 0.9492) (Figure 2F). Furthermore, although the DE intensity of response to 1-octen-3-ol was not as strong as that of GCaMP6s+/+, the response was seen to persist for a longer period of time (Supplementary Figure 8). Taken together, our results demonstrate *orco*'s role in the detection of numerous chemosensory stimuli. Additionally, we found that *orco* may play an important role in 1-octen-3-ol detection and response. A nonsignificant reduction of response in the DE yet a significant reduction in the muscles indicate that even strong yet insignificant decreases in neural response may lead to a significant reduction of muscle output.

In contrast to the GCaMP6s/*orco*5-/- mutants, GCaMP6s/Gr3-/- mutants showed more robust calcium-evoked responses, and were generally not significantly different from those of GCaMP6s/+/+ with the exclusion of muscle responses to 1-octen-3-ol (Supplementary Figure 5C-E). For instance, relative to the water control, 1-octen-3-ol and ethyl acetate elicited strong responses in both the DE and muscle (p-value < 0.05) (Supplementary Figure 4). In total, five stimuli evoked significant increases in fluorescence within muscles of GCaMP6s/Gr3/-/- mutants; including 1-octen-3-ol (max ΔF/F0 is 3.08 ±1.79, p-value = 0.009765), butylamine (max ΔF/F0 is 4.59±4.46, p-value = 0.01383), ethyl acetate (max ΔF/F0 is 4.51±1.85, p-value = 0.001199), VUAA1 (max ΔF/F0 is 1.86 ±1.11, p-value = 0.01393), and sucrose (max ΔF/F0 is 2.03±1.47, p-value = 0.04154) (Supplementary Figure 5C). Interestingly, the latency in response between the DE and muscle ROIs were near-simultaneous for butylamine (0.78±2.61 sec, p-value = 0.6565) and 1-octen-3-ol (2.72±6.75 sec, p-value = 0.9389), with the latter also demonstrating more persistent responses in both the DE and muscles, suggesting that gustation or other chemosensory channels may be involved in the processing of these odorants (Figure 2F, Supplementary Figure 8).

Odor-evoked behavior in free-swimming larvae

Previous studies have shown that mosquito larvae respond behaviorally to chemosensory stimuli including 1-octen-3-ol [26], but the genetic basis of these responses remain unclear. To investigate the behavioral responses of the GCaMP6s larvae in various genetic backgrounds (GCaMP6s/+/+, GCaMP6s/*orco*5-/-, and GCaMP6s/Gr3-/-), we examined free-swimming larval responses to a limited odor panel in a custom arena. Individual larvae were allowed to acclimate inside the dark behavior arena before a stimulus — either food extract, 1-octen-3-ol, or a water-only (negative) control — was added to one side of the arena, and responses were analyzed and compared for the 15-minute acclimation period and the following 15-minute experiment period (Figure 4). From the videos, we were able to quantify each larva's preference index (PI, defined as the proportion of time spent in the odor half of the arena minus the proportion of time spent in the non-odor half) (Figure 4). Importantly, prior to stimulation we found no differences in mean speed between larvae of the mutant backgrounds (Supplementary Figure 7), suggesting that these mutant backgrounds are not impaired in motility. In all strains, the addition of water had no significant influence on which side of the chamber the larvae preferred (p>0.05, pairwise t-test compared to acclimation period). Larvae of all strains significantly preferred the side of the chamber with the food extract (p<0.05), and this preference was not significantly different across strains (p>0.05, 2-way ANOVA by strain and odor). Larvae of all three strains showed no significant positional preference for 1-octen-3-ol (p>0.05).

Discussion

In these experiments, we have expanded the toolbox of techniques for investigating a globally important

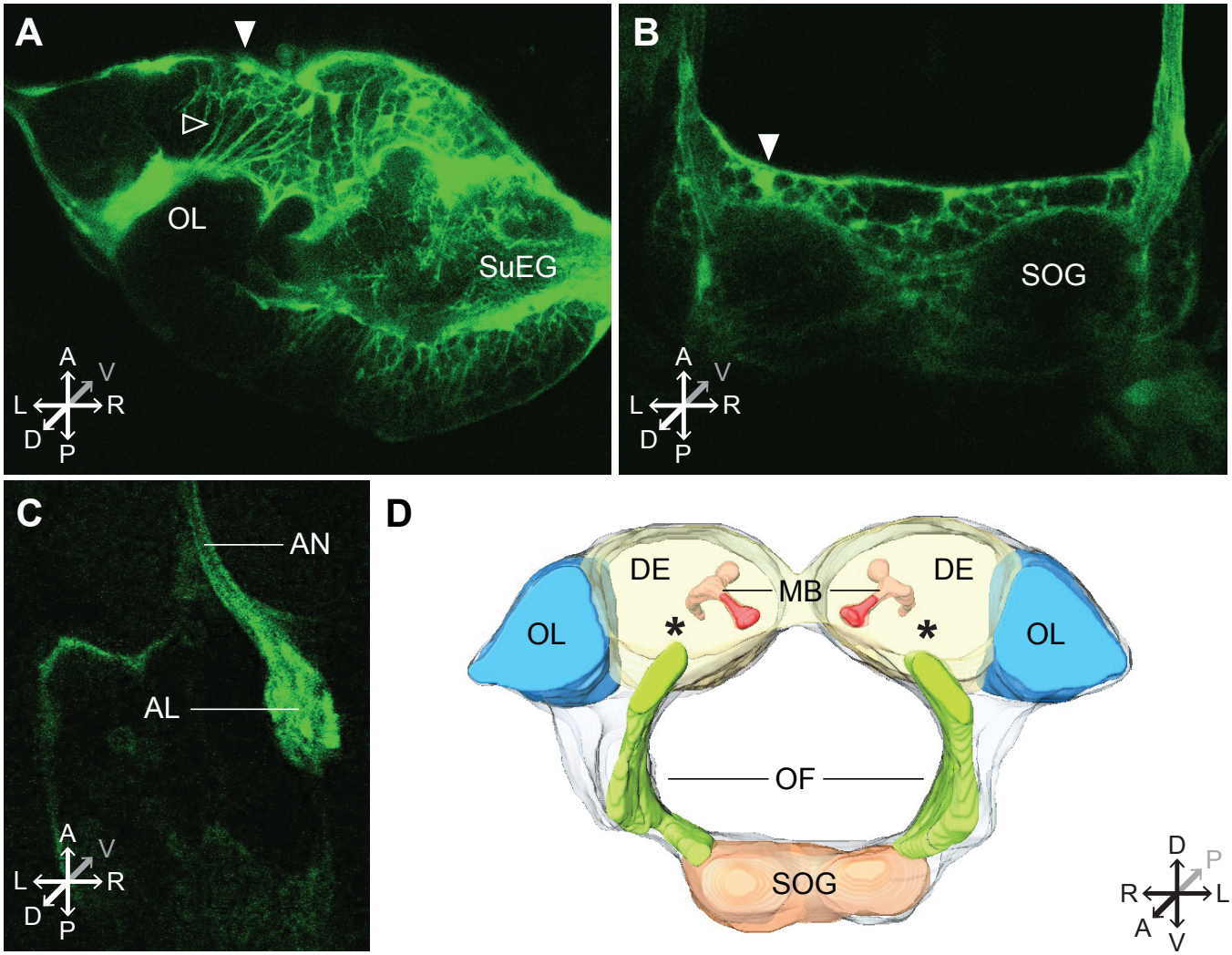

Figure 3: Two-photon imaging of *Ae. aegypti* larvae. Example images of 2-photon microscopy imaging of live *Ae. aegypti* larvae. Areas of interest included the optic lobe; OL, supra-esophageal ganglion; SuEG (upper DE, (**A**)), subesophageal ganglion; SOG (**B**), antennal nerve; AN and antennal lobe; AL. Cell bodies (labeled with a filled arrow), neuropil (labeled with an open arrow). (**C**). (**A; B:** L4 larvae with dorsal head cuticle removed. **C**: L2 larva imaged through transparent cuticle). **D:** Approximate 3D reconstruction of larval brain regions based on a confocal scan of the dissected larval brain. Asterisks indicate the rough location of the antennal lobe. Additional labeled brain regions include a general schematic of the optic lobe (OL), deutocerebrum (DE), mushroom bodies (MB), suboesophageal ganglion (SOG), and oesophageous foramen (OF) [46], Thermo Scientific Amira Software).

disease vector, *Ae. aegypti*, and explored the potential applications of these tools for investigating overarching questions in neurobiology such as sensory integration and information processing. Furthermore, our results from behavioral experiments suggest interesting avenues of future research in *Ae. aegypti* chemosensory processing. The robust expression of GCaMP6s in various mosquito tissues (Figure 1) allows quantification of stimulus-evoked responses in both motor and sensory systems, and in the adult and larval stages, including the adult antennae, adult maxillary palps, larval deutocerebrum (DE), and larval muscle (Figure 2, Supplementary Figure 1). This broad GCaMP6s expression allowed us to investigate both motor and sensory responses in *Ae. aegypti* larvae to an ecologically relevant panel of chemosensory stimuli. These cues elicited spatiotemporal patterns in GCaMP6/+/+ larval muscle and central nervous system (CNS), and revealed that key components of natural odors may be relevant across *Ae. aegypti* life stages (Supplementary Figure 1). In addition, monitoring both muscle and neural response allowed for visualization of stimuli specific relationships between the sensory and motor responses. Some stimuli elicited a neural response followed by a muscle output, however some demonstrated a neural response with no muscle output possibly due to a lack of behavior related to the stimulus. Also some stimuli generated a muscle response without the detection of a neural response possibly due to neural processing of that stimulus within a different region of the brain outside of our imaging plane. Further, when we crossed this GCaMP6s/+/+ line with *orco*5-/-

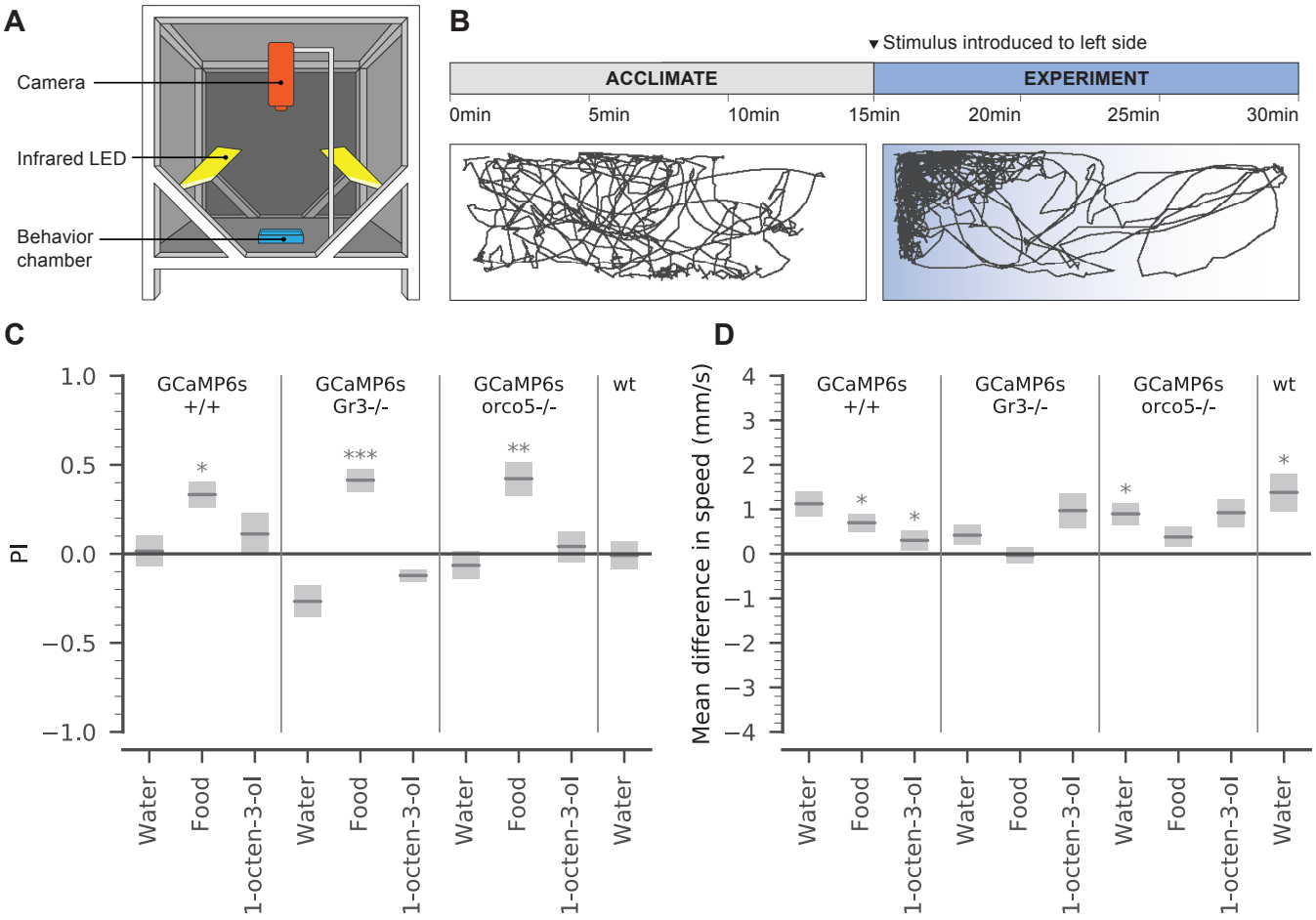

Figure 4: Behavioral analysis of stimulus-evoked responses in GCaMP6s/+/+, GCaMP6s/*orco*5-/-, GCaMP6s/Gr3-/-, and wt larvae. A: The dark experimental arena used for behavior testing. Animals were released individually into a custom 3D printed porcelain behavior chamber (blue), lit with infrared LED panels (yellow) and recorded with a Basler Scout Machine Vision Area Scan GigE camera (orange). **B:** In each experiment, the larva was allowed to acclimate in the arena for 15 minutes. Next, 100μL of one stimulus was introduced to the upper left side of the arena. In both stages, larval behavior was recorded at 2fps, and larval position in each frame was extracted using ImageJ and Python. This example trajectory shows the movement of a GCaMP6s/*orco*5-/- larva before and after the addition of 100μL food extract. **C:** Using these trajectories, we compared PI (defined as the proportion of time spent in the odor half of the arena minus the proportion of time spent in the non-odor half) across all larvae during the acclimation and experiment phase. Gray bars show mean ± SEM during the experiment phase. P-values: pairwise T-test comparing acclimation period to experiment period. *: p-value < 0.05, **: p-value < 0.01, ***: p-value < 0.001. GCaMP6s/+/+: water n=20; 1-octen-3-ol n=14; food extract n=20. GCaMP6s/*orco*5-/-: water n=24; 1-octen-3-ol n=16; food extract n=20. GCaMP6s/Gr3-/-: water n=16; 1-octen-3-ol n=17; food extract n=16; Liverpool wt: water n=19.

mutant to generate GCaMP6s/*orco*/-/-, we observed attenuation in these stimulus-evoked responses, particularly in response to known OR ligands (VUAA1 [47], 1-octen-3-ol [48], Supplementary Figure 4). By contrast, GCaMP6s/Gr3-/- larvae showed no significant impairment in response to any of the odorants tested, indicating that the heteromeric CO_2 receptor complex is not critical for the detection and response to these stimuli in the larval stage. This supports previous transcriptome work suggesting that the Gr3 receptor is expressed at very low levels in *Ae. aegypti* larvae [49]. Together, these results demonstrate the utility of these GCaMP6s/mutants for investigating the neural representation of chemosensory-mediated stimuli. Interestingly, our neuronal imaging showed no significant response to food odors, however muscle responses were observed. This may reflect the fact that our dorsal imaging plane did not extend into the ventral sub-oesophageal ganglion (SOG), which is innervated by sensory nerves from the mouthparts. Future experiments may look into imaging additional neuropils to detect any possible neural responses. Finally, our behavioral experiments contextualized some of these stimulus-evoked responses in a more naturalistic environment, revealing that ORs may act in parallel with other chemosensory channels during foraging behavior in *Ae. aegypti* larvae (Figure 4). Together, our combination of calcium imaging and behavior experiments highlights the importance of studying chemosensory behavior from multiple perspectives, and build on earlier work on the chemosensory repertoire [50, 51] and behaviors of mosquito larvae [52, 53]

to gain a more complete understanding of mosquito chemical ecology.

Although our GCaMP6s+/+ line has demonstrated the ability to generate useful insight in mosquito chemosensation, there remains a number of limitations that should be addressed if used for future research. Firstly, due to the nature of the *PUb* promoter, GCaMP6s expression can occur in all types of cells. The lack of specificity may make interpreting results and expression patterns difficult. For example, we observed muscle responses to VUAA1 (an olfactory receptor agonist) which likely represent activation of other sensory channels and subsequent downstream responses in the motor system rather than direct stimulus-evoked olfactory responses. Nevertheless, for the purpose of our experiments, the broad expression of GCaMP6s allowed for a general and holistic overview of a chemosensory responses to various stimuli. For future experiments that may want to utilize this strain to examine responses from specific cell types or neurons, it can be complemented with other neuronal recording techniques such as patch clamp to allow for the accurate quantification of specific cells while also the ability to generally visualize responses surrounding the cell of interest.

Conclusions

Our results highlight important avenues of future research in mosquito sensory processing. First, the mechanisms of chemosensory cue detection in *Ae. aegypti* larvae remains an open question. In terrestrial environments, long-range chemosensory stimuli are largely limited to volatile compounds with high vapor pressure at ambient temperatures [54]. However, *Ae. aegypti* larvae inhabit an aquatic environment that is a rich source of chemical signals far more varied in size, polarity, and structure, such as large proteins, amino acids, long hydrocarbon chains, and multi-molecular fragments of organic debris [55]. Interestingly, *Ae. aegypti* larvae express far fewer ORs than adults [50] and have a markedly smaller and physiologically less developed antennal lobes [35, 56]. Ae.aegypti larvae may rely on a more diverse assortment of IRs and GRs, in addition to ORs, to detect a wide range of water-borne chemicals relevant to behaviors such as foraging and predator avoidance [28, 57]. Characterization of the *Ae. aegypti* larval IRs and GRs may help identify chemical compounds that are most relevant to larval environments, and lend insight into the spectrum of larval chemical receptors. In addition to receptor-level chemical detection, the mechanism of chemosensory processing in the *Ae. aegypti* larval CNS is not well understood. Aquatic crustaceans integrate information from hydrodynamic detectors and two distinct types of chemosensory receptors within the CNS [58, 59], but it is unclear if *Ae. aegypti* sensory transduction follows this same model. From an evolutionary perspective, comparing the mechanism of *Ae. aegypti* larval olfaction to crustacean, amphibian, and fish models may also provide critical insight into the convergent evolution of aquatic chemosensation. Our *Ae. aegypti* GCaMP6/+/+ strain is of particular interest as it is, to our knowledge, the first example of GCaMP6 expression in an aquatic insect model.

Additionally, some odor components are shared among multiple ecologically relevant cues for mosquitoes, and neurobiological implications of these correlations are unclear. For example, 1-octen-3-ol is a component of both host odors [60] and microbial byproducts [61] that may function as food for larval mosquitoes. It is not unreasonable to hypothesize that there may be strong evolutionary selection on mosquito ORs that are beneficial in both life-history stages, and if so, identifying those chemicals that operate as both larval attractants and adult host cues may provide attractants that can be leveraged for mosquito control. Moreover, the mechanism of chemotaxis in *Ae. aegypti* larvae remains an open question. In other insect models such as *D. melanogaster*, larvae employ active sampling strategies to locate and navigate to food cues [62]. But it is unclear how *Ae. aegypti* larvae navigate chemosensory signals in an aquatic environment that is quite different in volume and turbidity from those experienced by *D. melanogaster*, or even *E. coli* [63] and *C. elegans* [64], which navigate chemosensory gradients at a significantly smaller scale. Quantitative modeling and further behavioral experiments may help better understand chemotaxis in an enigmatic aquatic insect model, and highlight interesting commonalities and differences in navigation strategy across different environments and spatial scales.

Generalizing further, the GCaMP6s/Gr3-/- and GCaMP6s/*orco*5-/- mutants could address critical gaps in our broader understanding of multisensory integration and sensorimotor responses, particularly in adult mosquitoes. Behavioral work in *Ae. aegypti* adults presents compelling evidence for the involvement of multisensory integration in host-seeking [65, 66]. However, little is known about the neural bases of these behaviors. In *D. melanogaster*, GCaMP6s imaging has revealed the functional basis of information convergence in higher-order brain areas [67, 68]. Future work with GCaMP6s/+/+ may similarly help decode the neural representations of multimodal host cues in mosquitoes, and provides motivation for the development of transcriptional control systems such as GAL4/UAS or the Q-system [69] for tissue-specific GCaMP6s expression. Importantly, we observed high GCaMP6s expression in both muscle and neuropil (Figure 2, Supplementary Figure 8). In *D. melanogaster*, concurrent analysis of neural response and motor output has facilitated

experiments in the integration of sensory processing and sensory-motor transformations [70–75]. By taking advantage of this simultaneous recording capacity in *Ae. aegypti*, additional experiments could investigate how these multisensory integration pathways mediate motor responses, and ultimately, determine behavioral decisions such as host choice and oviposition site preference. Finally, these GCaMP6s/+/+ mosquitoes and GCaMP6s/Gr3-/- and GCaMP6s/*orco*5-/- mutants could provide additional information and strategies for the control of disease-vector mosquitoes. Female mosquitoes may use olfactory indicators of larval habitat quality to choose oviposition sites [76]. A better understanding of chemosensory cues that elicit strong responses in larvae could help identify new attractants for use in oviposition traps, or oviposition deterrents for use in homes and outdoor water containers.

Materials and Methods

Insect rearing

Mosquitoes used in all experiments were derived from of the *Ae. aegypti* Liverpool strain, which was the source strain for the reference genome sequence. Mosquitoes were raised in incubators at 28°C with 70-80% relative humidity and a 12 hour light/dark cycle. Larvae were fed ground fish food (TetraMin Tropical Flakes, Tetra Werke, Melle, Germany) and adults were fed with 0.3M aqueous sucrose. Adult females were blood fed three to five days after eclosion using anesthetized mice. All animals were handled in accordance with the guide for the care and use of laboratory animals as recommended by the National Institutes of Health and supervised by the local Institutional Animal Care and Use Committee (IACUC).

Construct Assembly

To generate the GCaMP6s plasmid (plasmid sequence and DNA available for order at addgene ID# 106868), components were cloned into the *piggyBac* plasmid pBac-3xP3-dsRed [77] using Gibson assembly/EA cloning [78]. Specifically, pBac-3xP3-dsRed was digested with BstBI and SacII, and an attB site, amplified from a stock attB plasmid [79] with primers 997.C5 and 997.C6. The predicted *Ae. aegypti polyubiquitin* (*PUb*) promoter fragment [80] was amplified from *Ae. aegypti* genomic DNA using primers 997.C1 and 997.C2. While the GCaMP6s fragment [32] was amplified from vector pGP-CMV-GCaMP6s (Addgene plasmid #40753) using primers 997.C3 and 997.C4 and cloned in via EA cloning. The resulting plasmid was then digested with PacI and AvrII and the following fragments cloned in via EA cloning. P10 3'UTR [81] was amplified with primers 997.C7 and 997.C8 from vector pJFRC81-10XUAS-IVS-Syn21-GFP-p10 (Addgene plasmid 36432) and the OpIE-2 promoter region [82] amplified from vector pIZ/V5-His/CAT (Invitrogen) using primers 997.C9 and 997.C10. The plasmid was grown in strain JM109 chemically competent cells (Zymo Research #T3005) and isolated using Zyppy Plasmid Miniprep (Zymo Research #D4037) and maxiprep (Zymo Research #D4028) kits. The full plasmid sequence was verified using Source Bioscience Sanger sequencing services. A list of primer sequences used in the above construct assembly can be found in Supplementary Table 2.

Generation of GCaMP6s/+/+, GCaMP6s/Gr3-/-, and GCaMP6s/*orco*5-/- transgenic lines

GCaMP6s/+/+ mosquitoes were created by injecting 200 0-1hr pre-blastoderm stage embryos with a mixture of the GCaMP6s plasmid described above (200ng/μl) and a source of *piggyBac* transposase (phsp-Pbac, (200ng/μl)) [83–86]. Embryonic collection and microinjections were largely performed following previously established procedures [77, 87]. Injected embryos were hatched in deoxygenated water and surviving adults were placed into cages. Adult G0 females were allowed a blood-meal 4 days after eclosion. Following general rearing procedures described above, 3000 G1 larvae were screened for expected fluorescent markers, OpIE-2-dsRed, and *PUb*-GCaMP6s (Figure 1C, Supplementary Figure 6D). Larvae with positive fluorescent signals were collected under a fluorescent stereomicroscope (Leica M165FC). All positive larvae collected produced consistent *PUb*-GCaMP6s and OpIE-2-dsRed expression patterns hinting that these larvae contained the same insertion. Only one transgenic line was found. To strengthen our belief that this line was produced with a single chromosomal insertion, single individuals from each of the lines were backcrossed for four generations to our wild-type stock. Mendelian transmission ratios for each generation were measured. In all cases, we observed a 50% transmission ratio in each generation, indicating that our strain likely represented an insertion on a single chromosome. To obtain a nearly complete homozygous line, our GCaMP6s line was screened and selected for at least 20 generations. For each generation, wild-type individuals were removed and the remaining GCaMP6s+/+ individuals were mated together until the offspring from a colony reached nearly 99% GCaMP6s+/+ when screened. To obtain the GCaMP6s/*orco*5-/- homozygous line, GCaMP6s/+/+ (♂) was crossed with *orco*5-/- (♀), then G1 individuals (♂) with the GCaMP6s phenotype were backcrossed with *orco*5-/- individuals (♀) for at least 8 generations as single mosquito pairwise matings. Sanger sequencing was utilized to confirm GCaMP6s/*orco*5-/- homozygosity (Supplementary Figure 6A,B). Following, single pair matings between GCaMP6s/*orco*5-/- individuals were

conducted and screened for 100% inheritance of transgenic markers thus creating a line fully homozygous for *orco*5-/- and nearly homozygous for GCaMP6s. To obtain the GCaMP6s/Gr3-/- mutant homozygous line, GCaMP6s/+/+ (♂) was crossed with GR3-/- (♀, labeled with a CFP marker), then continually selected for individuals with correct markers (dsRed, GCaMP6s, and CFP) . Furthermore, single mosquito pairwise crosses were performed for at least 8 generations (Supplementary Figure 6C,D). To confirm homozygosity, single individuals starting from G8 were mated to wild-type. The resulting progeny was screened for 100% inheritance of the transgenic markers.The transgenic GCaMP6s/+/+ line has been deposited at BEI MR4 Resources (Accession # still waiting for acceptance of strain from BEI MR4).

Genetics and Molecular Characterization of Insertion Site

To characterize the insertion site of GCaMP6s, we modified an inverse PCR protocol described previously [77, 88]. Briefly, genomic DNA (gDNA) was extracted from 10 *Ae. aegypti* fourth instar larvae using the DNeasy Blood & Tissue Kit (Qiagen, Hilden, Germany) in accordance with the manufacturer's protocol. The eluted DNA was diluted, and two separate restriction digests were performed to characterize both the 5' and 3' ends using Sau3AI (5' reaction) or HinP1I (3' reaction) restriction enzymes. A ligation step using NEB T4 DNA Ligase was then performed on the restriction digest products to promote circularization of digested DNA. Two rounds of PCR were performed using primers 991.5F1, 991.5R1, 991.5F2, 991.5R2, 991.3F1, 991.3R1, 991.3F2 and 991.3R2 (with their corresponding restriction digest reaction) and sequence confirmation (1018) are listed in Supplementary Table 3. PCR products from the second round of PCR were cleaned using the MinElute PCR Purification Kit (Qiagen) in accordance with the manufacturer's protocol, and subsequently sequenced by Sanger sequencing (Source BioScience). Both the location and orientation (chromosome 2, with the flanking genomic regions for the 5' and 3' *piggyBac* ends positioned at the genomic loci 285,175,805-285,176,289 and 285,175,275-285,175,803, respectively) were confirmed by PCR using primers designed from the mapped genomic region in combination with both 3' *piggyBac* end forward primers. Sequencing data was then blasted to the AaegL5.0 reference genome. Alignment of the sequencing data was performed using EMBOSSWater (https://www.edi.ac.uk/Tools/psa/emboss_water/).

Odor-Evoked Confocal Imaging of Non-water Submerged Larvae/Adults

For larval imaging of GCaMP6s/+/+ calcium transients, using a slightly moistened fine tip paint brush, larva were placed ventral side down on double-sided tape adhered to a clean glass slide. Due to the larvae being exposed to air rather than its normal aquatic environment, to prevent dessication a moistened fine tip paint brush was used to periodically wet the larvae without affecting the sticky-tape adhesive. Imaging was focused on the full body and head. For adult imaging, mosquitoes were placed laterally on double-sided tape after being placed on ice for approximately 10 minutes. Antennae and proboscis were immobilized by using an artist brush and gently brushing the respective appendages onto the double sided tape. For both larvae and adults, a minimum of 15 seconds of inactivity was first captured recording the specimen. Recording continued for an additional 35 seconds. Images and recordings were taken using an Inverted Confocal microscope (Leica SP5).

Odor-Evoked Confocal Imaging of Larvae in Tethered-Swimming Assay

To immobilize each larval head, while allowing for movement of the larval body, less than one microliter of clear Aron Alpha high strength rapid bonding adhesive (Catalog # 72588) was applied to a Lab-Tek II chambered #1.5 German coverglass system composed of transparent borosilicate glass (Thermo Catalog #155382). Immediately following the application of the adhesive, the ventral side of a single larva was placed directly onto the adhesive, rapidly bonding the larval head to the coverglass in less than 1 minute. The chamber was then filled with 500μl of deionized water to fully submerge the larvae, while allowing for the larva's respiratory siphon to meet the surface of the water. Before any recordings, the larvae was allowed to rest for 12 hours to assimilate to the preparation. Recordings of stimulus-induced fluorescent responses were taken around the head. 100μl of 5% solution of odorants were injected into the chamber after 15 seconds of inactivity in larval brains. Activity was measured from 15 seconds prior to addition of stimulus to 90 seconds after. Following each trial, stimuli were removed by draining the water in chamber, gently flushing the larvae and chamber three times, and refilling with fresh deionized water. The same larva was used for multiple stimulants.

Selection and Preparation of Odorants

Stimulants were chosen from a list of known olfactory and/or gustatory stimuli of both *D. melanogaster* and adult *Ae. aegypti* [26, 27, 36–41]. These included ethyl acetate (Sigma Cat #319902), lactic acid (Sigma Cat #L1750), 1-octen-3-ol (Sigma Cat #O5284), butylamine (Sigma Cat#471305), VUAA1 (Vitas-M Cat#STK047588), sucrose (Sigma Cat#S0389), lobeline (Sigma Cat#141879), glutamate (Sigma Cat#49621), and water (negative control). All stock

solutions of odors were prepared as 5% solutions in water, with a final bioassayed concentration of $6\times10^{-}5$M. Food extract for larval experiments was prepared by mixing 0.5% fish food (Hikari Tropic First Bites: Petco, San Diego, CA, USA) in milliQ water. The solution was allowed to sit for one hour, then filtered through a 0.2μm sterile filter (#28145-477, VWR International, Radnor, PA, USA) to remove solid particulates. 1-octen-3-ol used in behavior experiments was prepared as a 10^{-4}M solution in water, based on preliminary experiments testing several odor concentrations (data not shown).

Imaging Data Analyses

To quantify fluorescence responses to various stimuli, Leica LAS X Core Offline version 3.3.0 software was used to export raw fluorescence data from relevant ROIs. Further analysis was done using GraphPad Prism and RStudio. To account for differences in fluorescence intensity that differed between each larva, raw fluorescence was normalized using $\Delta F/F0 = (F-F0)/F0$ where F is mean intensity of fluorescence at a certain time point and F0 is the baseline level of fluorescence using the average fluorescence intensity from the first 15 seconds of the recording without stimulation [89]. To determine the significance of responses to tested stimuli, a Welch's t-test was conducted between the max $\Delta F/F0$ of multiple replicates treated with one stimulant to that of water. Responses to each stimulant were compared to that of water.. To compare the differences between GCaMP6s/+/+, GCaMP6s/*orco*5-/-, and GCaMP6s/Gr3-/- calcium responses to our simulus panel, a Welch's t-test was conducted comparing the max $\Delta F/F0$ values between two larval backgrounds in response to the same stimulus. Importantly, due to the methodology of our larval imaging assay, the larval abdomen would occasionally be viewable behind the ROI. To confirm that this interference does not create any significant artifacts while measuring raw fluorescence, raw fluorescence 2 seconds before and during interference were compared and no significant interference was detected ($t = 0.237$, p-value = 0.8158). Additionally, to confirm that our data was not confounded by differing base levels of expression due to differences between the wild-type and mutant strains, we performed an ANOVA comparing the average base levels of fluorescence measured prior to the addition of each stimulus between each strain. When compared, the mean expressions were not significantly different (p-value = 0.3212) hence background extraneous differences between our wild-type and mutant background strains may be negligible. In two-photon imaging experiments, a larva was transferred to a Peltier-cooled holder that allows for the head to be fixed to the stage using ultraviolet glue. GCaMP6s expression was imaged at 2Hz using the Prairie Ultima IV two-photon excitation microscope (Prairie Technologies) and Ti-Sapphire laser (Chameleon Ultra; Coherent).

Muscle/DE Latency Analysis

Temporal differences between muscle and DE responses were calculated by subtracting DE timepoints at 50% of maximum $\Delta F/F0$ of the first peak following the addition of stimulus from that of muscles (Figure 2B,C). Recordings with both DE and muscles not displaying clear peaks in response to stimulants as well as latency values greater than 15 were treated as NA. Latency values were converted into ordinal values of 4 categories: NA, negative, 0 (no difference), and positive. A Mann-Whitney U test between latency values from each stimulus and that of water was used to determine significant differences.

Free-Swimming Larval Behavior Experiments

Larvae used for free-swimming behavior experiments were reared on Hikari Tropic First Bites (Petco, San Diego, CA, USA) under a 12 hour light/dark cycle. One day before the experiment, 5-day old larvae were isolated into individual Falcon^{TM} 50mL conical centrifuge tubes (Thermo Fisher Scientific, Waltham, MA, USA) containing ∼15mL milliQ water and no food. During the experiment, individual larvae were introduced to the center of a dark behavior arena developed for assaying mosquito larval chemosensory preference (Figure 4). No light was detected inside the arena under experimental conditions (LI-250A Lightmeter, instantaneous measurements, sensitive up to 0.01μmol $s^{-1}m^{-2}$ per μA. LI-COR Biosciences #Q40129). Animals were allowed to acclimate for 15 minutes in a custom 3D printed porcelain behavior chamber (ID #XWEEPACQA, Shapeways, New York, NY, USA) containing 20mL of milliQ water. 100μl of a chemical stimulus was then pipetted into the left side of the arena. Larvae were tested only during the day phase of the diurnal light cycle. Larvae were housed individually until eclosion to determine sex, and animals that died before eclosion were omitted from analyses.

Larval movement was recorded at 2fps for the 15 minute acclimation period, as well as the 15 minute experiment following stimulus introduction, using a Basler Scout Machine Vision Area Scan GigE camera (scA 1000-30gm, Ahrensburg, Germany) and Basler pylonViewer Windows software. Larval trajectories were analyzed using ImageJ Fiji [90] and custom software written in Python (http://www.python.org): Multitracker by Floris van Breugel (https://github.com/florisvb/multi_tracker), as well as a batch-processing Multitracker add-on, Multivideo Multitracker by Eleanor Lutz

(https://github.com/eleanorlutz/multivideo_multitracker) (Figure 4). In brief, videos were cropped and contrast-enhanced in ImageJ Fiji. Larval position was extracted using frame-by-frame subtraction in Multitracker. Trajectories were manually inspected in the Multitracker GUI, where missing data points were added and extraneous tracked objects removed. We then converted trajectory position from pixel values to mm using the ratio of the known width of the behavior container. Finally, we calculated the instantaneous speed of the larva, in mm, for each frame. Using these position and speed values, we then calculated the mean instantaneous speed (mm s^{-1}) and preference index (PI; proportion of time spent in the odor half - proportion of time spent in the non-odor half).

Fitness Experiments

To determine the impact our GCaMP6s transgene insertion on mosquito fitness, a series of fitness experiments comparing the female fecundity, male fertility, larval hatchability, and duration between larval and pupal stages between our GCaMP6s+/+ line and the wild-type line the line was originally derived from. Female fecundity was determined by mating 100 virgin females of both the GCaMP6s+/+ and wild-type line to 50 wild-type males. Females were allowed to mate for 3 days after eclosion and were given access to anesthetized mice for 15 minutes on the 5th and 6th day after eclosion. Two days after blood feeding, single bloodfed females were individually captured into vials lined with moistened filter paper. Non-bloodfed females were not collected. Bloodfed females were allowed 3 days in the vials to oviposit their eggs and were removed on the third day. Oviposited eggs were then counted. To determine male fertility, 25 males of both strains were mated to 100 virgin wild-type females and the same procedure for calculating female fecundity was used. To test egg hatching rate, eggs from single pair crosses of GCaMP6s+/+ (♀) × +/+ (♂) and +/+ (♀) × +/+ (♂) were counted and hatched 4 days after oviposition. Emerged larvae were then counted at the L2 stage. To calculate larvae-to-pupae development time, larvae of both strains were hatched and separate into 5 pans filled with 2.5L of water with 100 larvae per pan. The number of pupae emerged was counted every day post-hatching to estimate the number of days for larval developmental time.

Immunofluorescence and GCaMP6s Expression

To determine GCaMP6s' pattern of expression, whole larval brains were stained following a previously published method [69]. Brains were either stained with a mixture of rabbit anti-GFP (1:500, abcam) and either mouse anti-alpha tubulin (1:100, DHSB) or mouse anti-GS (1:200, BD Bio) as primary antibodies. Secondary antibodies used were Alexa-488 donkey anti-rabbit and Alexa-555 donkey anti-mouse (ThermoFisher). Images of stained brains were taken using a Leica SP8 confocal microscope (Supplementary Figure S3). In addition, to examine the baseline fluorescence in different chemosensory cell types, processes (glia) and the lateral and medial cell bodies were recorded before and during odor stimulation and image planes were analyzed using k-means clustering. Based on this analysis, the ROI cell type clusters could be distinguished based on cell size alone, rather than differences in fluorescence (Supplementary Figure S2).

Statistical Analysis

To compare response differences between individuals that differed by either genetic background or stimulus, we used a Welch's t-test due to the unequal sample size. To compare latency between neural and muscle responses, we used a Mann Whitney U test which allows for analysis of non normalized distributions as well as ordinal data.A pairwise t-test was used to compare larval behavior during the acclimation phase of the experiment to the odor stimulation phase (Figure 4). A 1-way ANOVA was used to compare overall behavioral differences across strains (Supplementary Figure 7).

Funding

This work was supported in part by NIH grants 1R21AI123937 to O.S.A, and 1RO1DCO13693-04, BMCB-D-18-00484 to J.A.R; National Science Foundation grants IOS-1354159 to J.A.R and DGE-1256082 to E.K.L; Air Force Office of Sponsored Research under grant FA9550-16-1-0167 to J.A.R; and the University of Washington Robin Mariko Harris Award to E.K.L, and the UCSD School of Medicine Microscopy Core which is supported by a NINDS P30 grant (NS047101).

Author Contributions

O.S.A and J.A.R conceived and designed the experiments. J.S., E.K.L., T..Y, M.L., M.B., K.T., R.A., and A.B. performed molecular, behavioral and genetic experiments. All authors contributed to the writing, analyzed the data, and approved the final manuscript.

Acknowledgements

We thank Christian Bowman for help with inverse PCR, Tjinder Grewal for assistance with larval behavior assays, Gabriella Wolff for her contribution of confocal images for Figure 3, the UCSD School of Medicine Microscopy Core, and David Kosman for his advice on immunostaining and confocal imaging for Supplementary Figure 3.

References

[1] S. C. Weaver, C. Charlier, N. Vasilakis, and M. Lecuit, "Zika, chikungunya, and other emerging vector-borne viral diseases," *Annu. Rev. Med.*, Aug. 2017.

[2] A. D. T. Barrett and S. Higgs, "Yellow fever: A disease that has yet to be conquered," *Annu. Rev. Entomol.*, vol. 52, pp. 209–229, 2007.

[3] S. B. Halstead, "Dengue virus-mosquito interactions," *Annu. Rev. Entomol.*, vol. 53, pp. 273–291, 2008.

[4] S. C. Weaver and A. D. T. Barrett, "Transmission cycles, host range, evolution and emergence of arboviral disease," *Nat. Rev. Microbiol.*, vol. 2, pp. 789–801, Oct. 2004.

[5] S. C. Weaver and W. K. Reisen, "Present and future arboviral threats," *Antiviral Res.*, vol. 85, pp. 328–345, Feb. 2010.

[6] A. F. Harris, A. R. McKemey, D. Nimmo, Z. Curtis, I. Black, S. A. Morgan, M. N. Oviedo, R. Lacroix, N. Naish, N. I. Morrison, A. Collado, J. Stevenson, S. Scaife, T. Dafa'alla, G. Fu, C. Phillips, A. Miles, N. Raduan, N. Kelly, C. Beech, C. A. Donnelly, W. D. Petrie, and L. Alphey, "Successful suppression of a field mosquito population by sustained release of engineered male mosquitoes," *Nat. Biotechnol.*, vol. 30, pp. 828–830, Sept. 2012.

[7] C. J. McMeniman, R. V. Lane, B. N. Cass, A. W. C. Fong, M. Sidhu, Y.-F. Wang, and S. L. O'Neill, "Stable introduction of a life-shortening *Wolbachia* infection into the mosquito *Aedes aegypti*," *Science*, vol. 323, pp. 141–144, Jan. 2009.

[8] T. Walker, P. H. Johnson, L. A. Moreira, I. Iturbe-Ormaetxe, F. D. Frentiu, C. J. McMeniman, Y. S. Leong, Y. Dong, J. Axford, P. Kriesner, A. L. Lloyd, S. A. Ritchie, S. L. O'Neill, and A. A. Hoffmann, "The *wMel Wolbachia* strain blocks dengue and invades caged *Aedes aegypti* populations," *Nature*, vol. 476, pp. 450–453, Aug. 2011.

[9] S. P. Sinkins, "*Wolbachia* and cytoplasmic incompatibility in mosquitoes," *Insect Biochem. Mol. Biol.*, vol. 34, pp. 723–729, July 2004.

[10] J. Champer, A. Buchman, and O. S. Akbari, "Cheating evolution: Engineering gene drives to manipulate the fate of wild populations," *Nat. Rev. Genet.*, vol. 17, pp. 146–159, Mar. 2016.

[11] J. M. Marshall and O. S. Akbari, "Can CRISPR-based gene drive be confined in the wild? A question for molecular and population biology," *ACS Chem. Biol.*, vol. 13, pp. 424–430, Feb. 2018.

[12] J. M. Marshall and O. S. Akbari, "Gene drive strategies for population replacement," in *Genetic Control of Malaria and Dengue*, pp. 169–200, 2016.

[13] N. P. Kandul, J. Liu, H. M. Sanchez, S. L. Wu, J. M. Marshall, and O. S. Akbari, "Transforming insect population control with precision guided sterile males," 2018.

[14] M. Li, T. Yang, N. P. Kandul, M. Bui, S. Gamez, R. Raban, J. Bennett, H. M. Sánchez C., G. C. Lanzaro, H. Schmidt, Y. Lee, J. M. Marshall, and O. S. Akbari, "Development of a confinable gene-drive system in the human disease vector, *Aedes aegypti*," 2019.

[15] D. Maoz, T. Ward, M. Samuel, P. Müller, S. Runge-Ranzinger, J. Toledo, R. Boyce, R. Velayudhan, and O. Horstick, "Community effectiveness of pyriproxyfen as a dengue vector control method: A systematic review," *PLoS Negl. Trop. Dis.*, vol. 11, no. 7, p. e0005651, 2017.

[16] C. L. Moyes, J. Vontas, A. J. Martins, L. C. Ng, S. Y. Koou, I. Dusfour, K. Raghavendra, J. Pinto, V. Corbel, J.-P. David, and D. Weetman, "Contemporary status of insecticide resistance in the major *Aedes* vectors of arboviruses infecting humans," *PLoS Negl. Trop. Dis.*, vol. 11, p. e0005625, July 2017.

[17] A. W. E. Franz, R. J. Clem, and A. L. Passarelli, "Novel genetic and molecular tools for the investigation and control of dengue virus transmission by mosquitoes," *Curr. Trop. Med. Rep.*, vol. 1, pp. 21–31, Mar. 2014.

[18] C. Montell and L. J. Zwiebel, "Chapter ten — Mosquito sensory systems," in *Advances in Insect Physiology* (A. S. Raikhel, ed.), vol. 51, pp. 293–328, Academic Press, Jan. 2016.

[19] E. K. Lutz, C. Lahondère, C. Vinauger, and J. A. Riffell, "Olfactory learning and chemical ecology of olfaction in disease vector mosquitoes: A life history perspective," *Curr. Opin. Insect Sci.*, vol. 20, pp. 75–83, Apr. 2017.

[20] Z. Syed, "Chemical ecology and olfaction in arthropod vectors of diseases," *Curr. Opin. Insect Sci.*, vol. 10, pp. 83–89, Aug. 2015.

[21] C. J. McMeniman, R. A. Corfas, B. J. Matthews, S. A. Ritchie, and L. B. Vosshall, "Multimodal integration of carbon dioxide and other sensory cues drives mosquito attraction to humans," *Cell*, vol. 156, pp. 1060–1071, Feb. 2014.

[22] M. DeGennaro, C. S. McBride, L. Seeholzer, T. Nakagawa, E. J. Dennis, C. Goldman, N. Jasinskiene, A. A. James, and L. B. Vosshall, "*Orco* mutant mosquitoes lose strong preference for humans and are not repelled by volatile DEET," *Nature*, vol. 498, no. 7455, pp. 487–491, 2013.

[23] F. van Breugel, J. Riffell, A. Fairhall, and M. H. Dickinson, "Mosquitoes use vision to associate odor plumes with thermal targets," *Curr. Biol.*, vol. 25, pp. 2123–2129, Aug. 2015.

[24] J. S. Kennedy, "The visual responses of flying mosquitoes," *Proc. Zool. Soc. Lond.*, vol. A109, no. 4, pp. 221–242, 2009.

[25] C. Vinauger, C. Lahondère, G. H. Wolff, L. T. Locke, J. E. Liaw, J. Z. Parrish, O. S. Akbari, M. H. Dickinson, and J. A. Riffell, "Modulation of host learning in *Aedes aegypti* mosquitoes," *Curr. Biol.*, vol. 28, pp. 333–344.e8, Feb. 2018.

[26] Y. Xia, G. Wang, D. Buscariollo, R. J. Pitts, H. Wenger, and L. J. Zwiebel, "The molecular and cellular basis of olfactory-driven behavior in *Anopheles gambiae* larvae," *Proc. Natl. Acad. Sci.*, vol. 105, pp. 6433–6438, Apr. 2008.

[27] C. Liu, R. Jason Pitts, J. D. Bohbot, P. L. Jones, G. Wang, and L. J. Zwiebel, "Distinct olfactory signaling mechanisms in the malaria vector mosquito *Anopheles gambiae*," *PLoS Biol.*, vol. 8, no. 8, p. e1000467, 2010.

[28] S. Rickard Christophers, *Aedes aegypti (L.) the yellow fever mosquito: Its life history, bionomics and structure.* Cambridge University Press, 1960.

[29] M. Ghaninia, M. Larsson, B. S. Hansson, and R. Ignell, "Natural odor ligands for olfactory receptor neurons of the female mosquito *Aedes aegypti*: Use of gas chromatography-linked single sensillum recordings," *J. Exp. Biol.*, vol. 211, pp. 3020–3027, Sept. 2008.

[30] D. F. Moffett, U. Jagadeshwaran, Z. Wang, H. M. Davis, H. Onken, and G. G. Goss, "Signaling by intracellular Ca2 and H in larval mosquito (*Aedes aegypti*) midgut epithelium in response to serosal serotonin and lumen pH," *J. Insect Physiol.*, vol. 58, no. 4, pp. 506–512, 2012.

[31] G. T. Macleod, M. Hegström-Wojtowicz, M. P. Charlton, and H. L. Atwood, "Fast calcium signals in *Drosophila* motor neuron terminals," *J. Neurophysiol.*, vol. 88, pp. 2659–2663, Nov. 2002.

[32] T.-W. Chen, T. J. Wardill, Y. Sun, S. R. Pulver, S. L. Renninger, A. Baohan, E. R. Schreiter, R. A. Kerr, M. B. Orger, V. Jayaraman, L. L. Looger, K. Svoboda, and D. S. Kim, "Ultrasensitive fluorescent proteins for imaging neuronal activity," *Nature*, vol. 499, pp. 295–300, July 2013.

[33] M. A. E. Anderson, T. L. Gross, K. M. Myles, and Z. N. Adelman, "Validation of novel promoter sequences derived from two endogenous ubiquitin genes in transgenic *Aedes aegypti*," *Insect Mol. Biol.*, vol. 19, pp. 441–449, Aug. 2010.

[34] O. S. Akbari, I. Antoshechkin, H. Amrhein, B. Williams, R. Diloreto, J. Sandler, and B. A. Hay, "The developmental transcriptome of the mosquito *Aedes aegypti*, an invasive species and major arbovirus vector," *G3*, vol. 3, pp. 1493–1509, Sept. 2013.

[35] K. Mysore, S. Flister, P. Müller, V. Rodrigues, and H. Reichert, "Brain development in the yellow fever mosquito *Aedes aegypti*: a comparative immunocytochemical analysis using cross-reacting antibodies from *Drosophila melanogaster*," *Dev. Genes Evol.*, vol. 221, pp. 281–296, Dec. 2011.

[36] R. W. Taylor, I. M. Romaine, C. Liu, P. Murthi, P. L. Jones, A. G. Waterson, G. A. Sulikowski, and L. J. Zwiebel, "Structure-activity relationship of a broad-spectrum insect odorant receptor agonist," *ACS Chem. Biol.*, vol. 7, no. 10, pp. 1647–1652, 2012.

[37] G. V. P. Reddy and A. Guerrero, "Interactions of insect pheromones and plant semiochemicals," *Trends Plant Sci.*, vol. 9, no. 5, pp. 253–261, 2004.

[38] F. Acree, R. B. Turner, H. K. Gouck, M. Beroza, and N. Smith, "L-lactic acid: A mosquito attractant isolated from humans," *Science*, vol. 161, no. 3848, pp. 1346–1347, 1968.

[39] D. F. Hoel, D. L. Kline, S. A. Allan, and A. Grant, "Evaluation of carbon dioxide, 1-octen-3-ol, and lactic acid as baits in mosquito magnet pro traps for *Aedes albopictus* in north central Florida," *J. Am. Mosq. Control Assoc.*, vol. 23, pp. 11–17, Mar. 2007.

[40] P. V. Gonzalez, P. A. González Audino, and H. M. Masuh, "Behavioral response of *Aedes aegypti* (diptera: *Culicidae*) larvae to synthetic and natural attractants and repellents," *J. Med. Entomol.*, vol. 52, pp. 1315–1321, Nov. 2015.

[41] E. G. Freeman, Z. Wisotsky, and A. Dahanukar, "Detection of sweet tastants by a conserved group of insect gustatory receptors," *Proc. Natl. Acad. Sci.*, vol. 111, pp. 1598–1603, Jan. 2014.

[42] C. Montell, "A taste of the *Drosophila* gustatory receptors," *Curr. Opin. Neurobiol.*, vol. 19, no. 4, pp. 345–353, 2009.

[43] Y. Xia, G. Wang, D. Buscariollo, R. J. Pitts, H. Wenger, and L. J. Zwiebel, "The molecular and cellular basis of olfactory-driven behavior in *Anopheles gambiae* larvae," *Proc. Natl. Acad. Sci.*, vol. 105, pp. 6433–6438, Apr. 2008.

[44] G. S. Chitarra, T. Abee, F. M. Rombouts, M. A. Posthumus, and J. Dijksterhuis, "Germination of *Penicillium paneum* conidia is regulated by 1-octen-3-ol, a volatile self-inhibitor," *Appl. Environ. Microbiol.*, vol. 70, pp. 2823–2829, May 2004.

[45] I. V. F. Broek and C. J. Otter, "Odour sensitivity of antennal olfactory cells underlying grooved pegs of *Anopheles gambiae s.s.* and *An. quadriannulatus*," *Entomol. Exp. Appl.*, vol. 96, no. 2, pp. 167–175, 2000.

[46] K. Mysore, S. Flister, P. Müller, V. Rodrigues, and H. Reichert, "Brain development in the yellow fever mosquito *Aedes aegypti*: A comparative immunocytochemical analysis using cross-reacting antibodies from *Drosophila melanogaster*," *Dev. Genes Evol.*, vol. 221, pp. 281–296, Dec. 2011.

[47] B. N. Kumar, R. W. Taylor, G. M. Pask, L. J. Zwiebel, R. D. Newcomb, and D. L. Christie, "A conserved aspartic acid is important for agonist (VUAA1) and odorant/tuning receptor-dependent activation of the insect odorant co-receptor (*Orco*)," *PLoS One*, vol. 8, p. e70218, July 2013.

[48] J. D. Bohbot and J. C. Dickens, "Characterization of an enantioselective odorant receptor in the yellow fever mosquito *Aedes aegypti*," *PLoS One*, vol. 4, p. e7032, Sept. 2009.

[49] C. N. G. Erdelyan, T. H. Mahood, T. S. Y. Bader, and S. Whyard, "Functional validation of the carbon dioxide receptor genes in *Aedes aegypti* mosquitoes using RNA interference," *Insect Mol. Biol.*, vol. 21, pp. 119–127, Feb. 2012.

[50] J. Bohbot, R. J. Pitts, H.-W. Kwon, M. Rützler, H. M. Robertson, and L. J. Zwiebel, "Molecular characterization of the *Aedes aegypti* odorant receptor gene family," *Insect Mol. Biol.*, vol. 16, pp. 525–537, Oct. 2007.

[51] Y. Xia, G. Wang, D. Buscariollo, R. J. Pitts, H. Wenger, and L. J. Zwiebel, "The molecular and cellular basis of olfactory-driven behavior in *Anopheles gambiae* larvae," *Proc. Natl. Acad. Sci.*, vol. 105, pp. 6433–6438, Apr. 2008.

[52] P. V. Gonzalez, P. A. González Audino, and H. M. Masuh, "Behavioral response of *Aedes aegypti* (diptera: *Culicidae*) larvae to synthetic and natural attractants and repellents," *J. Med. Entomol.*, vol. 52, pp. 1315–1321, Nov. 2015.

[53] R. W. Merritt, R. H. Dadd, and E. D. Walker, "Feeding behavior, natural food, and nutritional relationships of larval mosquitoes," *Annu. Rev. Entomol.*, vol. 37, pp. 349–376, 1992.

[54] J. A. Riffell, L. Abrell, and J. G. Hildebrand, "Physical processes and real-time chemical measurement of the insect olfactory environment," *J. Chem. Ecol.*, vol. 34, pp. 837–853, July 2008.

[55] R. L. Burks and D. M. Lodge, "Cued in: Advances and opportunities in freshwater chemical ecology," *J. Chem. Ecol.*, vol. 28, pp. 1901–1917, Oct. 2002.

[56] K. Mysore, E. M. Flannery, M. Tomchaney, D. W. Severson, and M. Duman-Scheel, "Disruption of *Aedes aegypti* olfactory system development through chitosan/siRNA nanoparticle targeting of semaphorin-1a," *PLoS Negl. Trop. Dis.*, vol. 7, p. e2215, May 2013.

[57] J. G. Crespo, "A review of chemosensation and related behavior in aquatic insects," *J. Insect Sci.*, vol. 11, p. 62, 2011.

[58] D. Mellon, Jr, "Combining dissimilar senses: Central processing of hydrodynamic and chemosensory inputs in aquatic crustaceans," *Biol. Bull.*, vol. 213, pp. 1–11, Aug. 2007.

[59] M. Thiel and T. Breithaupt, "Research challenges for the twenty-first century," in *Chemical Communication in Crustaceans*, pp. 3–22, New York, NY: Springer New York, 2011.

[60] W. Takken and D. L. Kline, "Carbon dioxide and 1-octen-3-ol as mosquito attractants," *J. Am. Mosq. Control Assoc.*, vol. 5, pp. 311–316, Sept. 1989.

[61] G. Fischer and W. Dott, "Relevance of airborne fungi and their secondary metabolites for environmental, occupational and indoor hygiene," *Arch. Microbiol.*, vol. 179, pp. 75–82, Jan. 2003.

[62] A. Gomez-Marin, G. J. Stephens, and M. Louis, "Active sampling and decision making in *Drosophila* chemotaxis," *Nat. Commun.*, vol. 2, p. 441, Aug. 2011.

[63] V. Sourjik and N. S. Wingreen, "Responding to chemical gradients: Bacterial chemotaxis," *Curr. Opin. Cell Biol.*, vol. 24, pp. 262–268, Apr. 2012.

[64] M. A. Hilliard, C. I. Bargmann, and P. Bazzicalupo, "*C. elegans* responds to chemical repellents by integrating sensory inputs from the head and the tail," *Curr. Biol.*, vol. 12, pp. 730–734, Apr. 2002.

[65] C. J. McMeniman, R. A. Corfas, B. J. Matthews, S. A. Ritchie, and L. B. Vosshall, "Multimodal integration of carbon dioxide and other sensory cues drives mosquito attraction to humans," *Cell*, vol. 156, pp. 1060–1071, Feb. 2014.

[66] F. van Breugel, J. Riffell, A. Fairhall, and M. H. Dickinson, "Mosquitoes use vision to associate odor plumes with thermal targets," *Curr. Biol.*, vol. 25, pp. 2123–2129, Aug. 2015.

[67] L. B. Bräcker, K. P. Siju, N. Varela, Y. Aso, M. Zhang, I. Hein, M. L. Vasconcelos, and I. C. Grunwald Kadow, "Essential role of the mushroom body in context-dependent CO_2 avoidance in *Drosophila*," *Curr. Biol.*, vol. 23, pp. 1228–1234, July 2013.

[68] L. P. C. Lewis, K. P. Siju, Y. Aso, A. B. Friedrich, A. J. B. Bulteel, G. M. Rubin, and I. C. Grunwald Kadow, "A higher brain circuit for immediate integration of conflicting sensory information in *Drosophila*," *Curr. Biol.*, vol. 25, pp. 2203–2214, Aug. 2015.

[69] O. Riabinina, D. Task, E. Marr, C.-C. Lin, R. Alford, D. A. O'Brochta, and C. J. Potter, "Organization of olfactory centres in the malaria mosquito *Anopheles gambiae*," *Nat. Commun.*, vol. 7, p. 13010, Oct. 2016.

[70] C.-L. Chen, L. Hermans, M. C. Viswanathan, D. Fortun, M. Unser, A. Cammarato, M. H. Dickinson, and P. Ramdya, "Imaging neural activity in the ventral nerve cord of behaving adult *Drosophila*." Jan. 2018.

[71] B. Schnell, I. G. Ros, and M. H. Dickinson, "A descending neuron correlated with the rapid steering maneuvers of flying *Drosophila*," *Curr. Biol.*, vol. 27, pp. 1200–1205, Apr. 2017.

[72] A. J. Kim, L. M. Fenk, C. Lyu, and G. Maimon, "Quantitative predictions orchestrate visual signaling in *Drosophila*," *Cell*, vol. 168, pp. 280–294.e12, Jan. 2017.

[73] S. Namiki, M. H. Dickinson, A. M. Wong, W. Korff, and G. M. Card, "The functional organization of descending sensory-motor pathways in *Drosophila*," 2017.

[74] T. Lindsay, A. Sustar, and M. Dickinson, "The function and organization of the motor system controlling flight maneuvers in flies," *Curr. Biol.*, vol. 27, pp. 345–358, Feb. 2017.

[75] J. M. Melis, T. Lindsay, and M. H. Dickinson, "Mapping steering muscle activity to 3-dimensional wing kinematics in fruit flies," Integrative and Comparative Biology, Mar. 2018.

[76] J. Pelletier, A. Guidolin, Z. Syed, A. J. Cornel, and W. S. Leal, "Knockdown of a mosquito odorant-binding protein involved in the sensitive detection of oviposition attractants," *J. Chem. Ecol.*, vol. 36, pp. 245–248, Mar. 2010.

[77] M. Li, M. Bui, T. Yang, C. S. Bowman, B. J. White, and O. S. Akbari, "Germline Cas9 expression yields highly efficient genome engineering in a major worldwide disease vector, *Aedes aegypti*," *Proc. Natl. Acad. Sci.*, vol. 114, pp. E10540–E10549, Dec. 2017.

[78] D. G. Gibson, L. Young, R.-Y. Chuang, J. Craig Venter, C. A. Hutchison, and H. O. Smith, "Enzymatic assembly of DNA molecules up to several hundred kilobases," *Nat. Methods*, vol. 6, pp. 343–345, Apr. 2009.

[79] J. Bischof, R. K. Maeda, M. Hediger, F. Karch, and K. Basler, "An optimized transgenesis system for *Drosophila* using germ-line-specific φC31 integrases," *Proc. Natl. Acad. Sci.*, vol. 104, pp. 3312–3317, Feb. 2007.

[80] M. A. E. Anderson, T. L. Gross, K. M. Myles, and Z. N. Adelman, "Validation of novel promoter sequences derived from two endogenous ubiquitin genes in transgenic *Aedes aegypti*," *Insect Mol. Biol.*, vol. 19, pp. 441–449, Aug. 2010.

[81] B. D. Pfeiffer, J. W. Truman, and G. M. Rubin, "Using translational enhancers to increase transgene expression in *Drosophila*," *Proc. Natl. Acad. Sci.*, vol. 109, no. 17, pp. 6626–6631, 2012.

[82] D. A. Theilmann and S. Stewart, "Tandemly repeated sequence at the 3' end of the IE-2 gene of the baculovirus *Orgyia pseudotsugata* multicapsid nuclear polyhedrosis virus is an enhancer element," *Virology*, vol. 187, pp. 97–106, Mar. 1992.

[83] A. M. Handler and R. A. Harrell, Ii, "Germline transformation of *Drosophila melanogaster* with the *piggyBac* transposon vector," *Insect Mol. Biol.*, vol. 8, no. 4, pp. 449–457, 1999.

[84] V. Kokoza, A. Ahmed, E. A. Wimmer, and A. S. Raikhel, "Efficient transformation of the yellow fever mosquito *Aedes aegypti* using the *piggyBac* transposable element vector pBac[3xP3-EGFP afm]," *Insect Biochem. Mol. Biol.*, vol. 31, pp. 1137–1143, Nov. 2001.

[85] N. F. Lobo, A. Hua-Van, X. Li, B. M. Nolen, and M. J. Fraser, Jr, "Germ line transformation of the yellow fever mosquito, *Aedes aegypti*, mediated by transpositional insertion of a *piggyBac* vector," *Insect Mol. Biol.*, vol. 11, pp. 133–139, Apr. 2002.

[86] O. S. Akbari, P. A. Papathanos, J. E. Sandler, K. Kennedy, and B. A. Hay, "Identification of germline transcriptional regulatory elements in *Aedes aegypti*," *Sci. Rep.*, vol. 4, p. 3954, Feb. 2014.

[87] A. Aryan, K. M. Myles, and Z. N. Adelman, "Targeted genome editing in *Aedes aegypti* using TALENs," *Methods*, vol. 69, pp. 38–45, Aug. 2014.

[88] A. M. Huang, E. J. Rehm, and G. M. Rubin, "Recovery of DNA sequences flanking p-element insertions in *Drosophila*: Inverse PCR and plasmid rescue," *Cold Spring Harb. Protoc.*, vol. 2009, p. db.prot5199, Apr. 2009.

[89] H. Jia, N. L. Rochefort, X. Chen, and A. Konnerth, "In vivo two-photon imaging of sensory-evoked dendritic calcium signals in cortical neurons," *Nat. Protoc.*, vol. 6, pp. 28–35, Jan. 2011.

[90] J. Schindelin, I. Arganda-Carreras, E. Frise, V. Kaynig, M. Longair, T. Pietzsch, S. Preibisch, C. Rueden, S. Saalfeld, B. Schmid, J.-Y. Tinevez, D. J. White, V. Hartenstein, K. Eliceiri, P. Tomancak, and A. Cardona, "Fiji: An open-source platform for biological-image analysis," *Nat. Methods*, vol. 9, pp. 676–682, June 2012.

Supplementary Tables

Supplemental Table 1: Evaluating fitness cost of GCaMP6s insertion.

	GCaMP6s+/+	WT+/+	p-value
♂ Fertility (# eggs laid)	76.42±18.97 (n=59)	79.23±21.65 (n=74)	0.4276
♀ Fecundity (# eggs laid)	96.08±30.29 (n=72)	79.23±21.65 (n=74)	>0.05
Egg hatching rate (% eggs hatched)	64.48±32.56 (n=72)	71.78±28.57 (n=74)	0.1536
Larval development time (days)	6.21±0.82 (n=434)	6.27±0.49 (n=516)	0.2034

Supplemental Table 2: Primer sequences used in this study.

Primer Name	Primer Sequence (5' to 3')	Source
997.C1	CGACGGTCACGGCGGGCATGTCGACGCGGCCGCTATCTTTACATGTA GCTTGTGCATTGA	*Ae. aegypti* genomic DNA
997.C2	AGCCATACCATGATGATGATGATGATGAGAACCCATCTCGAGATTCG TTGAAATCTCTGT	
997.C3	TTTTCTGCTCAACAGAGATTTCAACGAATCTCGAGATGGGTTCTCAT CATCATCATCATC	Addgene plasmid #740753
997.C4	GTCAGATCCGAGATCGGCCGGCCTAGGGCGCGCCTTAATTAATCACT TCGCTGTCATCAT	
997.C5	CGGTATCTCGCGTTTGTTTGATCGCACGGTTCCCACAATGGTTAATT CGAGCTCGCCCGG	attB plasmid
997.C6	ATTGGATTCAATGCACAAGCTACATGTAAAGATAGCGGCCGCGTCGA CATGCCCGCCGTG	
997.C7	GTTTGTACAAATGATGACAGCGAAGTGATTAATTAACTAGAATGAAT CGTTTTTAAAATA	Addgene plasmid #36432
997.C8	AAAAAGTTGGTGGTGGGGAGGCCACCGAGTATGGGCGCGCCCCGGCC GTTAACTCGAATC	
997.C9	TGGCTTGGATAGCGATTCGAGTTAACGGCCGGGGCGCGCCCATACTC GGTGGCCTCCCCA	Invitrogen pIZ/V5-His/CAT
997.C10	GCATGAACTCCTTGATGACGTTCTTGGAGGAGCGCACCATCACCAGA GACAGGTTGCGGC	
997. C11	GCTAACGGCAAACACCATAAC	*orco*5-/- confirmation primers
997. C12	CGAAGAAAGCTCTCAGGTAACA	

Supplemental Table 3: Inverse PCR primer sequences used in this study.

Reaction	Primer Name	Primer Sequence (5' to 3')
5' (1st Round PCR)	991.5F1	GACGCATGATTATCTTTTACGTGAC
	991.5R1	TGACACTTACCGCATTGACA
5' (2nd Round PCR)	991.5F2	GCGATGACGAGCTTGTTGGTG
	991.5R2	TCCAAGCGGCGACTGAGATG
3' (1st Round PCR)	991.3F1	CAACATGACTGTTTTTAAAGTACAAA
	991.3R1	GTCAGAAACAACTTTGGCACATATC
3' (2nd Round PCR)	991.3F2	CCTCGATATACAGACCGATAAAAC
	991.3R2	TGCATTTGCCTTTCGCCTTAT
Confirmation of 3'	1018.S6	CAGGCGCTGGAAAAATAATGTGAG
	1018.S7	CTCACATTATTTTTCCAGCGCCTG
Confirmation of 5'	1018.S8	TTTCCACGAAATGAACTCAAACGC
	1018.S9	CACACTAATGTACAGTCAGTCTATGCTACGC
	1018.S10	AGAAGAACAGAGGCAATCAACTACATTGA

Supplementary Figures

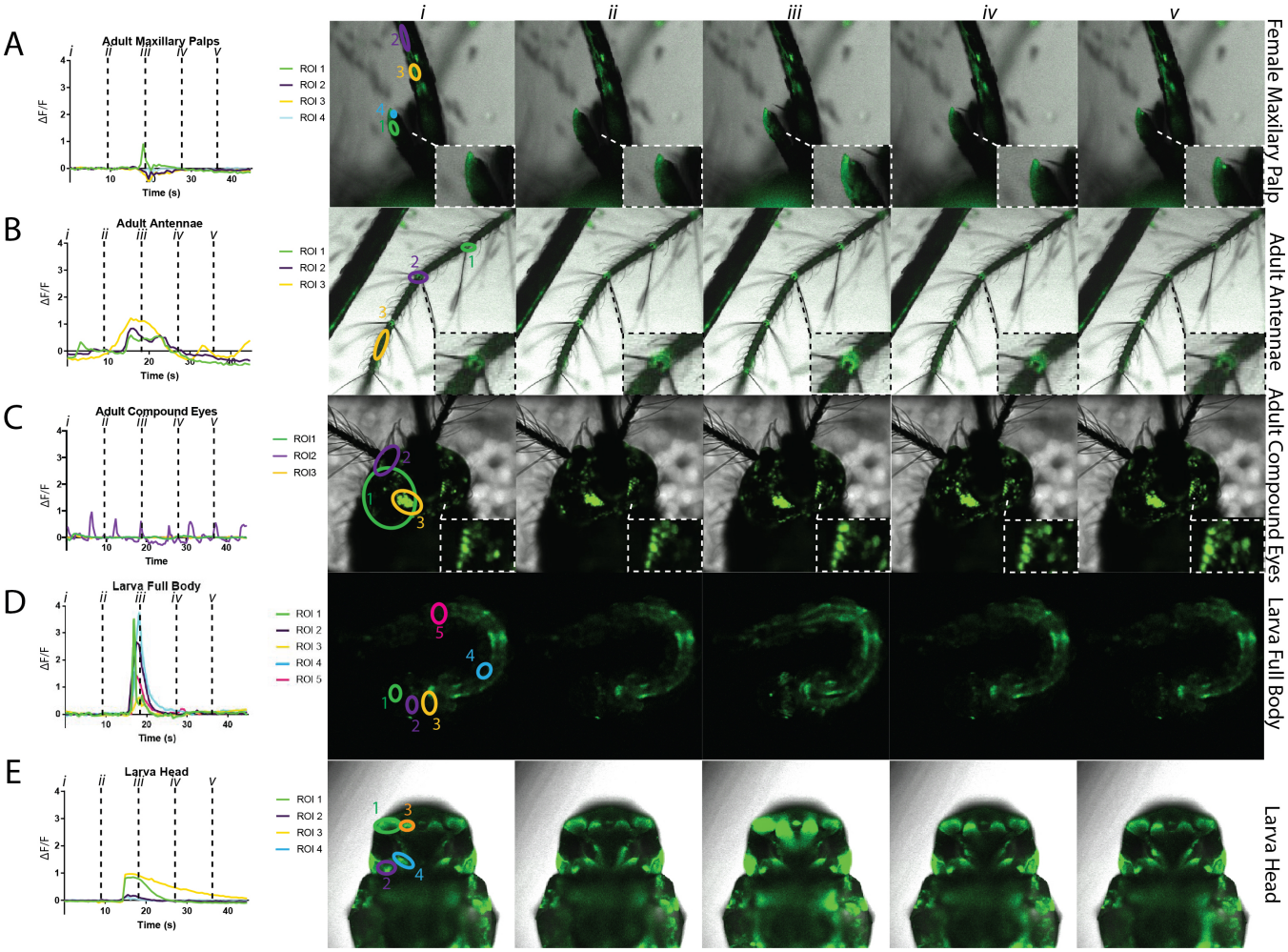

Figure S1: GCaMP6s is a general tool to record calcium responses in multiple tissues. Calcium responses were imaged in multiple tissues (**A-E**, *left*) at varying developmental stages. Frames were taken every 9s, starting at 0s (i) until 36s (v) (**A-E**, *right*). Calcium transients were seen in regions within the adult female maxillary palp (ROI 1,4) and labium (ROI 2,3) (**A**). The female adult antennae also exhibited calcium transients within the nodes (ROI 1,2) and internodes (ROI 3) of the antennal flagellum (**B**). Stochastic patterns of fluorescence were seen when looking at clusters of ommatidia (ROI 1-3) within the right adult compound eye (**C**). Calcium transients were also visualized throughout the 2nd instar larvae. For example, responses were recorded in the medial retractor muscles (ROI 1), brain (ROI 2), longitudinal muscles in the thorax (ROI 3), longitudinal muscles in the 3rd abdominal segment (ROI 4), and muscles and neurons in the 6th abdominal segment (ROI 5) (**D**). When imaging the dorsal side of the larval head, calcium transients were visible in the transverse retractor (ROI 1), optic lobe (ROI 2), medial retractor (ROI 3), and antennal lobe (ROI 4) (**E**). Full videos have been provided in the supplement (Supplementary videos 1-5).

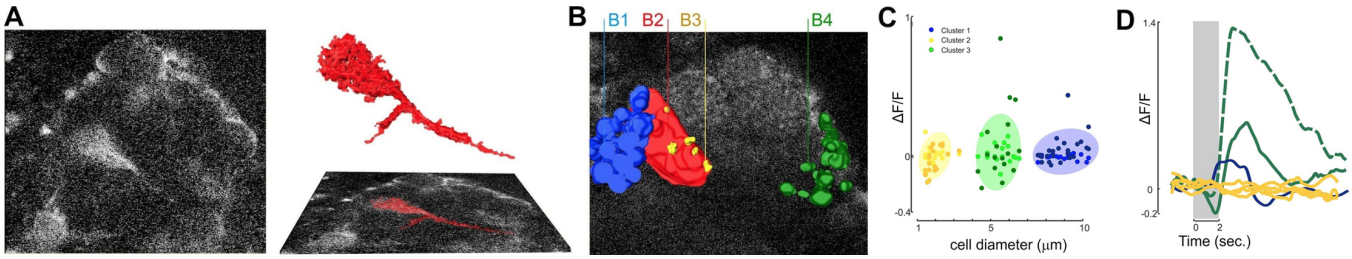

Figure S2: GCaMP6s labeling is sufficient to morphologically distinguish various cell types of interest within the antennal lobe. GCaMP6s could be used to morphologically characterize diverse cell types including the volumes of individual glomeruli (**A**), (**B**) lateral cell cluster neurons (**B1**), volume of the PL2 glomerulus (**B2**), glia (**B3**), and medial cell cluster neurons (**B4**). (**C**) k-means clustering significantly identified ($p<0.05$) three distinct cell classes based on their cell sizes, rather than differences in GCaMP expression levels, such as those in the lateral cell cluster (blue, possibly reflecting local interneurons), cells in the medial cell cluster (green, possibly projection neurons), and glial-like blebs on the glomerular surface (yellow). Cells were imaged at baseline levels and during odor stimulation (darker dots). Soma in the medial cell cluster exhibited greater changes in calcium dynamics during odor stimulation compared to the other cell types. Shaded areas denote the confidence interval around each cluster. (**D**) Responses of the different cell types during odor stimulation. Small, glia-like processes (yellow) showed small changes in calcium (less than 5%) compared to the soma in the medial (green) and lateral (blue) cell clusters. The projection neuron in the glomerulus (dashed green line) exhibited the largest calcium dynamic during odor stimulation.

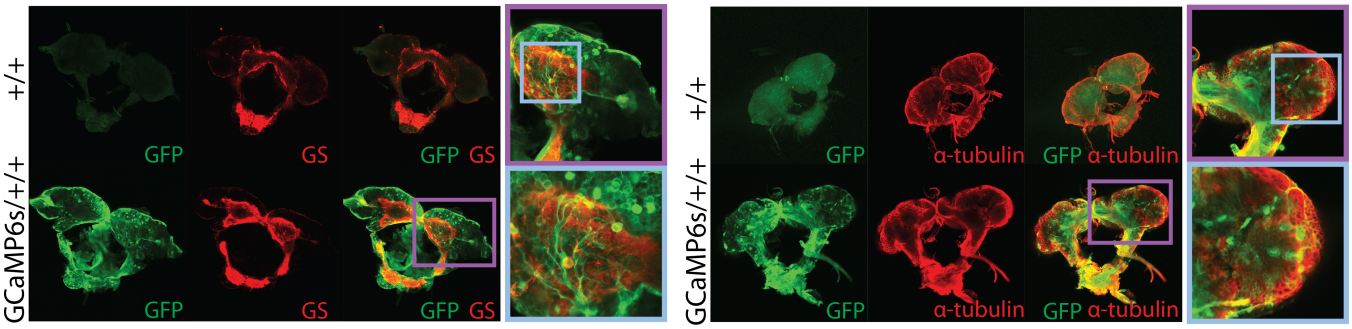

Figure S3: *PUb*-GCaMP6s pattern of expression within the mosquito larval brain. GCaMP6s+/+ larval brains were dissected, fixed and stained for GFP and either alpha-tubulin or glutamine synthetase (GS). Confocal imaging show colocalization between the respective neural or astrocyte-like glial cell antibodies with fixed GFP, demonstrating ubiquitous expression of GCaMP6s in both neural and glial cells.

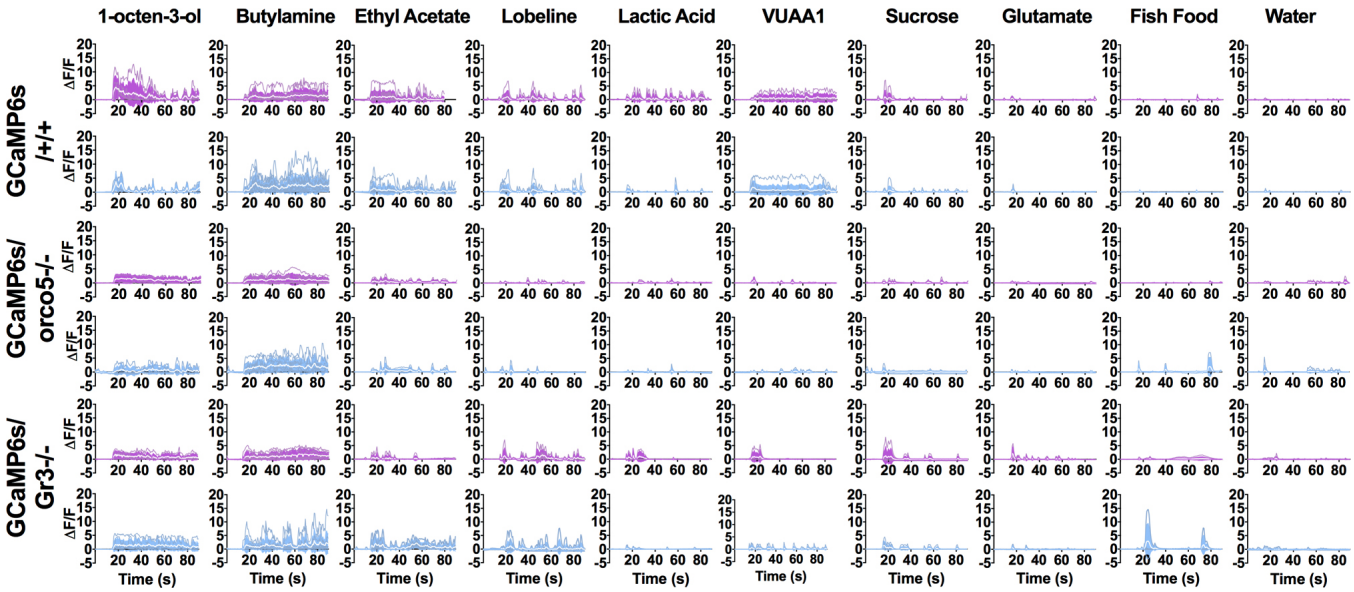

Figure S4: Calcium responses of GCaMP6s/+/+, GCaMP6s/*orco*5-/-, GCaMP6s/Gr3-/- to various stimulants. Time courses for GCaMP6s+/+, GCaMP6s/*orco*5-/-, and GCaMP6s/Gr3-/- DE (purple) and muscle (blue) responses to a stimulus panel including 1-octen-3-ol, butylamine, ethyl acetate, lobeline, lactic acid, VUAA1, sucrose, glutamate, fish food, and water (control). The number of biological replicates used for each experiment were 3 or greater (GCaMP6s/+/+ DE: 1-octen-3-ol n=6; butylamine n=11; ethyl acetate n=10; lobeline n=8; lactic acid n=6; VUAA1 n=6; sucrose n=8; glutamate n=5; fish food n=4; water n=12. GCaMP6s/+/+ Muscle: 1-octen-3-ol n=7; butylamine n=15; ethyl acetate n=15; lobeline n=13; lactic acid n=7; VUAA1 n=8; sucrose n=10; glutamate n=7; fish food n=3; water n=12. GCaMP6s/*orco*5-/- DE: 1-octen-3-ol n=4; butylamine n=8; ethyl acetate n=6; lobeline n=6; lactic acid n=6; VUAA1 n=4; sucrose n=7; glutamate n=5; fish food n=4; water n=7. GCaMP6s/*orco*5-/- Muscle: 1-octen-3-ol n=6; butylamine n=10; ethyl acetate n=6; lobeline n=6; lactic acid n=6; VUAA1 n=5; sucrose n=7; glutamate n=5; fish food n=4; water n=9. GCaMP6s/Gr3-/- DE: 1-octen-3-ol n=6; butylamine n=5; ethyl acetate n=5; lobeline n=4; lactic acid n=4; VUAA1 n=6; sucrose n=4; glutamate n=4; fish food n=6; water n=4. GCaMP6s/Gr3-/- Muscle: 1-octen-3-ol n=7; butylamine n=11; ethyl acetate n=7; lobeline n=9; lactic acid n=6; VUAA1 n=8; sucrose n=7; glutamate n=5; fish food n=5; water n=10).

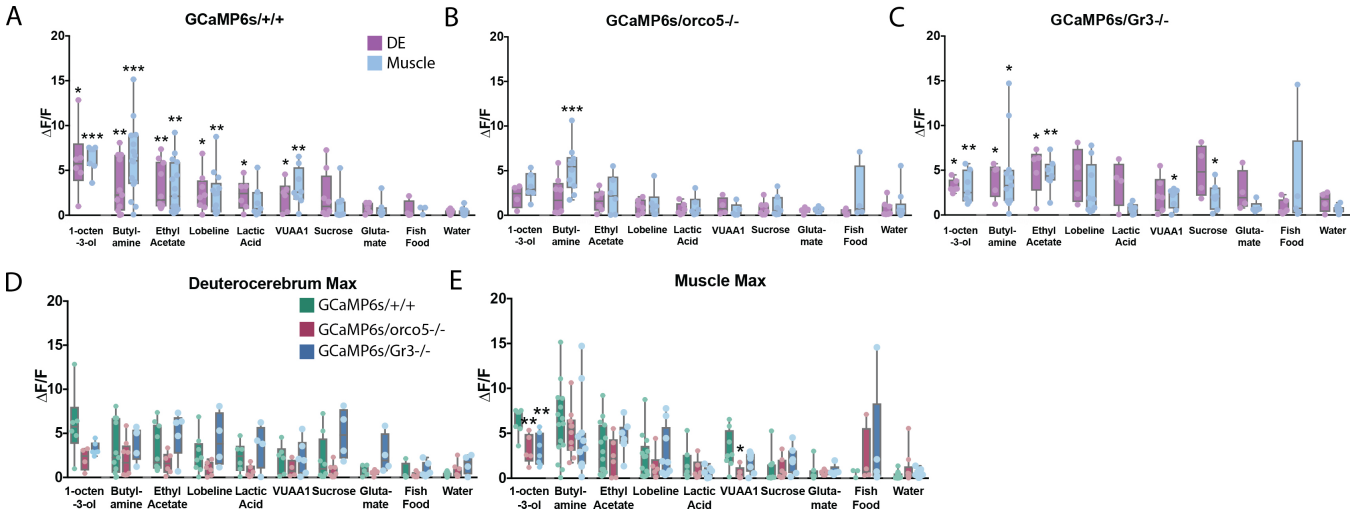

Figure S5: Analysis of stimuli-evoked responses of GCaMP6s/+/+, GCaMP6s/*orco*5-/-, GCaMP6s/Gr3-/-. Maximum fluorescence values of the DE (purple) and Muscle (blue) in response to each stimulus was compared to that of water (control) to test for significance (**A-C**). Maximum changes in fluorescence in response to each stimulus was also compared between the DE and muscles of GCaMP6s/+/+ (green) and both GCaMP6s/*orco*5-/- (red) and GCaMP6s/Gr3-/- (blue) (**D,E**). The number of biological replicates used for each experiment were 3 or greater. *: p-value < 0.05, **: p-value < 0.01, ***: p-value < 0.001, Welch's T-test (GCaMP6s/+/+ DE: 1-octen-3-ol n=6; butylamine n=11; ethyl acetate n=10; lobeline n=8; lactic acid n=6; VUAA1 n=6; sucrose n=8; glutamate n=5; fish food n=4; water n=12. GCaMP6s/+/+ Muscle: 1-octen-3-ol n=7; butylamine n=15; ethyl acetate n=15; lobeline n=13; lactic acid n=7; VUAA1 n=8; sucrose n=10; glutamate n=7; fish food n=3; water n=12. GCaMP6s/*orco*5-/- DE: 1-octen-3-ol n=4; butylamine n=8; ethyl acetate n=6; lobeline n=6; lactic acid n=6; VUAA1 n=4; sucrose n=7; glutamate n=5; fish food n=4; water n=7. GCaMP6s/*orco*5-/- Muscle: 1-octen-3-ol n=6; butylamine n=10; ethyl acetate n=6; lobeline n=6; lactic acid n=6; VUAA1 n=5; sucrose n=7; glutamate n=5; fish food n=4; water n=9. GCaMP6s/Gr3-/- DE: 1-octen-3-ol n=6; butylamine n=5; ethyl acetate n=5; lobeline n=4; lactic acid n=4; VUAA1 n=6; sucrose n=4; glutamate n=4; fish food n=6; water n=4. GCaMP6s/Gr3-/- Muscle: 1-octen-3-ol n=7; butylamine n=11; ethyl acetate n=7; lobeline n=9; lactic acid n=6; VUAA1 n=8; sucrose n=7; glutamate n=5; fish food n=5; water n=10).

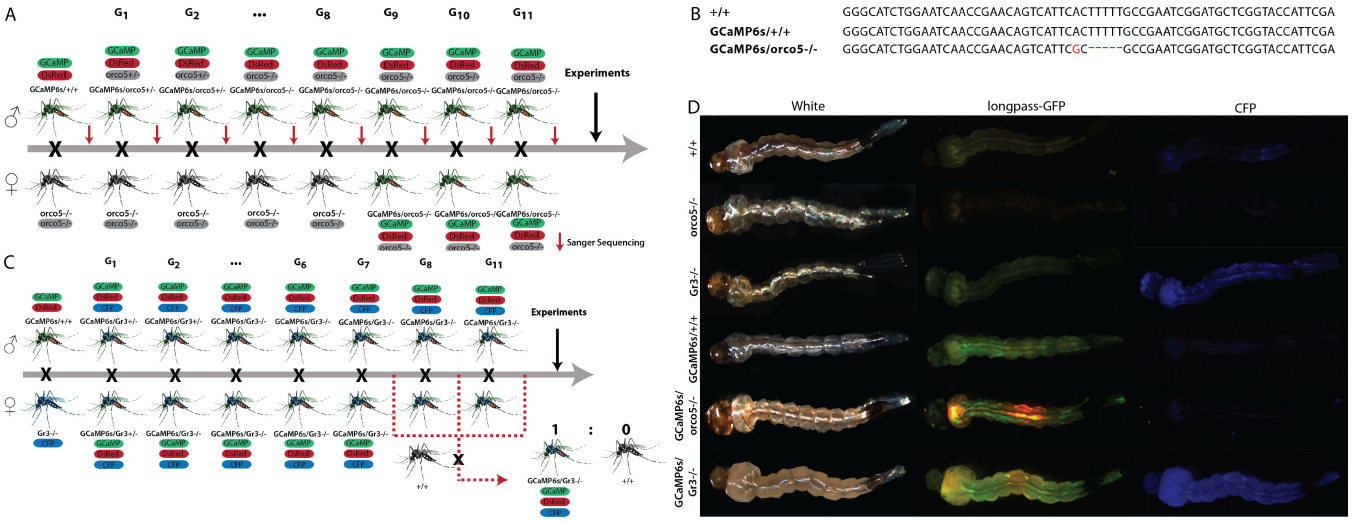

Figure S6: GCaMP6s/*orco*5-/- and GCaMP6s/Gr3-/- line generation and confirmation. GCaMP6s+/+ mosquitos were mated to *orco*5-/- mosquitoes. Resulting individuals were mated to *orco*5-/- mosquitoes in a single pairwise cross for at least 8 generations and sequenced using Sanger Sequencing to confirm the presence of the *orco* gene (**A**). Mutations are indicated in red (**B**). GCaMP6s/+/+ mosquitos were crossed with Gr3-/- mosquitos. Individuals containing both GCaMP6s and Gr3-/- markers, dsRed/GFP transients and CFP respectively, were crossed in single pairwise matings for at least 8 generations to generate homozygous lines, individuals were then crossed to +/+ to confirm homozygosity by mendelian inheritance (**C**). All mosquito lines used were screened and sorted during the larval stage using a longpass-GFP and CFP filter to confirm OpIE-DsRed/GCaMP and CFP respectively (**D**).

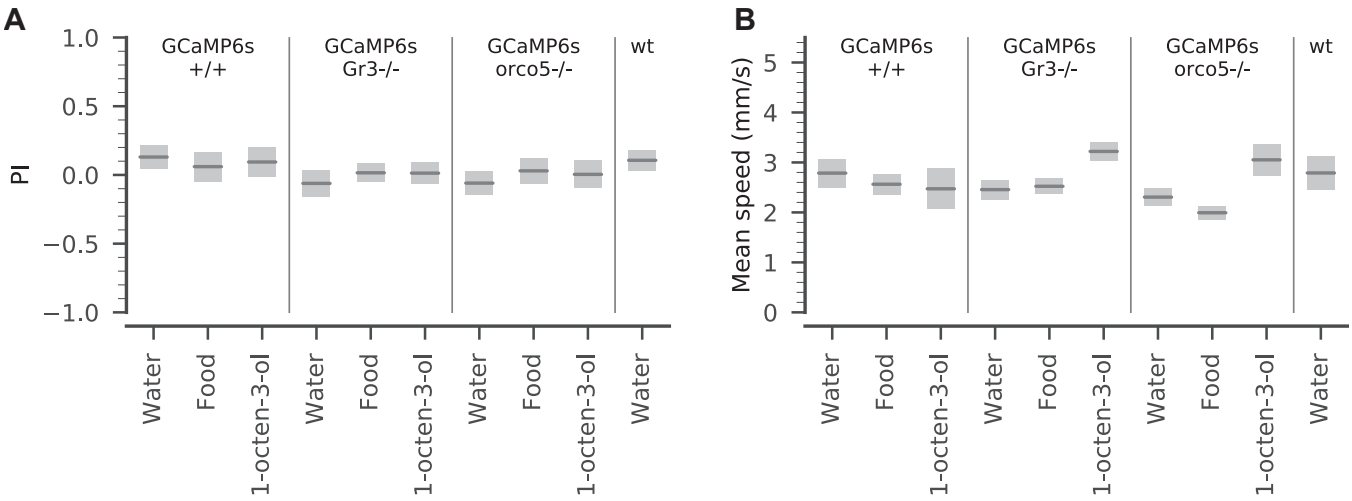

Figure S7: Larvae of different strains do not exhibit motility defects. Prior to stimulation we found no differences in positional preference (**A**) or mean speed (**B**) between larvae of the mutant and wild-type backgrounds (1-way ANOVA by background, p>0.05). Our results suggest that our arena is fair in the absence of odors (**A**) and that larvae of different strains do not exhibit motility defects (**B**). Gray bars show mean +/- SEM. n=14~24 per treatment (GCaMP6s/+/+: water n=20, 1-octen-3-ol n=14, food extract n=20. GCaMP6s/*orco*5-/-: water n=24, 1-octen-3-ol n=16, food extract n=20. GCaMP6s/Gr3-/-: water n=16, 1-octen-3-ol n=17, food extract n=16, Liverpool wt: water n=19).

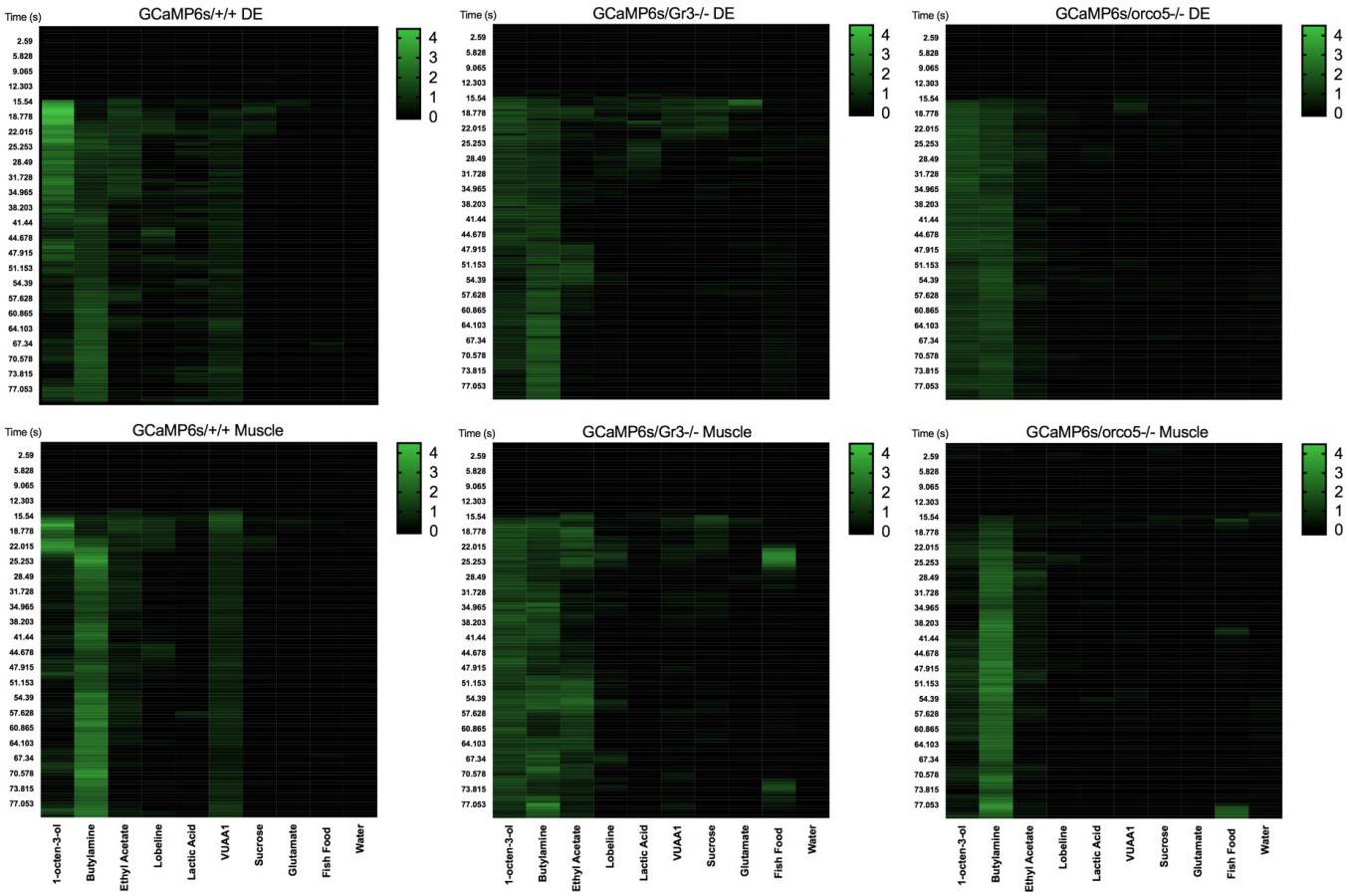

Figure S8: Average calcium responses of GCaMP6s+/+, GCaMP/*orco*5-/-, and GCaMP6s/Gr3-/- over time. Responses to various stimuli were averaged over multiple replicates for each time point.(GCaMP6s/+/+ DE: 1-octen-3-ol n=6; butylamine n=11; ethyl acetate n=1015; lobeline n=813; lactic acid n=67; VUAA1 n=68; sucrose n=810; glutamate n=57; fish food n=43; water n=12. GCaMP6s/+/+ Muscle: 1-octen-3-ol n=7; butylamine n=15; ethyl acetate n=15; lobeline n=13; lactic acid n=7; VUAA1 n=8; sucrose n=10; glutamate n=7; fish food n=3; water n=12. GCaMP6s/*orco*5-/- DE: 1-octen-3-ol n=46; butylamine n=811; ethyl acetate n=6; lobeline n=6; lactic acid n=6; VUAA1 n=45; sucrose n=7; glutamate n=5; fish food n=4; water n=712. GCaMP6s/*orco*5-/- Muscle: 1-octen-3-ol n=6; butylamine n=10; ethyl acetate n=6; lobeline n=6; lactic acid n=6; VUAA1 n=5; sucrose n=7; glutamate n=5; fish food n=4; water n=9. GCaMP6s/Gr3-/- DE: 1-octen-3-ol n=6; butylamine n=511; ethyl acetate n=57; lobeline n=49; lactic acid n=46; VUAA1 n=68; sucrose n=47; glutamate n=45; fish food n=65; water n=412. GCaMP6s/Gr3-/- Muscle: 1-octen-3-ol n=7; butylamine n=11; ethyl acetate n=7; lobeline n=9; lactic acid n=6; VUAA1 n=8; sucrose n=7; glutamate n=5; fish food n=5; water n=10).

Chapter 2

Computational and experimental insights into the chemosensory navigation of *Aedes aegypti* mosquito larvae

Eleanor K. Lutz, Tjinder S. Grewal and Jeffrey A. Riffell

Published in: Proceedings of the Royal Society B: Biological Sciences. 2020

Abstract

Mosquitoes are prolific disease vectors that affect public health around the world. Although many studies have investigated search strategies used by host-seeking adult mosquitoes, little is known about larval search behavior. Larval behavior affects adult body size and fecundity, and thus the capacity of individual mosquitoes to find hosts and transmit disease. Understanding vector survival at all life stages is crucial for improving disease control. In this study we use experimental and computational methods to investigate the chemical ecology and search behavior of *Aedes aegypti* mosquito larvae. We first show that larvae do not respond to several olfactory cues used by adult *Ae. aegypti* to assess larval habitat quality, but perceive microbial RNA as a potent foraging attractant. Second, we demonstrate that *Ae. aegypti* larvae use chemokinesis, an unusual search strategy, to navigate chemical gradients. Finally, we use computational modeling to demonstrate that larvae respond to starvation pressure by optimizing exploration behavior — possibly critical for exploiting limited larval habitat types. Our results identify key characteristics of foraging behavior in an important disease vector mosquito. In addition to implications for better understanding and control of disease vectors, this work establishes mosquito larvae as a tractable model for chemosensory behavior and navigation.

Introduction

The mosquito *Aedes aegypti* is a global vector of diseases such as Dengue, Zika, and Chikungunya [1]. This synanthropic mosquito is evolutionarily adapted to human dwellings, with some populations breeding exclusively indoors [2, 3]. The urban microhabitat features unique climatic regimes, photoperiod, and resource availability. In response to these selective pressures, successful synanthropic animals including cockroaches [4], rats [5], and crows [6] exhibit many behaviors absent in non-urbanized sibling species. Understanding these behaviors is of major importance to public health. Throughout human history, synanthropic disease vectors have caused devastating pandemics like the Black Death, which killed an estimated 30-40% of the Western European population [7, 8]. Like rats or cockroaches, adult *Ae. aegypti* mosquitoes exhibit many behavioral adaptations to human microhabitats [2, 9]. However, comparatively little is known about larval adaptations. The larval environment directly affects adult body size [10, 11], fecundity [11], and biting persistence [12], and understanding vector survival at all life stages is crucial for improving disease control [13]. Despite growing interest [14–16], it remains an open question how environmental stimuli affect larval behavior to regulate these responses and processes.

In addition to the above public health implications, the behavior of synanthropic mosquito larvae is fascinating from a theoretical search strategy perspective. *Ae. aegypti* larvae are aquatic detritivores that live in constrained environments such as vases and tin cans [10]. In such limited environments, do larva exhibit a chemotactic search strategy (in which animals change their direction of motion in response to a chemical stimuli), or do they use a chemokinetic response (in which animals change a non-directional component of motion, such as speed or turn frequency, in response to a chemical stimuli) [17]? Mechanistic understanding of larval foraging behavior may provide insight into chemosensory systems controlling the behavior as well as the evolutionary adaptations for these systems in synanthropic environments.

In this work, we investigate larval *Ae. aegypti* behavior from a chemical ecological and search theory perspective. First, we explore chemosensory cues involved in larval foraging. Although many olfactory cues are used by adult females to select oviposition sites [18], it is unclear if larvae and adults use the same chemicals to assess larval habitat quality. Second, we consider larval search behavior in spatially restricted environments using empirical data and computational modeling. Our work identifies the lack of chemotaxis in foraging *Ae. aegypti* larvae — an example of how environmental restrictions may drive the evolution of animal behavior. We further identify microbial RNA as a potent and unusual larval foraging attractant. Together, our results identify *Ae. aegypti* larvae as a tractable model in bio-

logical search theory, and highlight the importance of investigating synanthropic disease vectors at all life history stages.

Results

Effects of Sex, Physiological State, and Circadian Timing on Larval Physiology

Behavioral experiments in insects have demonstrated the importance of circadian timing, starvation, and age [19]. However, little is known about the effects of these variables on *Ae. aegypti* larvae. To better understand the effects of nutritional state and sex on our study organism, we used machine vision to track individual 4th instar *Ae. aegypti* larvae in a custom arena before each experiment (Fig 1A). For both fed and starved animals, female larvae were larger than males (fed larvae: n=135♀, 153♂, $p<0.0001$, effect size=0.53mm; starved larvae: n=89♀, 122♂, $p<0.01$, effect size=0.26mm, Fig S1A). Starved larvae were also smaller than fed animals for both females ($p<0.0001$, effect size=0.51mm) and males ($p<0.01$, effect size=0.23mm, Fig S1A). Because adult *Ae. aegypti* exhibit crepuscular activity [10], we also investigated the effects of circadian timing on larval behavior. We found no effects of circadian timing on larval movement speed ($p=0.40$), time spent moving ($p=0.41$), or time spent next to arena walls ($p=0.55$). These observations support previous findings that mosquito larvae, unlike adults, exhibit little behavioral variation during the day [20, 21].

Quantifying the Chemosensory Environment in Naturalistic Larval Habitat Sizes

Previous research has shown that other species of mosquito larvae detect many different chemosensory stimuli [23]. In *Ae. aegypti*, it is unclear what chemical cues, if any, larvae use to navigate their environment. Nevertheless, chemosensory cues may be essential in avoiding predation or foraging efficiently. Using our arena and machine vision methods, we investigated larval preference for eight putatively attractive and aversive sets of stimuli. First, we experimentally verified the chemical diffusion in the arena and found that larval movement significantly increased the diffusion of stimuli within the arena ($p<0.0001$, Fig S2). We next created a chemical diffusion map for analyzing stimuli preference using only experiments containing larvae (Fig 1B, Fig S2A-D). For chemosensory stimuli, we used predicted attractive stimuli including a 0.5% mixture of food (Hikari Tropic First Bites fish food) suspended in water, as well as food extract filtered through a 0.2μm filter to remove solid particulates. Quinine was used as a putative aversive stimulus (a bitter tastant aversive to many insects including *Drosophila melanogaster* and *Apis mellifera* [24, 25]). We also tested indole and o-cresol, two microbial

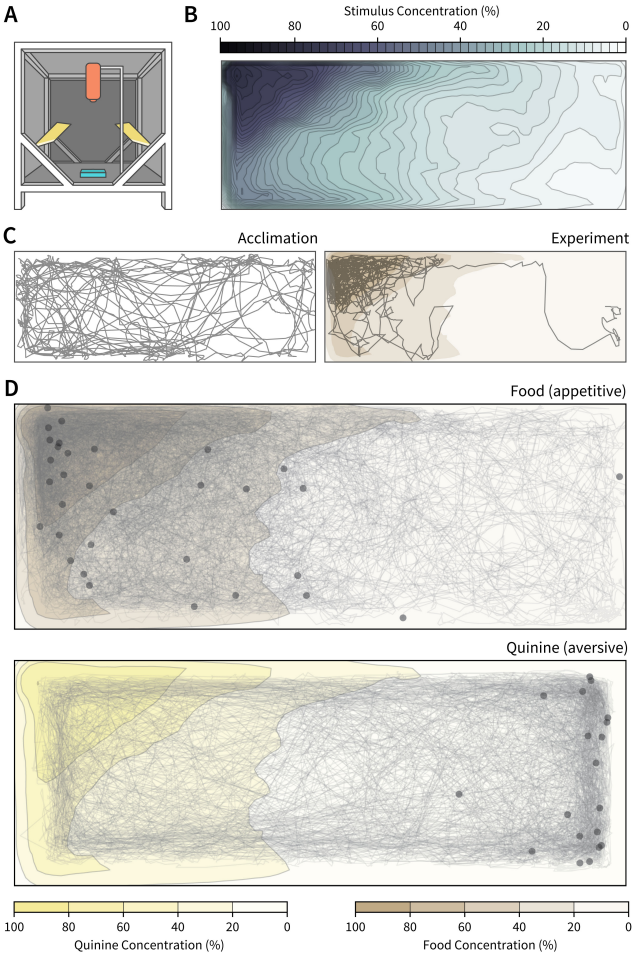

Figure 1: Quantifying the chemosensory environment in naturalistic larval habitat sizes. A: Diagram of experimental conditions, adapted from [22], including a Basler Scout Machine Vision GigE camera (orange), infrared lighting (yellow) and a behavior arena (blue). **B:** Chemosensory diffusion map of the behavior arena at the end of the 15 minute experiment. **C:** Example of an individual larval trajectory during the 15 minute acclimation phase (left). Trajectory of same individual during the 15 minute experiment phase, responding to food added to the left side of the arena (right). **D:** Trajectory of all starved animals presented with food (top) or quinine (bottom). Although trajectories are shown aggregated into one image, all animals were tested individually. Scatter points show the position of each animal at the end of the experiment and color overlays show the chemosensory diffusion map at the end of the 15 minute experiment.

compounds that attract adult mosquitoes for oviposition [26]. Finally, we tested the response of larvae to RNA, glucose, and a mixture of 9 amino acids required for *Ae. aegypti* larval growth. All three components are essential for *Ae. aegypti* survival [27], and RNA polynucleotides serve as attractants or essential nutrients for larvae of other mosquito species [28–31]. Moreover, dissolved RNA is released at high levels ($\mu g \cdot L^{-1}\ h^{-1}$) from growing populations of microbes in freshwater habitats [32], and could provide valuable foraging information to omnivores such as *Ae. aegypti*. By contrast, other isolated macronutrients such as salts,

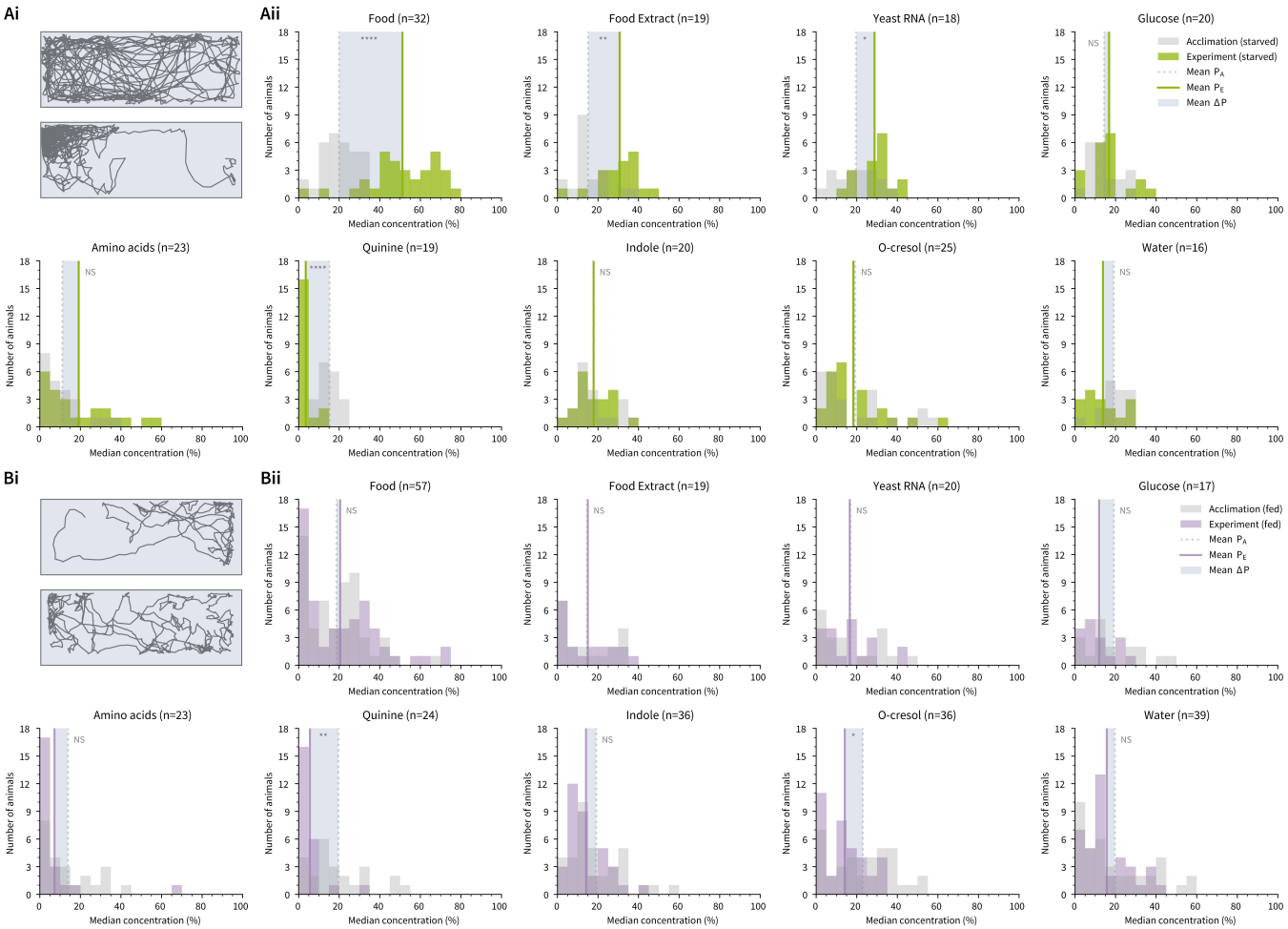

Figure 2: Physiological feeding state affects larval attraction towards ecologically relevant odors. Ai: Example trajectory of a starved larva during the acclimation (top) and the experiment phase (below), responding to food introduced to the top left. **Aii:** Distribution of larvae during the acclimation phase (grey) and experiment phase (green), median concentration. The shaded box visualizes the mean ΔP across all individuals. Note that due to the unequal distribution of high and low concentration areas in the behavior arena, animals naturally appear to distribute near lower concentrations when no stimulus is present. **Bi:** Example trajectory of a fed larva during the acclimation (top) and experiment phase (below), responding to food introduced to the top left. **Bii:** Distribution of fed larval preference during the acclimation (grey) and experiment phase (purple). In **Aii** and **Bii**, asterisks denote the significance level of paired-sample Welch's t-tests comparing acclimation P and experiment P (*:p<0.05; **:p<0.01; ***:p<0.001; ****:p<0.0001; NS: not significant). n-values reported next to each stimulus describe the number of animals in the treatment.

	Potential Chemosensory Search Strategies				
	Anosmic	*Chemotaxis*	*Klinokinesis*	*Chemokinesis*	**Experiment Observations**
Stimulus preference ΔP	no	yes	yes	yes	yes (p<0.0001)
Directional preference ΔDP	no	yes	no	no	no (p=0.98)
Δ Concentration speed ΔDS	no	no	no	no	no (p=1)
Concentration speed ΔCS	no	no	no	yes	yes (p<0.0001)
Δ Concentration turns ΔDTI	no	yes	no	no	no (p=1)
Concentration turns ΔCTI	no	no	yes	no	no (p=1)

Table 1: Comparing larval exploration behavior to canonical animal search strategy models. Four different chemosensory search strategies are listed (central columns) along with the expected observable behavior metrics for each strategy (left column). By comparing the experimental observations (right column) with the expected results, we determined that *Ae. aegypti* larval chemosensory navigation is best explained by an chemokinesis search strategy model.

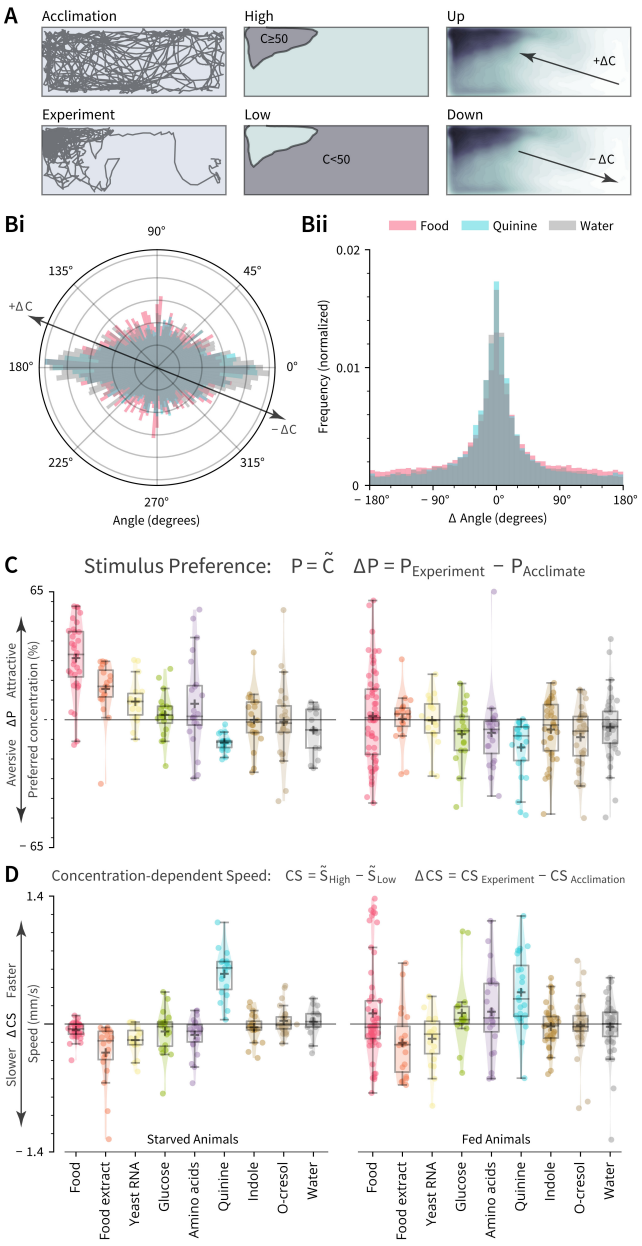

Figure 3: Larval exploration behavior is best explained by a chemokinesis search model. A: Diagram of behavioral quantifications. Larvae were observed during a 15 minute acclimation period in clean water, followed by a 15 minute experiment in the presence of the stimulus. The arena was divided into an area of high (≥50%) and low concentration (<50%). Larvae could move in a direction that increased local concentration (+ΔC) or decreased local concentration (-ΔC). **Bi:** Orientation of animals in the arena throughout the experiment. Larvae did not exhibit directional movement in response to appetitive or aversive stimuli. Note that larvae spend more time moving horizontally (0°, 180°) because the rectangular arena is longer in the horizontal direction. **Bii:** Larvae did not change frequency of turns (Δ Angle) in response to appetitive or aversive stimuli. **C:** Box plots for the population median ± 1 quartile, population mean (+ marker) and mean response for each individual (dots) for larval preference (ΔP). A horizontal line at 0 represents no change in behavior following stimulus addition. **D:** As in **C**, except for stimulus-dependent changes in Concentration-dependent Speed (ΔCS).

sugars, and amino acids elicit little to no attraction in other larval mosquito species [33].

Physiological Feeding State Affects Larval Attraction Towards Ecologically Relevant Odors

For each of these eight sets of stimuli, in addition to water, we compared the stimulus preference of larvae before and after stimulus addition (Fig 1C, Fig 2A, Fig S3, Fig S4, Fig S5). Preference was defined as the median concentration chosen by the larvae throughout the 15-minute experiment, normalized to behavior during the previous 15-minute acclimation phase. Starved larvae were attracted to food (n=32, p<0.0001) and spent significantly less time near the aversive cue quinine (n=19, p<0.0001). Food extract filtered through a 0.2μm filter remained attractive (n=19, p=0.004), suggesting that larvae use small, waterborne chemical cues to forage. To further investigate these foraging cues, we next examined responses to microbial RNA, glucose, and an amino acid mixture. We found that RNA was significantly attractive (n=18, p=0.049), while glucose (n=20, p=1), and the amino acid mixture (n=23, p=1) were not. Addition of water — a negative control for mechanical disturbance — had no impact on larval positional preference (n=16, p=1). Although we expected indole and o-cresol, which are attractive to adult *Ae. aegypti*, to elicit attraction from larvae, neither odorant elicited a change in behavior from the acclimation phase (indole: n=20, p=1; o-cresol: n=25, p=1). Indole tested at a higher concentration (10mM) also had no effect (n=19, p=0.31). Together, these results suggest that larvae and adults may not necessarily rely on similar cues to assess larval habitat quality.

The physiological feeding state of an adult mosquito has a strong impact on subsequent behavioral preferences [34], but it remains unknown how feeding status influences responses to chemosensory stimuli in larvae. We thus fed larvae ad libitum to fish food before testing their responses to each of the eight stimuli and a water control (Fig 2B). Fed larvae showed no significant attraction to food (n=57, p=1), food extract (n=19, p=1), and RNA (n=20, p=1), supporting the prediction that microbial RNA functions as an attractant in the context of foraging. Nonetheless, fed larvae still exhibited aversive responses to quinine (n=24, p=0.003), demonstrating that the lack of response to foraging cues is not due to a global reduction in chemosensory behavior. Similar to starved larvae, fed animals showed no preference for the water control (n=39, p=1), indole (100μM: n=36, p=0.98; 10mM: n=17, p=1), glucose (n=17, p=1), or the amino acid mixture (n=23, p=1). Fed larvae exhibited significant aversion to o-cresol (n=36, p=0.026).

A Chemokinesis Navigation Strategy is Most Consistent with Larval Aggregation Toward Cues Investigated in this Study

Next we investigated the behavioral mechanism by which *Ae. aegypti* larvae locate sources of odor, since such information could provide insight into the chemosensory pathways that mediate the behaviors. We hypothesized that larval aggregation near attractive cues such as food is mediated by chemotaxis — a common form of directed motion observed in many animals and microbes [35–37]. In chemo-klino-taxis (hereafter chemotaxis), animals exhibit directed motion with respect to a chemical gradient. Alternatively, larvae may exhibit chemo-ortho-kinesis (hereafter chemokinesis) — a process in which animals respond to local conditions by regulating speed rather than direction — or chemo-klino-kinesis (hereafter klinokinesis) — in which animals respond to local conditions by regulating turning frequency. Finally, larvae may be unable to detect chemosensory stimuli, and thus exhibit purely random behavior (hereafter anosmic). To differentiate between these strategies, we quantified six observable metrics used to characterize navigation behavior (Table 1). By breaking down larval trajectories into several different components (Fig 3A-B) and identifying which variables correlate with stimulus preference (Fig 3C-D), we can infer which search strategy best explains larval behavior.

Surprisingly, we found no evidence for chemotaxis near attractive or aversive chemicals. Starved larvae did not exhibit kinematic changes characteristic of chemotaxis, such as directional preference (ΔDP, p=0.98, Fig 3Bi, Fig S6A). Further, larvae could not increase odor localization efficiency above random chance: discovery time for all cues was comparable across treatments (ΔD, p=1, Fig S6B). Larvae also did not perform klinokinesis: Turning frequency was unaffected by either the instantaneous concentration the larvae experienced (ΔCTI, p=1, Fig 3Bii, Fig S6C) or change in concentration (ΔDTI, p=1, Fig S6D). Instead, we found that larval activity was most consistent with chemokinesis for the eight cues tested in these experiments. Larvae altered movement speed when experiencing high local stimuli conditions (ΔCS, p<0.0001, Fig 3D) but not when moving up or down the concentration map (ΔDS, p=1, Fig S6E). When grouped into aversive, attractive, and neutral chemosensory cues, the correlation between preference (ΔP) and chemokinetic response (ΔCS) similarly separated into three clusters (Fig S7). We did not observe a strong linear relationship in our dataset, perhaps because the majority of cues tested did not elicit a strong behavioral preference.

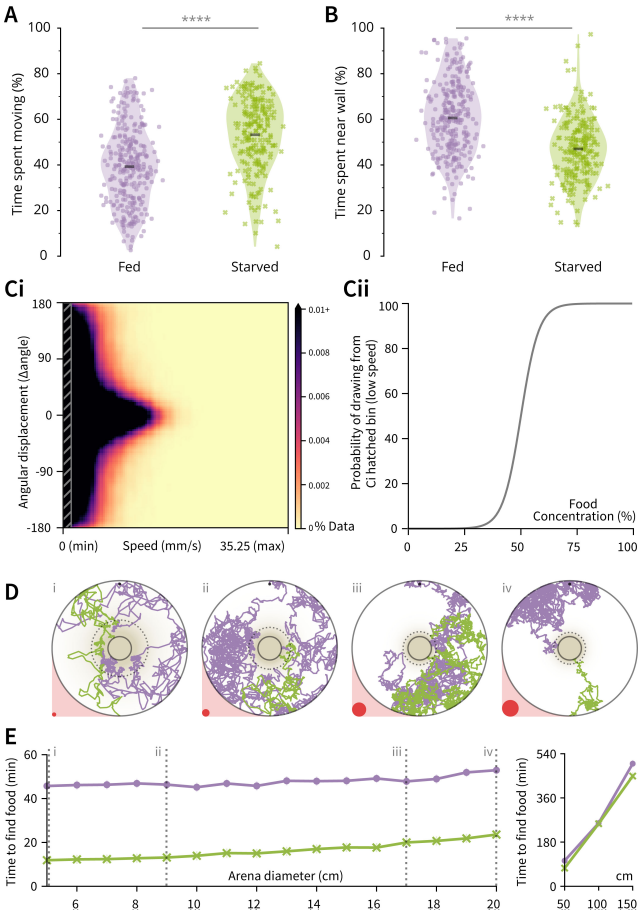

Figure 4: Starved *Ae. aegypti* optimize exploration behavior to increase the probability of finding food. A: Starved larvae spend more time exploring the arena than fed larvae (p<0.0001). **B:** Starved larvae spend less time within one body length of an arena wall (p<0.0001). **A-B:** Violin plot. Dots are the means for each individual, and black bar is the mean across all individuals (n>168 per treatment); asterisks denote p<0.0001 (Welch's t-test). **C:** We developed a computational model to approximate the chemokinetic behavior observed in experimental data. **Ci:** Probability Density Function of the relationship between movement speed and instantaneous angle for starved animals. The shaded grey rectangle to the left visualizes the area encompassing half of the available data. **Cii:** Trajectories were constructed by sampling values from the shaded rectangle when larvae were in areas of high food concentration, and sampling values from outside the shaded rectangle when in areas of low food concentration. The probability function for drawing from the two distributions was smoothed to avoid threshold artifacts. **D:** Simulated trajectories of fed (purple) and starved (green) larvae foraging in ecologically relevant arena sizes. Relative size of each arena is visualized as red circles. In this figure larvae began at the top center (fed) or the bottom center (starved). However in actual simulations starting location was randomized for each individual. **Di:** 5cm, **Dii:** 9cm, **Diii:** 17cm, and **Div:** 20cm simulated arena diameters. In all cases, the solid black circle outlines the food target goal, and the dashed circle represents the boundary of 50% food concentration. **E:** Simulated chemokinetic larvae using empirical data from starved animals (green × markers) found the food source consistently faster than the same model using data from fed animals (purple dots). Mean of 1000 simulations ± standard error. Dashed grey lines correspond to ecologically relevant habitat sizes described in Table S1 and in **D**.

Starved *Ae. aegypti* Optimize Exploration Behavior to Increase the Probability of Finding Food

Many organisms change their speed or activity rate when starved [38], and we predicted that starved *Ae. aegypti* may also alter their exploration behavior to increase the probability of discovering food. Experimental observations showed evidence for starvation-mediated behavior changes — starved animals spent more time exploring ($p<0.0001$, Fig 4A) and spent less time near walls and corners ($p<0.0001$, Fig 4B). We were interested in understanding whether or not these behavioral changes might be adaptive in ecologically relevant container sizes. We thus created two chemokinesis foraging models using empirical data from fed and starved animals (n=248 fed larvae during the acclimation phase: n=445,925 trajectory data points; n=168 starved larvae during the acclimation phase: n=302,096 trajectory data points). This computational model explored circular arenas of various ecologically relevant diameter sizes 5 to 20cm in diameter (Table S1) by randomly sampling instantaneous speed and turn angle from experimental data (Fig 4C). Individual simulations using this model were tasked with finding a food source at the center of one of these arenas (Fig 4D), starting from a randomized location. Similar to the trajectories of starved larvae (Fig 2D), our simulated trajectories exhibited tortuous paths that ultimately encountered the food patch. Nonetheless, the chemokinesis model using empirical data from starved animals discovered the food source more than 20 minutes faster than fed animals across all habitat sizes (Fig 4E), supporting our hypothesis that starvation-mediated changes in larval behavior increase the probability of finding food in larval environments. Moreover, simulated starved larvae could find the food source in under 25 minutes across these smaller environment sizes (Fig 4E). Given that *Ae. aegypti* larvae can survive up to a week without food [10], our results suggest that a chemokinetic search strategy is sufficient to successfully forage in diverse and realistic larval habitats. Although our simulation assumptions are less suitable for understanding larger breeding sites[1], we further simulated habitats 50, 100, and 150cm in diameter for comparison. We found that larvae still discovered the food source in several hours (fed simulations: 1.7, 4.3, and 8.3 hours; starved simulations: 1.2, 4.2, and 7.5 hours for 50, 100, and 150cm arenas, Fig 4E). Finally, the slope for starved animals in smaller habitats was about twice that of fed animals (starved: 45.3 seconds $\cdot$ cm^{-1}; fed: 22.9 s $\cdot$ cm^{-1}), suggesting that the benefit of behavioral modification in starved animals is more pronounced in smaller arena sizes (slope of difference between fed - starved simulations: -22.4 s $\cdot$ cm^{-1}).

[1] Large breeding sites are probably more likely to contain multiple small patches of food distributed throughout the environment, rather than our simulated model of one single patch.

Discussion

In this study we quantify essential characteristics of *Ae. aegypti* larval behavior that are crucial for the development of future studies. Further, we identify previously unknown behaviors that highlight the unique evolutionary history and developmental biology of these disease vector mosquitoes. First, we show that larvae perceive microbial RNA as a foraging attractant, but do not respond to several olfactory cues that attract adult *Ae. aegypti* for oviposition. Second, we demonstrate that *Ae. aegypti* larvae use chemokinesis, rather than chemotaxis, to navigate with respect to chemical sources. Finally, we use experimental observations and computational analyses to demonstrate that larvae respond to starvation pressure by changing their behavior to increase the probability of finding food sources in realistic habitat sizes.

Although adult *Ae. aegypti* feeding is regulated by ATP perception [39], we are unaware of other work demonstrating perception of nucleotides or nucleic acids such as RNA in *Ae. aegypti* larvae. In our state-dependent preference experiments, we investigate the ecological basis of larval RNA attraction, and propose that RNA may function as one of the foraging indicators in the larval environment. However, 44 different nutrients are required for *Ae. aegypti* larval survival [27], and the attractiveness of other potential phagostimulants including vitamins and carbohydrates have not been tested with the sensitivity of our experimental methods. In addition, the concentration and relative composition of phagostimulants may have complex effects on larval preference, and these combinatorial effects were not examined in this study. In a natural environment *Ae. aegypti* larvae likely rely on a combination of stimuli to locate food sources. Nevertheless, an earlier study demonstrated that olfactory receptor deficient (*orco -/-*) *Ae. aegypti* larvae showed no defects in attraction to food [22]. Taken together, our results support the hypothesis that sensory information gained from gustatory or ionotropic receptors may be more integral to larval chemosensation than olfactory receptors. Further, larval attraction to RNA suggests that the importance of nucleotide phagostimulation is preserved throughout a mosquito's life cycle, from larval foraging to adult blood engorgement and oviposition.

Our study also raises a number of comparative questions that could be addressed in future research. For instance, is chemokinesis in mosquito larvae associated with human association and man-made containers? Future studies could compare chemotactic ability in other spatially constrained mosquitoes, such as *Toxorhynchites* (which inhabit tree holes) or *Aedes albopictus*

(another container-breeding mosquito) [40], to species that oviposit in larger bodies of water such as *Aedes togoi* (marine rock pools) or opportunistic species such as *Culex nigripalpus* that oviposit in a wide range of habitat sizes [40,41]. Additionally, computational modeling of fluid dynamics and larval movement may help determine whether chemotaxis is physiologically and physicochemically challenging in small, man-made environments. Due to the diffusive environment in the small containers, where shallow gradients dominate and turbulence is lacking, the change in time or space of the chemical signal may be too small for the larvae to detect. This is particularly relevant considering our results showing that larval movement significantly modifies the stimulus gradient [42].

Synanthropic mosquitoes are increasingly important to global health as urbanization progresses: Currently over half of all humans live in urban environments, and this proportion is only expected to increase [43]. Adaptations that facilitate human cohabitation, like specialized larval foraging strategies, are vital to our understanding of mosquito behavior and success as a disease vector [9].

Materials and Methods

Details on the Insects, Selection of Preparation of Odorants, and Statistical Analyses, can be found in the Electronic Supplementary Materials.

Behavior Arena and Experiment

We previously developed a paradigm to investigate chemosensory preference in larval *Ae. aegypti* [22]. In this study we expanded our protocol by mapping the chemosensory environment in our arena using fluorescein dye. Importantly, because larval swimming activity increases chemical movement within the arena, we mapped the dye distribution from experiments containing an actively swimming larva. 100μL of fluorescein dye was added to a white arena of the same material and dimensions, each containing one *Ae. aegypti* larva. Dye color was converted to concentration values using a standardization dataset of 13 reference concentrations (Fig S2C). Dye diffusion through time was quantified by the mean of all values in each 1mm^2 area, linearly interpolated throughout time (n=10, Fig S2B).

During behavior experiments, we recorded animals for 15 minutes before each experiment to analyze baseline activity and confirm that the arena was fair in the absence of chemosensory cues. Subsequently, 100μL of a chemical stimulus was gently pipetted into the left side of the arena to minimize mechanosensory disturbances, and larval activity was recorded for another 15 minutes (Fig 1C).

Video Analyses

Video data was obtained and processed as previously described [22] using Multitracker software by Floris van Breugel [44] and Python version 3.6.2. Additionally, approximate larval length was measured for each animal in ImageJ Fiji [45], as the pixel length from head to tail, in a selected video frame that showed the larva in a horizontal position. Lengths were converted to mm using the known inner container width as the conversion ratio. Experimenters were blind to larval sex when measuring lengths. Throughout our analyses, the arena was divided into areas of high concentration ($\geq$50% initial stimulus) and low concentration (<50%). Larvae could move in a direction that increased local concentration or decreased local concentration. We discounted concentration changes caused by diffusion while the larvae remained immobile. A threshold of Δ2%/s was required to qualify as moving up or down the concentration map.

Computational Modeling

We developed a chemokinetic computational model to investigate larval foraging success in different environments. This model resampled the observed trajectories of *Ae. aegypti* larvae to investigate the consequences of a chemokinetic search strategy using realistic larval behavioral metrics. In the experimental foraging task, simulated animals explored a circular arena until they encountered a food source at the center of the arena. These arenas included a range of 19 different arena sizes representing many of the ecologically realistic habitats reported in literature (Table S1). The food target was scaled to arena size (comprising 3% of total area) under the assumption that habitats of larger diameter would also contain higher absolute amounts of food. Each simulated larvae began at a random point within the arena, and then explored the environment at each time step by sampling a paired speed-angle data point from experimental data (Fig 4Ci). We elected to pair these data points in our model because we observed that the two variables were correlated at higher speeds (Fig 4Ci). The time step was re-sampled if the selected data point would cause the trajectory of the simulated larvae to leave the boundary of the experimental arena. Data from animals tested with glucose and amino acids were not included. These experiments were conducted during the manuscript review process, and it was not possible to rerun simulations in the allotted time. Nevertheless, our simulations were sampled from over 700,000 data points from 416 individual larvae. To approximate chemokinetic behavior, simulated larvae in areas of high food concentration ($\sim$>50%) moved slower, and larvae in areas of low food concentration ($\sim\leq$50%) moved faster. These differences were implemented by splitting the paired speed-angle data into two bins of equal size, with one bin containing the

slowest half of all data points and the other containing the faster half. The probability of sampling from each half was determined as a function of the instantaneous food concentration (Fig 4Cii), with the addition of an exponentially smoothed decision boundary to reduce thresholding artifacts. The empirical data pairs used in these models represented all data taken from larvae observed in clean water before the addition of experimental stimuli, with fed simulations sampling data from fed animals and starved simulations sampling data from starved animals only (n=248 fed, n=168 starved). To define the boundary of 50% food concentration for chemokinetic behavioral decisions, we defined the simulated chemical conditions using an exponential regression model of distance and concentration based on our empirical chemical map (Fig S2E). When the simulated larvae entered the food patch at the center of the arena, the simulation was stopped and the time taken to discover the food was recorded (in seconds). We conducted 1,000 simulations for each arena size and nutritional state (fed vs. starved).

Acknowledgements

This work was supported in part by grants from the National Institute of Health grant 1RO1DCO13693 and 1R21AI137947 to J.A.R.; National Science Foundation grants IOS-1354159 to J.A.R. and DGE-1256082 to E.K.L.; Air Force Office of Sponsored Research under grant FA9550-16-1-0167 to J.A.R.; and the Robin Mariko Harris Award to E.K.L. We thank Floris van Breugel for assistance with video data analysis, the University of Washington Biostatistics Consulting Group for statistical advice, and Binh Nguyen and Kara Kiyokawa for maintaining the Riffell lab mosquito colony. We also thank Thomas Daniel, Bingni Brunton, Kameron Harris, and the Kincaid 320 Python Club for insightful discussions on programming and data management. Finally, we thank two anonymous reviewers for their contribution of time, expertise, and thoughtful advice that significantly improved this manuscript.

Author Contributions

Conceptualization: E.K.L. and J.A.R.; Methodology: E.K.L. and J.A.R.; Software: E.K.L.; Investigation: E.K.L. and T.S.G.; Resources: E.K.L. and J.A.R.; Data Curation: E.K.L; Writing — Original Draft: E.K.L; Writing — Review and Editing: E.K.L, J.A.R, and T.S.G.; Visualization: E.K.L; Supervision: J.A.R; Project administration: J.A.R; Funding acquisition: E.K.L. and J.A.R.

Declaration of Interests

The authors declare no competing interests.

Additional Files

Code associated with this manuscript can be found at:
`https://github.com/eleanorlutz/aedes-aegypti-2019`.
Data associated with this manuscript can be found at Dryad:
`doi:10.5061/dryad.s1rn8pk3n`.

References

[1] S. C. Weaver, C. Charlier, N. Vasilakis, and M. Lecuit, "Zika, Chikungunya, and other emerging vector-borne viral diseases," *Annu. Rev. Med.*, vol. 69, pp. 395–408, Jan. 2018.

[2] J. R. Powell and W. J. Tabachnick, "History of domestication and spread of *Aedes aegypti* — a review," *Mem. Inst. Oswaldo Cruz.*, vol. 108, pp. 11–17, 2013.

[3] J. E. Brown, B. R. Evans, W. Zheng, V. Obas, L. Barrera-Martinez, A. Egizi, H. Zhao, A. Caccone, and J. R. Powell, "Human impacts have shaped historical and recent evolution in *Aedes aegypti*, the Dengue and yellow fever mosquito," *Evolution.*, vol. 68, pp. 514–525, Feb. 2014.

[4] C. Schapheer, G. Sandoval, and C. A. Villagra, "Pest cockroaches may overcome environmental restriction due to anthropization," *J. Med. Entomol.*, vol. 55, pp. 1357–1364, June 2018.

[5] A. Y. T. Feng and C. G. Himsworth, "The secret life of the city rat: A review of the ecology of urban Norway and black rats (*Rattus norvegicus* and *Rattus rattus*)," *Urban Ecosyst.*, vol. 17, pp. 149–162, Mar. 2014.

[6] J. M. Marzluff, K. J. McGowan, R. Donnelly, and R. L. Knight, "Causes and consequences of expanding American crow populations," in *Avian Ecology and Conservation in an Urbanizing World* (J. M. Marzluff, R. Bowman, and R. Donnelly, eds.), pp. 331–363, Boston, MA: Springer US, 2001.

[7] K. P. Aplin, H. Suzuki, A. A. Chinen, R. T. Chesser, J. Ten Have, S. C. Donnellan, J. Austin, A. Frost, J. P. Gonzalez, V. Herbreteau, F. Catzeflis, J. Soubrier, Y. Fang, J. Robins, E. Matisoo-Smith, A. D. S. Bastos, I. Maryanto, M. H. Sinaga, C. Denys, R. A. Van Den Bussche, C. Conroy, K. Rowe, and A. Cooper, "Multiple geographic origins of commensalism and complex dispersal history of black rats," *PLoS One.*, vol. 6, p. e26357, Nov. 2011.

[8] D. Raoult, G. Aboudharam, E. Crubézy, G. Larrouy, B. Ludes, and M. Drancourt, "Molecular identification by "suicide PCR" of *Yersinia pestis* as the agent of medieval black death," *Proc. Natl. Acad. Sci. U.S.A.*, vol. 97, pp. 12800–12803, Nov. 2000.

[9] D. J. Gubler, E. E. Ooi, S. Vasudevan, and J. Farrar, *Dengue and Dengue Hemorrhagic Fever, 2nd Edition*. CABI, Aug. 2014.

[10] S. Christophers, *Aedes aegypti (L.) the Yellow Fever Mosquito: Its Life History, Bionomics and Structure*. Cambridge University Press, 1960.

[11] H. Briegel, "Metabolic relationship between female body size, reserves, and fecundity of *Aedes aegypti*," *J. Insect Physiol.*, vol. 36, pp. 165–172, Jan. 1990.

[12] R. S. Nasci, "Influence of larval and adult nutrition on biting persistence in *Aedes aegypti* (*Diptera*: *Culicidae*)," *J. Med. Entomol.*, vol. 28, pp. 522–526, July 1991.

[13] E. K. Lutz, C. Lahondère, C. Vinauger, and J. A. Riffell, "Olfactory learning and chemical ecology of olfaction in disease vector mosquitoes: A life history perspective," *Curr. Opin. Insect Sci.*, vol. 20, pp. 75–83, Apr. 2017.

[14] J. J. Skiff and D. A. Yee, "Behavioral differences among four co-occurring species of container mosquito larvae: Effects of depth and resource environments," *J. Med. Entomol.*, vol. 51, no. 2, pp. 375–381, 2014.

[15] M. H. Reiskind and M. Shawn Janairo, "Tracking *Aedes aegypti* (*Diptera: Culicidae*) larval behavior across development: Effects of temperature and nutrients on individuals' foraging behavior," *J. Med. Entomol.*, vol. 55, no. 5, pp. 1086–1092, 2018.

[16] J. B. Z. Zahouli, B. G. Koudou, P. Müller, D. Malone, Y. Tano, and J. Utzinger, "Urbanization is a main driver for the larval ecology of *Aedes* mosquitoes in arbovirus-endemic settings in south-eastern Côte d'Ivoire," *PLoS Negl. Trop. Dis.*, vol. 11, no. 7, p. e0005751, 2017.

[17] S. Benhamou and P. Bovet, "How animals use their environment: A new look at kinesis," *Anim. Behav.*, vol. 38, no. 3, pp. 375–383, 1989.

[18] S. G. Pavlovich and C. L. Rockett, "Color, bacteria, and mosquito eggs as ovipositional attractants for *Aedes aegypti* and *Aedes albopictus* (*Diptera: Culicidae*)," *Great Lakes Entomol.*, vol. 33, no. 2, p. 7, 2018.

[19] M. Kaiser and M. Cobb, "The behaviour of *Drosophila melanogaster* maggots is affected by social, physiological and temporal factors," *Anim. Behav.*, vol. 75, pp. 1619–1628, May 2008.

[20] R. Van Pletzen, "Larval and pupil behavior in *Culiseta longiareolata*," *J. Limnol. Soc. S. Afr.*, vol. 7, no. 1, pp. 24–28, 1981.

[21] J. R. Clopton, "A circadian rhythm in spontaneous locomotor activity in the larvae and pupae of the mosquito, *Culiseta incidens*," *Physiol. Entomol.*, vol. 4, pp. 201–207, Sept. 1979.

[22] M. Bui, J. Shyong, E. K. Lutz, T. Yang, M. Li, K. Truong, R. Arvidson, A. Buchman, J. A. Riffell, and O. S. Akbari, "Live calcium imaging of *Aedes aegypti* neuronal tissues reveals differential importance of chemosensory systems for life-history-specific foraging strategies," *BMC Neurosci.*, vol. 20, June 2019.

[23] Y. Xia, G. Wang, D. Buscariollo, R. J. Pitts, H. Wenger, and L. J. Zwiebel, "The molecular and cellular basis of olfactory-driven behavior in *Anopheles gambiae* larvae," *Proc. Natl. Acad. Sci. U.S.A.*, vol. 105, pp. 6433–6438, Apr. 2008.

[24] C. Rusch, E. Roth, C. Vinauger, and J. A. Riffell, "Honeybees in a virtual reality environment learn unique combinations of colour and shape," *J. Exp. Biol.*, vol. 220, pp. 3478–3487, Dec. 2017.

[25] A. El-Keredy, M. Schleyer, C. König, A. Ekim, and B. Gerber, "Behavioural analyses of quinine processing in choice, feeding and learning of larval *Drosophila*," *PLoS One.*, vol. 7, p. e40525, July 2012.

[26] A. Afify and C. G. Galizia, "Chemosensory cues for mosquito oviposition site selection," *J. Med. Entomol.*, vol. 52, pp. 120–130, Mar. 2015.

[27] Singh and Brown, "Nutritional requirements of *Aedes aegypti* l.," *J. Ins. Physiol*, vol. 1, pp. 199–220, 1957.

[28] E. Barber and Herskowitz, "The attraction of larvae of *Culex pipiens quinquefasciatus* say to ribonucleic acid and nucleotides," *J. Ins. Physiol*, vol. 28, no. 7, pp. 585–588, 1982.

[29] Dadd and Kleinjan, "Phagostimulation of larval *Culex pipiens* l. by nucleic acid nucleotides, nucleosides and bases," *Physiol. Entomol*, vol. 10, no. 1, pp. 37–44, 1985.

[30] C. Ellgaard and Barber, "Preferential accumulation of *Culex quinquefasciatus* (*Diptera: Culicidae*) larvae in response to adenine nucleotides and derivatives," *J. Med. Entomol*, vol. 24, no. 6, pp. 633–636, 1987.

[31] Dadd, "Nucleotide, nucleoside and base nutritional requirements of the mosquito *Culex pipiens*," *J. Insect Physiol*, vol. 25, no. 4, pp. 353–359, 1979.

[32] J. Paul, W. Jeffrey, and J. Cannon, "Production of dissolved DNA, RNA, and protein by microbial populations in a Florida reservoir," *Appl Environ Microbiol.*, vol. 56, pp. 2957–2962, Oct. 1990.

[33] R. W. Merritt, R. H. Dadd, and E. D. Walker, "Feeding behavior, natural food, and nutritional relationships of larval mosquitoes," *Annu. Rev. Entomol.*, vol. 37, pp. 349–376, 1992.

[34] W. Takken, J. J. A. van Loon, and W. Adam, "Inhibition of host-seeking response and olfactory responsiveness in *Anopheles gambiae* following blood feeding," *J. Insect Physiol.*, vol. 47, no. 3, pp. 303–310, 2001.

[35] H. C. Berg and D. A. Brown, "Chemotaxis in *Escherichia coli* analyzed by three-dimensional tracking," *Nature.*, vol. 239, pp. 500–504, Oct. 1972.

[36] G. Röder, M. Mota, and T. C. J. Turlings, "Host plant location by chemotaxis in an aquatic beetle," *Aquat. Sci.*, vol. 79, pp. 309–318, Apr. 2017.

[37] Y. H. Hussain, J. S. Guasto, R. K. Zimmer, R. Stocker, and J. A. Riffell, "Sperm chemotaxis promotes individual fertilization success in sea urchins," *J. Exp. Biol.*, vol. 219, pp. 1458–1466, May 2016.

[38] M. de Jager, F. Bartumeus, A. Kölzsch, F. J. Weissing, G. M. Hengeveld, B. A. Nolet, P. M. J. Herman, and J. van de Koppel, "How superdiffusion gets arrested: Ecological encounters explain shift from Lévy to Brownian movement," *Proc. Biol. Sci.*, vol. 281, Jan. 2014.

[39] R. Galun, L. C. Koontz, R. W. Gwadz, and J. M. C. Ribeiro, "Effect of ATP analogues on the gorging response of *Aedes aegypti*," *Physiol. Entomol.*, vol. 10, pp. 275–281, Sept. 1985.

[40] D. F. Hoel, P. J. Obenauer, M. Clark, R. Smith, T. H. Hughes, R. T. Larson, J. W. Diclaros, and S. A. Allan, "Efficacy of ovitrap colors and patterns for attracting *Aedes albopictus* at suburban field sites in north-central Florida," *J. Am. Mosq. Control Assoc.*, vol. 27, pp. 245–251, Sept. 2011.

[41] M. Bentley, "Chemical ecology and behavioral aspects of mosquito oviposition," *Annu. Rev. Entomol.*, vol. 34, no. 1, pp. 401–421, 1989.

[42] A. M. Hein, D. R. Brumley, F. Carrara, R. Stocker, and S. A. Levin, "Physical limits on bacterial navigation in dynamic environments," *J. R. Soc. Interface.*, vol. 13, p. 20150844, Jan. 2016.

[43] M. A. Goddard, A. J. Dougill, and T. G. Benton, "Scaling up from gardens: Biodiversity conservation in urban environments," *Trends Ecol. Evol.*, vol. 25, pp. 90–98, Feb. 2010.

[44] F. van Breugel, A. Huda, and M. H. Dickinson, "Distinct activity-gated pathways mediate attraction and aversion to CO_2 in *Drosophila*," *Nature.*, vol. 564, no. 7736, pp. 420–424, 2018.

[45] J. Schindelin, I. Arganda-Carreras, E. Frise, V. Kaynig, M. Longair, T. Pietzsch, S. Preibisch, C. Rueden, S. Saalfeld, B. Schmid, J.-Y. Tinevez, D. J. White, V. Hartenstein, K. Eliceiri, P. Tomancak, and A. Cardona, "Fiji: An open-source platform for biological-image analysis," *Nat. Methods.*, vol. 9, pp. 676–682, June 2012.

[46] K. L. Chan, B. C. Ho, and Y. C. Chan, "*Aedes aegypti* (L.) and *Aedes albopictus* (*Skuse*) in Singapore City. 2. Larval habitats," *Bull. World Health Organ.*, vol. 44, no. 5, pp. 629–633, 1971.

[47] C. Vinauger, E. K. Lutz, and J. A. Riffell, "Olfactory learning and memory in the disease vector mosquito *Aedes aegypti*," *J. Exp. Biol.*, vol. 217, pp. 2321–2330, July 2014.

[48] "R core team (2013). R: A language and environment for statistical computing. http://www.R-project.org/. Accessed: 2019-3-18."

Supplementary Figures

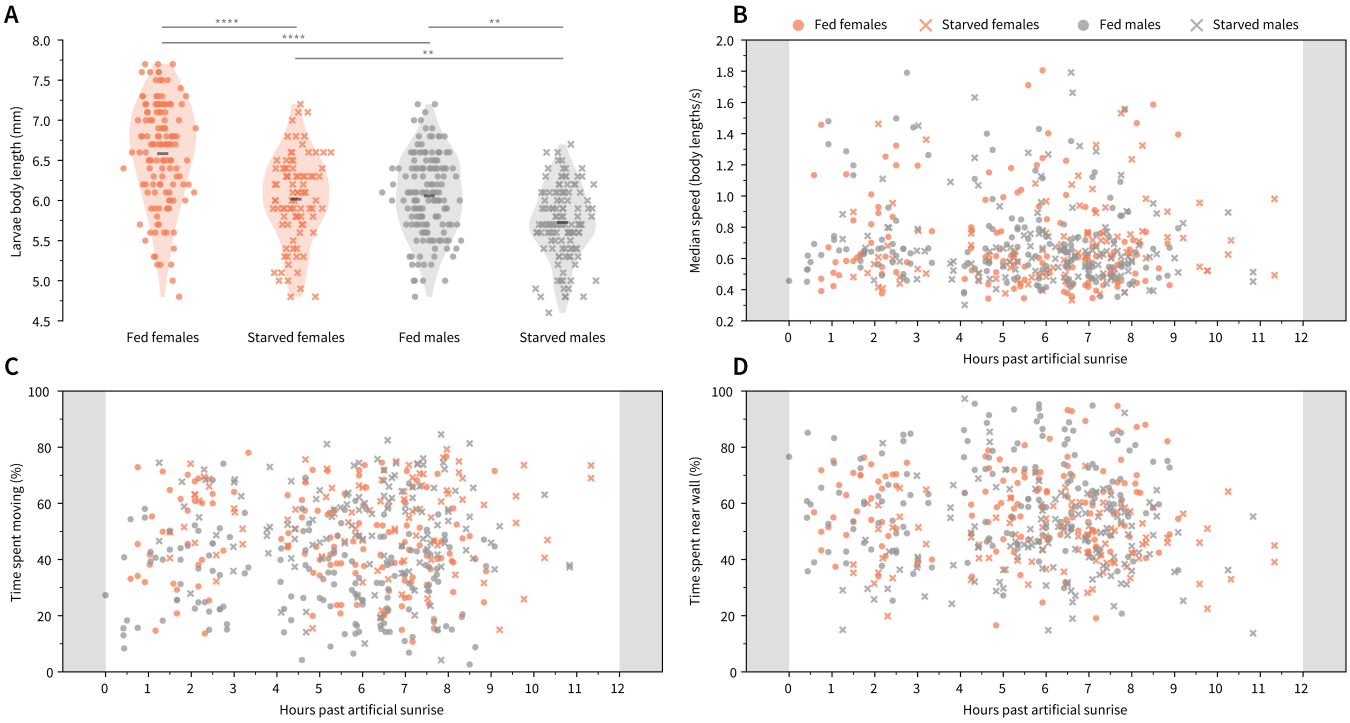

Figure S1: Effects of sex, physiological state, and circadian timing on larval physiology. A-D: Fed females (orange dots, n=135) and males (grey dots, n=153), starved females (orange × markers, n=89) and males (grey × markers, n=122). **A:** Violin plot. Scatter points show the body length (mm) for each individual, and the black bar is the mean across all individuals; asterisks denote significance values (Welch's t-test: *:p<0.05; **:p<0.01; ***:p<0.001; ****:p<0.0001). Larval body length is influenced by sex and starvation state. **B:** No change was observed in median speed (body lengths·s^{-1}) as a function of circadian timing. Note that the sampling rate throughout the day was not consistent due to the work schedule of experimenters involved in the project. **C:** No change was observed in time spent moving throughout daylight hours. **D:** No change was observed in proportion of time spent within one body length of the wall throughout daylight hours. **A-D:** For all effects shown above, we pooled measurements of all animals from the acclimation period. Our experiment results for each individual stimulus have far fewer animals for each sex, and we did not have sufficient power to analyze stimulus-specific sex differences. Nevertheless, we accounted for possible sex-specific confounds such as larval size or movement speed by normalizing the stimulus response of each animal to its activity during the pre-experiment acclimation period. In addition, we have included the sex information for each animal in our open-source code and data. We hope that the availability of this data can help inform researchers developing future experiments, even if statistical comparisons of stimulus response cannot be drawn with our current sample size.

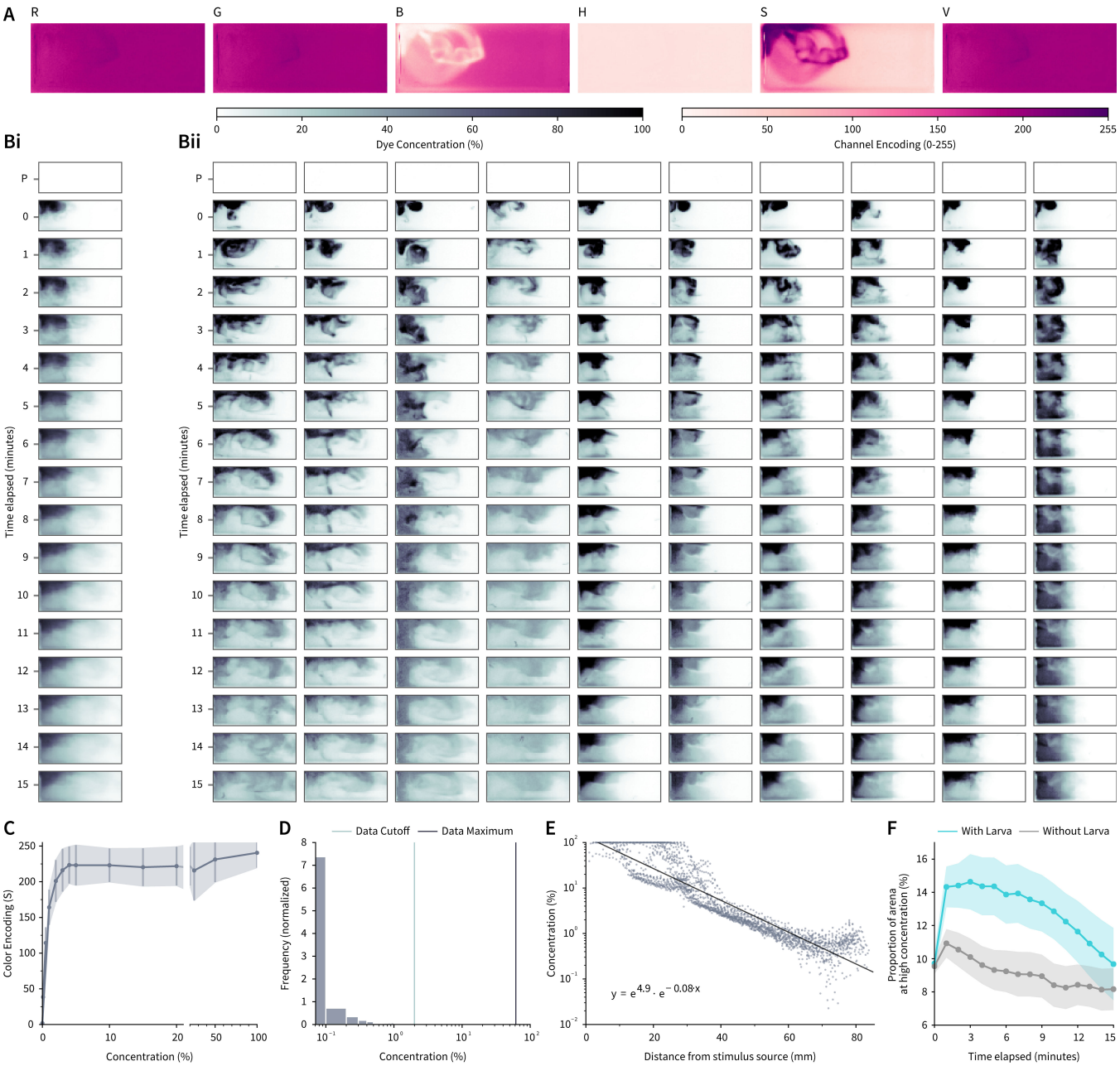

Figure S2: Creating a concentration gradient map to analyze and model larval search behavior. A: To quantify fluorescein dye diffusion, photographs were taken every minute using a Canon PowerShot ELPH 320 HS camera. Of the available color information channels (RGB, HSV), the saturation channel (S) contained the most information and was used to represent dye color throughout image analyses. **Bi:** Dye diffusion through time was quantified by the mean of all values in each 1mm^2 area, linearly interpolated through time (n=10 experiments containing larvae). A control photograph was taken before the start of each experiment (P) but was not used to construct the chemical gradient map. **Bii:** Individual variation between trials. Each column represents data from one experiment through time. **C:** Dye color (S) was converted to raw concentration values using a standardization dataset of 13 reference concentrations. 20mL of each reference concentration was poured into the entire arena and photographed. **D:** Because 100μL of dye is immediately diluted in the 20mL behavior arena water volume, reference concentration colors could not be used to directly convert color to % maximum concentration. Instead, the maximum concentration value was normalized to $\geq$95% of all color measurements across all experiments. **E:** To create a concentration map for computational simulations in different arena sizes, we analyzed the relationship between concentration and distance from stimulus source at time=0. Concentration values for individual 1$\times$1mm^2 sections across all 10 experiments at time=0 (dots), best fit line (black). **F:** Presence of a larva within the container significantly increases the spread of fluorescein dye. As a proxy for dye distribution, we measured the proportion of 1mm^2 segments within the arena with a concentration of >50%. Blue: Proportion of >50% segments in experiments with larvae; Gray: Proportion of >50% segments in experiments without larvae (n=10 each, mean $\pm$ standard error). Initial dye distribution (time=0) was not significantly different between treatments (p=0.76, Mann-Whitney U test), suggesting that subsequent observation differences are not due to experimenter bias in dye addition. Linear regression of dye distribution for all subsequent time steps (time>0) showed significant differences between containers with and without larvae (p<0.0001).

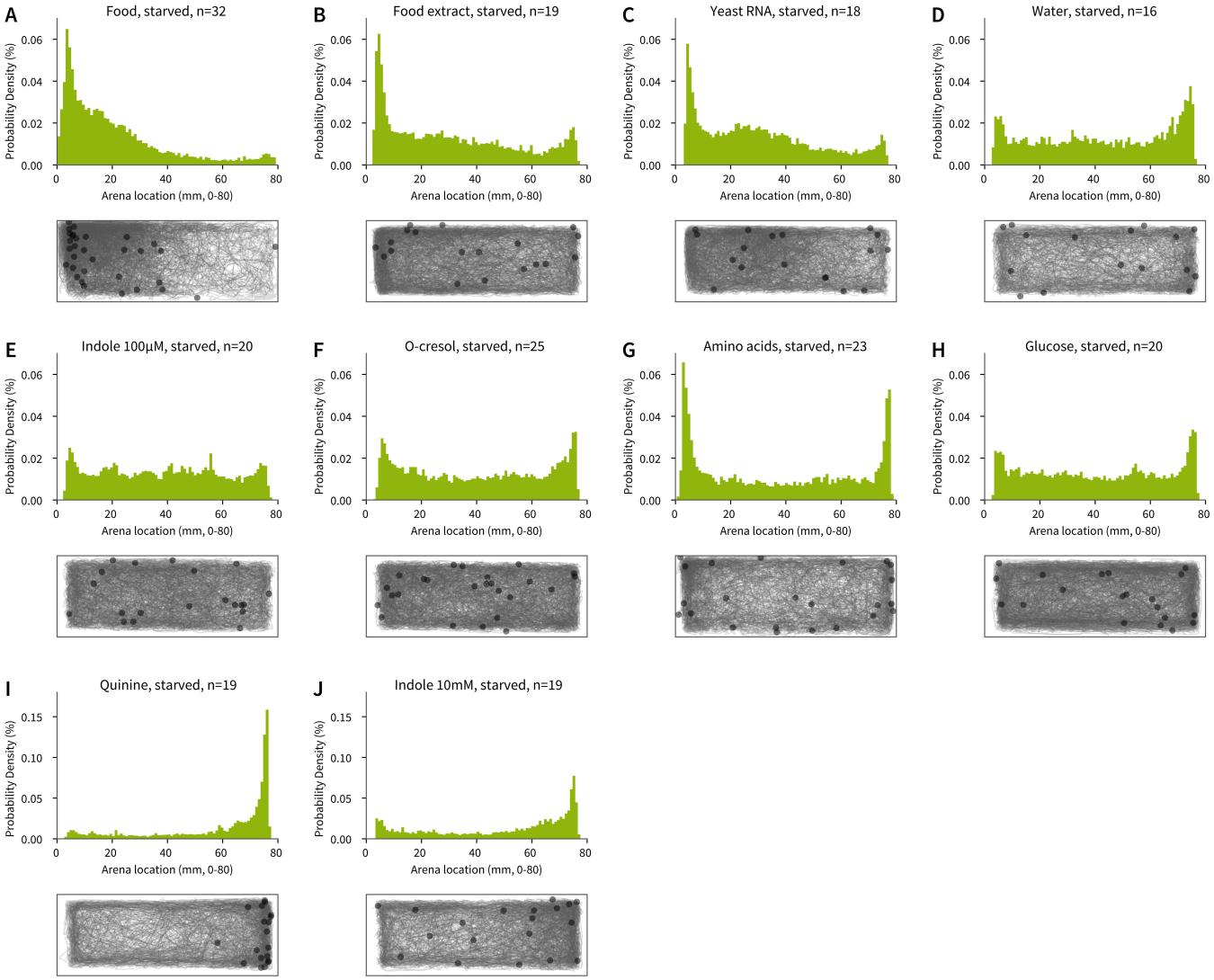

Figure S3: Response of starved larvae to experimental stimuli. A-J: Distribution and trajectories of all starved animals during the experiment phase for food (**A**), food extract (**B**), yeast RNA (**C**), water (**D**), 100μM indole (**E**), o-cresol (**F**), amino acid mixture (**G**), glucose (**H**), quinine (**I**), and 10mM indole (**J**). Although trajectories are shown aggregated into one image for each panel, all animals were tested individually. Scatter points show the position of each animal at the end of the experiment. It is important to note that these histograms show the aggregated position data from all animals throughout the entire 15 minute experiment. Thus, a single animal exhibiting strong attraction or aversion may disproportionately influence this data visualization. For statistical tests reported in this paper, a single preference value was calculated for each animal (Figure 3C) to avoid such effects.

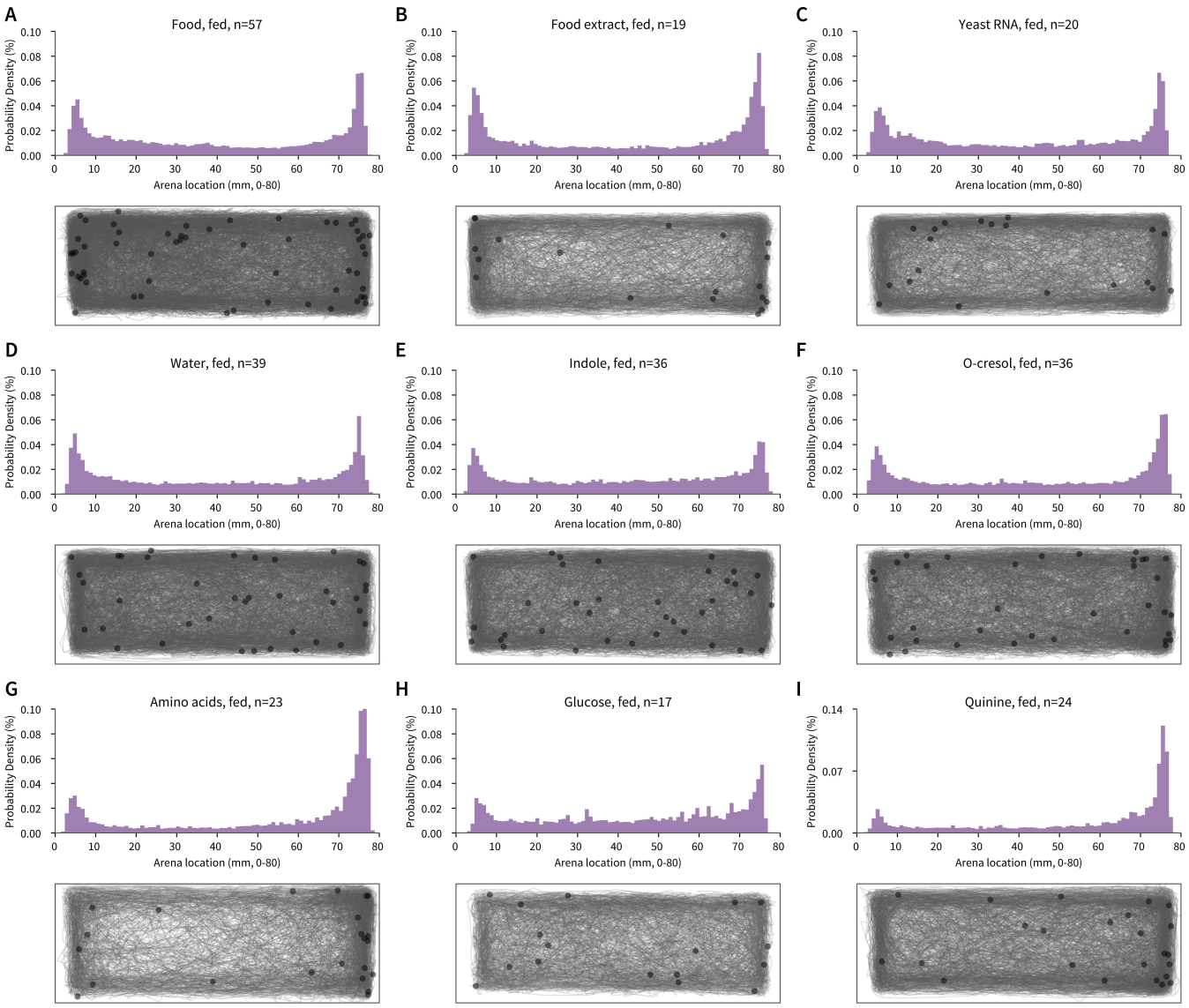

Figure S4: Response of fed larvae to experimental stimuli. A-I: Distribution and trajectories of all starved animals during the experiment phase for food (**A**), food extract (**B**), yeast RNA (**C**), water (**D**), 100μM indole (**E**), o-cresol (**F**), amino acid mixture (**G**), glucose (**H**), and quinine (**I**). Although trajectories are shown aggregated into one image for each panel, all animals were tested individually. Scatter points show the position of each animal at the end of the experiment. Note that the high distribution peaks observed at each side of the arena visualize the higher preference for walls observed in fed animals (Fig 4B). As in Fig S3, it is important to note that these histograms show the aggregated position data from all animals throughout the entire 15 minute experiment. Thus, a single animal exhibiting strong attraction or aversion may disproportionately influence this data visualization. For statistical tests reported in this paper, a single preference value was calculated for each animal (Figure 3C) to avoid such effects.

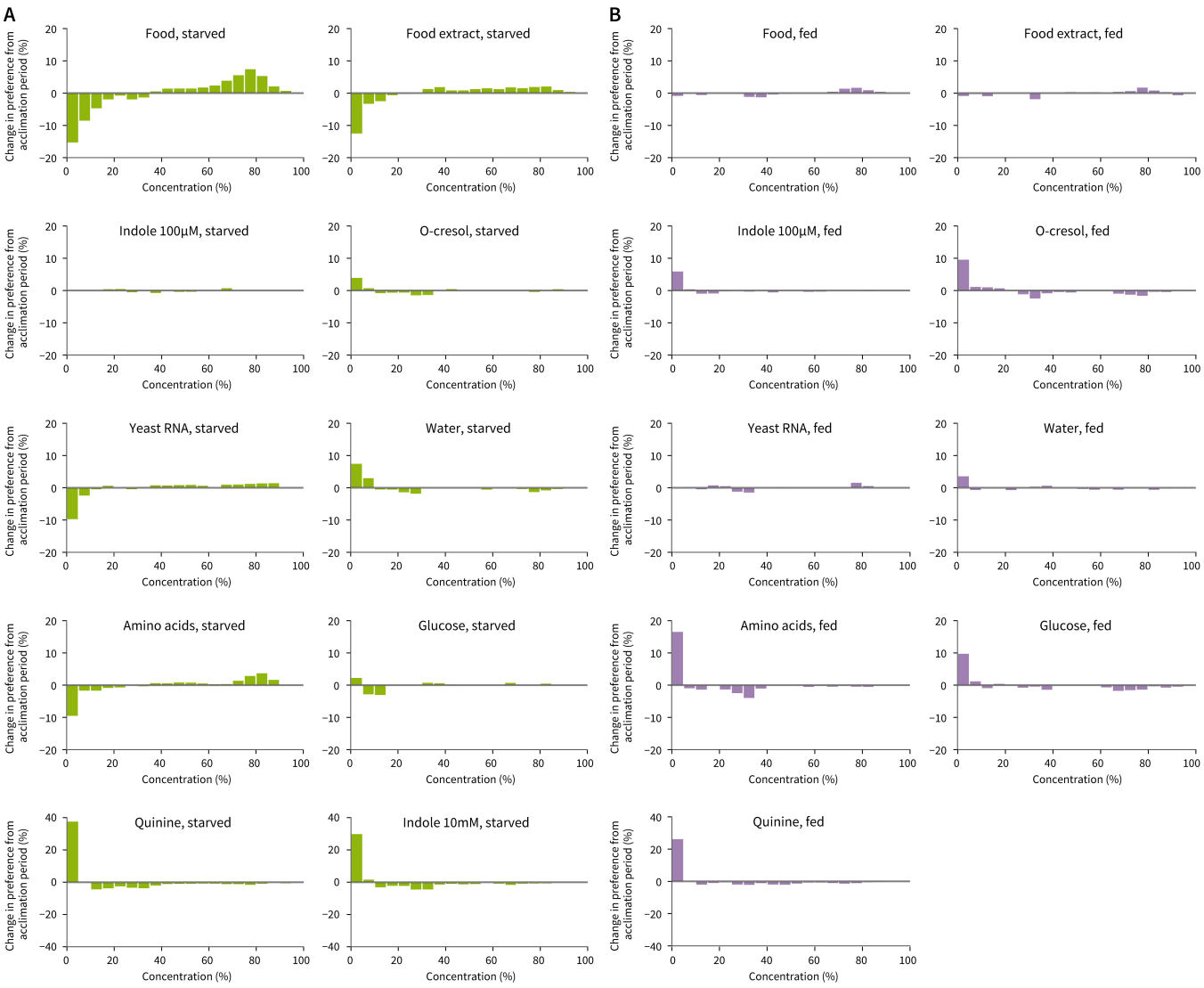

Figure S5: Behaviorally relevant stimuli concentration thresholds for starved and fed larvae. Distribution of starved (**A**) and fed (**B**) animals across the stimulus concentration map. **A-B:** Histograms visualize the change in preference for each concentration bin, normalized to larval distribution during the acclimation phase. This visualization is provided to suggest an estimate for the stimulus concentration thresholds that may be behaviorally relevant for larvae. As in Fig S3 and S4, it is important to note that these histograms show the aggregated position data from all animals throughout the entire 15 minute experiment. Thus, a single animal exhibiting strong attraction or aversion may disproportionately influence this data visualization. For statistical tests reported in this paper, a single preference value was calculated for each animal (Figure 3C) to avoid such effects.

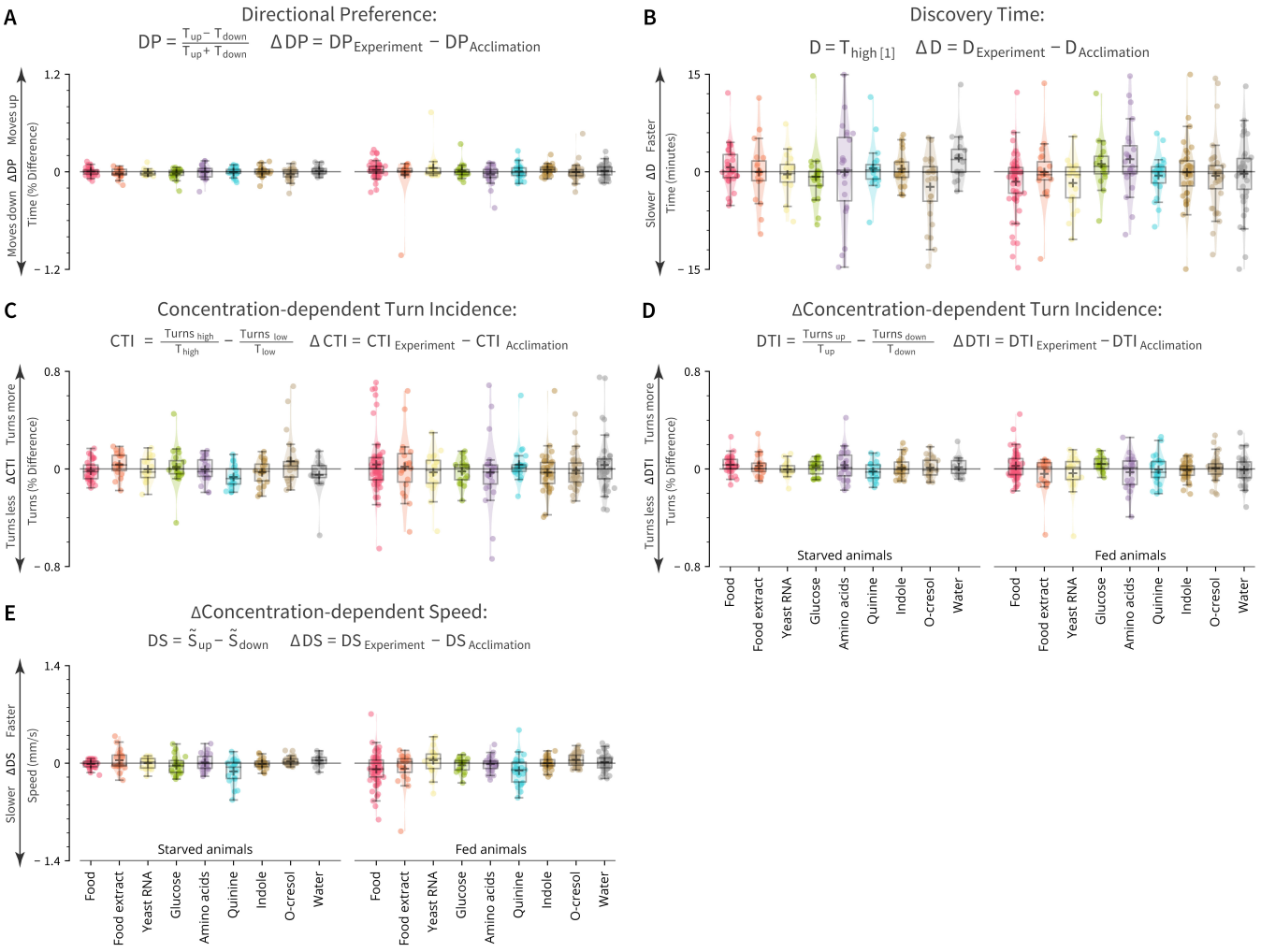

Figure S6: Larval behavior is not consistent with chemotaxis or klinokinesis search strategy models. A-E: Box plots for the population median ± 1 quartile, population mean (+ marker) and mean response for each individual (dots). We observed no significant changes across stimuli for any of these five behavioral metrics ($p>0.05$, Kruskal-Wallis test). Equations above plots denote how the behavioral metrics were calculated. **A:** Directional Preference ΔDP, difference in time (T) moving up or down the concentration map. **B:** Discovery time ΔD, time (T) elapsed before initial encounter of high concentration ($\geq$50%). **C:** Concentration-dependent Turn Incidence ΔCTI, difference in turning rate at high and low local concentrations. **D:** ΔConcentration-dependent Turn Incidence ΔDTI, difference in turning rate while moving up or down concentration. **E:** ΔConcentration-dependent Speed ΔDS, difference in mean speed ($\tilde{S}$) while moving up or down the concentration map.

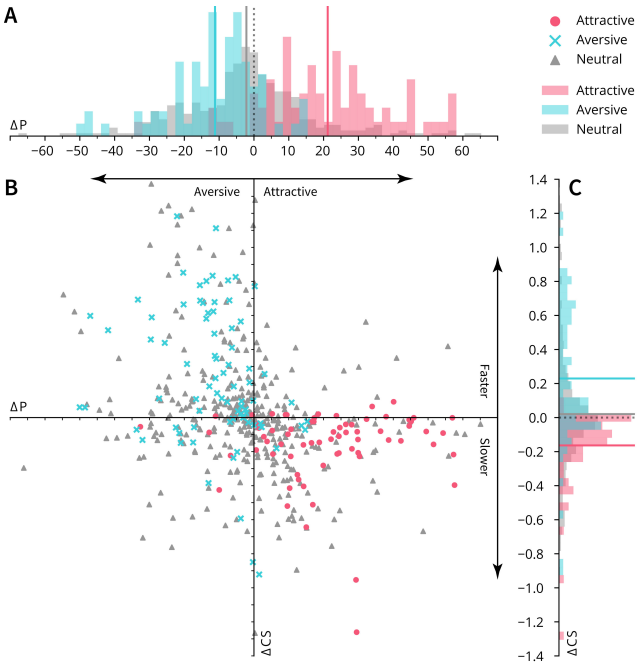

Figure S7: Larval stimulus preference is correlated to concentration-dependent movement speed. A: Normalized frequency histograms of ΔP. Mean response to aversive, neutral, and appetitive cues are visualized as solid vertical lines in the corresponding color. A dotted black line at zero indicates the expected outcome if the added stimulus had no effect on larval behavior. **B:** Larval preference (ΔP) significantly correlates with Concentration-dependent Speed (ΔCS). Results from all experiments are shown grouped into three categories: attractive (pink dots: food, food extract, and yeast RNA in starved larvae), aversive (blue × markers: quinine in fed and starved larvae; o-cresol in fed larvae), and neutral (grey triangle markers: water, indole, glucose, and amino acids in fed and starved larvae; o-cresol in starved larvae; food, food extract, and yeast RNA in fed larvae). **C:** As in **B**, except for normalized frequency histograms of larval ΔCS.

	Radius	Frequency	Examples
i	<5cm	27.8% of habitats	Ant traps
ii	5-9cm	9.7% of habitats	Tin cans, bottles
iii	9-17cm	32.3% of habitats	Jars, bowls, vases
iv	17-20cm	3.1% of habitats	Plates, pails

Table S1: Ecologically realistic habitat sizes analyzed through computational modeling. A range of habitat sizes were selected from a literature search of realistic habitat sizes for *Ae. aegypti* larvae ([46] and references therein).

Supplementary Materials and Methods

Insects

Wild-type *Ae. aegypti* (Costa Rica strain MRA-726, MR4, ATCC Manassas Virginia) were maintained in a laboratory colony as previously described [47]. Experiment larvae were separated within 24 hours of hatching and reared at a density of 75 per tray (26×35×4cm). One day before the experiment, 4-day-old larvae were isolated in Falcon^{TM} 50mL conical centrifuge tubes (Thermo Fischer Scientific, Waltham, MA, USA) containing ∼15mL milliQ water. Starved larvae were denied food for at least 24 hours before the experiment. Animals that died before eclosion or pupated during the experiment were omitted. Because it was not possible to detect younger larvae using our video tracking paradigm, we mitigated possible age-related behavioral confounds by standardizing the age of experimental larvae.

Selection and Preparation of Odorants

Odorants (indole, o-cresol) were prepared at 100μM in milliQ water (Aldrich #W259306; Aldrich #44-2361) — a concentration previously shown to be significantly attractive to *An. gambiae* mosquito larvae [23]. Indole was also prepared similarly at 10mM, a concentration that is significantly aversive to *An. gambiae* larvae [23]. Quinine hydrochloride was prepared at 10mM in milliQ water (Aldrich #Q1125). Larval food (Petco; Hikari Tropic First Bites) was prepared at 0.5% by weight in milliQ water and mixed thoroughly before each experiment to resuspend food particles. To prepare the food extract solution, 0.5% food was dissolved in milliQ water for one hour and filtered through a 0.2μm filter (VWR International #28145-477). For the yeast RNA solution, total RNA from *Saccharomyces cerevisiae* yeast was prepared at 0.1% by weight in DEPC-treated, autoclaved 0.2μm filtered water (Aldrich #10109223001; Ambion #AM9916). Yeast RNA, food, and food extract were prepared fresh daily. Glucose and the amino acid mixture were prepared at concentrations previously shown to be optimal for rearing *Ae. aegypti* larvae [27]: D-(+)-Glucose (Aldrich #G8270) was prepared at 10g·L^{-1}, and the amino acid solution consisted of L-lysine (Aldrich #L5501, 0.66g·L^{-1}), L-tryptophan (Aldrich #T0254, 0.36g·L^{-1}), L-histidine (Aldrich #H8000, 0.25g·L^{-1}), L-leucine (Aldrich #L8000, 1g·L^{-1}), L-isoleucine (Aldrich #I2752, 1.12g·L^{-1}), L-threonine (Aldrich #T8625, 0.75g·L^{-1}), L-methionine (Aldrich #M9625, 0.7g·L^{-1}), L-valine (Aldrich #V0500, 1.2g·L^{-1}), and L-arginine (Aldrich #A8094, 0.39g·L^{-1}). Although chemicals diffuse at different rates depending on molecular size and physico-chemical properties, diffusion coefficients in water were unavailable for the majority of mixtures tested. Therefore, it is important to note

that our chemical diffusion map is an approximation of the actual chemosensory environment experienced by larvae. Nonetheless, active behavior of the larva modified the chemical distribution in the arena to such a degree that any differences would be negligible.

Statistical Analyses

Statistical analyses were performed in R version 3.5.1 [48]. A Bonferroni-Holm correction was applied to all statistical analyses. A non-parametric Mann-Whitney test was used to compare body length of fed and starved males and females, because a Shapiro-Wilk normality test demonstrated that the data was not normally distributed ($p<0.05$) (Fig S1A). Linear least squares regression was used to assess the effect of time of day to animal speed, time spent moving, and time spent near walls during the acclimation phase (Fig S1B-D). Paired-samples Welch's t-tests were used to compare the median chemical concentration chosen by the larvae throughout the 15-minute experiment to the behavior of the same larvae throughout the 15-minute acclimation phase. This preference metric was also quantified as a single value (ΔP, $P_{Experiment}$-$P_{Acclimation}$, Fig 3, Fig S4). For all subsequent analyses on behavioral mechanisms, larval behavior during the acclimation phase was subtracted from larval activity during the experiment phase to normalize for differences between individuals and larval preference for corners and walls. When investigating potential differences between attraction and aversion behaviors, we grouped stimuli into cues that elicited significant attraction ($\Delta P>0$, $p<0.05$), significant repulsion ($\Delta P<0$, $p<0.05$), or neutral response ($p\geq0.05$). A non-parametric Kruskal-Wallis test was used to compare behavioral metrics among these three stimuli classes, because a Shapiro-Wilk normality test demonstrated that the data was not normally distributed ($p<0.05$) (Fig 3D, Fig S3, Fig S4). These other behavioral metrics included Directional Preference (ΔDP), defined as the difference in time moving up or down the concentration map; Discovery time (ΔD), defined as the time elapsed before initial encounter of high ($\geq$50%) concentration of the stimulus; Concentration-dependent Speed (ΔCS), defined as the difference in speed at high ($\geq$50%) and low ($<$50%) local concentrations; ΔConcentration-dependent Speed (ΔDS), defined as the difference in speed while moving up or down the concentration map; Concentration-dependent Turn Incidence (ΔCTI), defined as the difference in turning rate (turns per second, turns defined as instantaneous change in angle of $>30°$) at high and low local concentrations; and ΔConcentration-dependent Turn Incidence (ΔDTI), defined as the difference in turning rate while moving up or down the concentration map. For statistical analyses, larvae that never entered areas of high concentration were assigned a ΔD of 15 minutes, corresponding to the end of the experiment, and a ΔCS and ΔCTI of 0 (placeholder values chosen to reduce Type I error). We did not conduct statistical analyses on simulated data, and instead report overall trends in the results throughout the manuscript. This approach was chosen because the large number of replicates — which were necessary for reducing the noise introduced by randomizing the larval starting location — would artificially inflate the significance of statistical comparisons.

Chapter 3

Distinct navigation behaviors in *Aedes*, *Anopheles*, and *Culex* mosquito larvae

Eleanor K. Lutz, Kim T. Ha and Jeffrey A. Riffell

Published in: Journal of Experimental Biology. 2020

Abstract

Mosquitoes spread deadly diseases that impact millions of people every year. Understanding mosquito physiology and behavior is vital for public health and disease prevention. However, many important questions remain unanswered in the field of mosquito neuroethology, particularly in our understanding of the larval stage. In this study, we investigate the innate exploration behavior of six different species of disease vector mosquito larvae. We show that these species exhibit strikingly different movement paths, corresponding to a wide range of exploration behaviors. We also investigate the response of each species to an appetitive food cue, aversive cue or neutral control. By contrast to the large differences in exploration behavior, all species appeared to gather near preferred cues through random aggregation rather than directed navigation. Our results identify key behavioral differences among important disease vector species, and suggests that navigation and exploration among even closely related mosquito species may be much more distinct than previously thought.

Introduction

Mosquitoes are global disease vectors that transmit diseases such as malaria, Chikungunya, and dengue fever. To limit the spread of these disease vector mosquitoes, researchers have identified larval mosquito control as a highly effective public health tool [1]. In particular, naturally occurring larvicides such as methionine and *Bacillus sp.* bacteria have recently increased in popularity as an environmentally safe alternative to synthetic insecticides like DDT [1,2]. These larvicides must be ingested by larvae to be effective, and many factors affect larval feeding rate, including foraging strategy, chemosensory preference, and competition with conspecifics or individuals from other species [3–5]. In addition, larval behaviors and development rate also play an important role in adult population levels. For instance, direct competition for limited food resources at the larval stage is thought to be a major factor in the presence of certain disease vectors [6, 7]. Qualitative studies of mosquito larvae have shown different patterns of feeding and swimming behaviors [4, 5, 8], although these inter-species differences appear to be flexible and dependent upon the environment [8]. Despite growing interest [9–11], the strategies larvae use to locate sources of food, or respond to environmental stimuli, including sources of nutrients or toxic chemicals, remain poorly understood across many disease vector species. A better understanding of larval navigation and foraging behavior across mosquito species may help inform vector control techniques by suggesting where, when, and how much ingestible larvicide to apply to maximize mosquito control while minimizing cost and environmental impact.

Comparative approaches can provide important insights into the sensory and evolutionary bases of behavior. Despite the limited data on chemosensory behaviors by mosquito larvae, previous work has demonstrated differences across species in locomotion and responses to food-related stimuli [9], with these differences attributed to the adaptive use of nutrient resources and impacts of competition. For instance, multiple species of *Culex* or *Aedes* larvae may inhabit spatially-restricted containers where individuals experience interspecific competition for limited resources [6,8,12,13]. Although these species may exhibit differences in locomotory and feeding responses, like suspension feeding or browsing on surfaces, they can exhibit similar behaviors when experiencing similar environmental resources, like browsing on the surface of a leaf [8]. Larval resource use and competition have important effects on adult body size, and in the case of *Aedes albopictus*, can increase arboviral infection. Characterizing larval behaviors under different chemosensory conditions may allow determining how different species respond to different microhabitats or competitive environments.

Mosquito larvae may also provide important insight into the algorithms associated with search behaviors by aquatic insects. A previous study has shown that *Aedes aegypti* larvae find food randomly, rather than demonstrating directed motion toward preferred cues. Once a food-rich area is located, larvae decrease their swimming speed to remain in the favorable environment [14]. Previous studies in *Anopheles albimanus* [15]

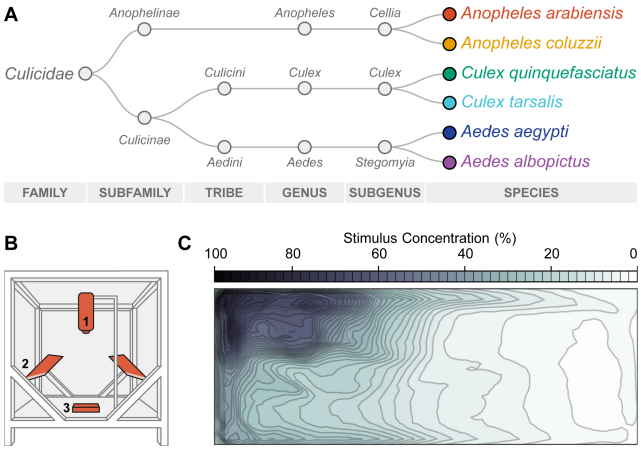

Figure 1: Summary of experimental design and methods. A: A simplified phylogeny of the six mosquito species investigated in this manuscript, adapted from [18] (branch lengths are not representative of phylogenetic distance). **B:** Diagram of the experimental rig, adapted from [14], including a Basler Scout Machine Vision GigE camera (**1**), infrared lighting (**2**) and a behavior arena filled with water (**3**). **C:** A map of stimulus distribution within the arena at 15 minutes post-stimulus addition, adapted from [14].

and *Aedes vexans* [16] larvae showed that these species also discover food at random, although the methods used in these studies prevented deeper analysis into the mechanism of navigation. This is an unusually simple foraging strategy rarely found in other insects, or even in adult mosquitoes [17]. Do other disease vector mosquito species also forage by randomly encountering food cues?

In this study we investigated the foraging and navigation behavior of six species of mosquito larvae, drawn from the three major disease vector genera *Aedes*, *Anopheles*, and *Culex* [18] (Fig 1A). These species were selected for their importance to public health and for their diversity in ecological specialization and habitat choice. In the *Aedes* genus we investigated *Ae. aegypti* and *Ae. albopictus* — the most important vectors of dengue fever and yellow fever. Although these two species are closely related, *Ae. aegypti* preferentially breeds in manmade containers [19] while *Ae. albopictus* is a generalist that may also inhabit rural and forested areas [20]. In the *Anopheles* genus we examined the malaria vectors *Anopheles arabiensis* and *Anopheles coluzzii*. Interestingly, although *An. arabiensis* and *An. coluzzii* inhabitat similar human-associated larval habitats [21,22], *An. arabiensis* drastically outcompetes *An. coluzzii* in mixed-species larval competition [3]. This suggests that these closely related species may rely on different foraging strategies, and that larval habitat specialization may not solely predict foraging behavior. Finally, we investigated *Culex quinquefasciatus*, a container-breeding mosquito, and *Culex tarsalis*, which breed in large vegetative areas such as rice fields. These two *Culex* species exhibit oviposition behavior that correspond to predation risk in their natural larval habitat (high risk and high predator avoidance for *C. tarsalis*, low risk and low predator avoidance for container-dwelling *C. quinquefasciatus*) [23]. Our exploratory study reveals striking differences in exploration behavior between all six species.

Results

Larval exploration behavior in clean water

To study the navigation behavior of each mosquito species, we used a semi-automated video analysis method previously reported in [14] (Fig 1B). We first investigated behavior in clean water during the 15 minute acclimation period (*Ae. aegypti* n=67; *Ae. albopictus* n=70; *An. arabiensis* n=93; *An. coluzzii* n=108; *C. quinquefasciatus* n=110; *C. tarsalis* n=53). The arena size used in these experiments (3×8cm) was chosen based on previous field research showing that 95% of *Ae. aegypti* and *Ae. albopictus* oviposition sites in the field were man-made containers, and that more than a quarter of these observed oviposition sites were under 5cm in radius [24], comparable to our experimental arena. Similarly, *An. gambiae* larvae were most commonly found in very small pools such as animal hoofprints in a different field study [25].

We observed striking behavioral differences across mosquito species in many aspects of exploration behavior (Fig 2A). For example, *C. tarsalis* explored the environment slowly using distinctive sweeping circles (mean number of spirals = 13.1), while the two *Anopheles* species interspersed long rests with fast, straight sprints (*An. arabiensis* mean number of spirals = 0.2; *An. coluzzii* 0.4). The two *Aedes* species, as well as *C. tarsalis*, spent the majority of the time moving (*Ae. aegypti* 56%; *Ae. albopictus* 52%; *C. tarsalis* 46%), albeit at a much lower mean speed (*Ae. aegypti* 0.8 body lengths·s^{-1}; *Ae. albopictus* 0.7 BL·s^{-1}; *C. tarsalis* 0.7 BL·s^{-1}) compared to other species (mean speed 1.3∼1.9 BL·s^{-1}; time spent moving 9∼35%). To further investigate these observations, we quantified ten different aspects of each larval trajectory, based on metrics we believed to be relevant to foraging and exploration behavior (Fig 2B-K). We found significant differences across species in all quantified measures (Fig 2B-K; $p<0.001$, Kruskal-Wallis test with Holm-Bonferroni correction).

For example, some metrics measure the frequency of exploration behavior in starved larvae, such as time spent moving and total distance traveled. Other metrics quantify known search behavior patterns in insects, such as the looping spirals observed in local-search behavior [26], frequency of sharp turns, and the number of continuous straight-line paths. Some metrics were added to assess larval response to disturbance. For example, introducing animals to the arena during the ac-

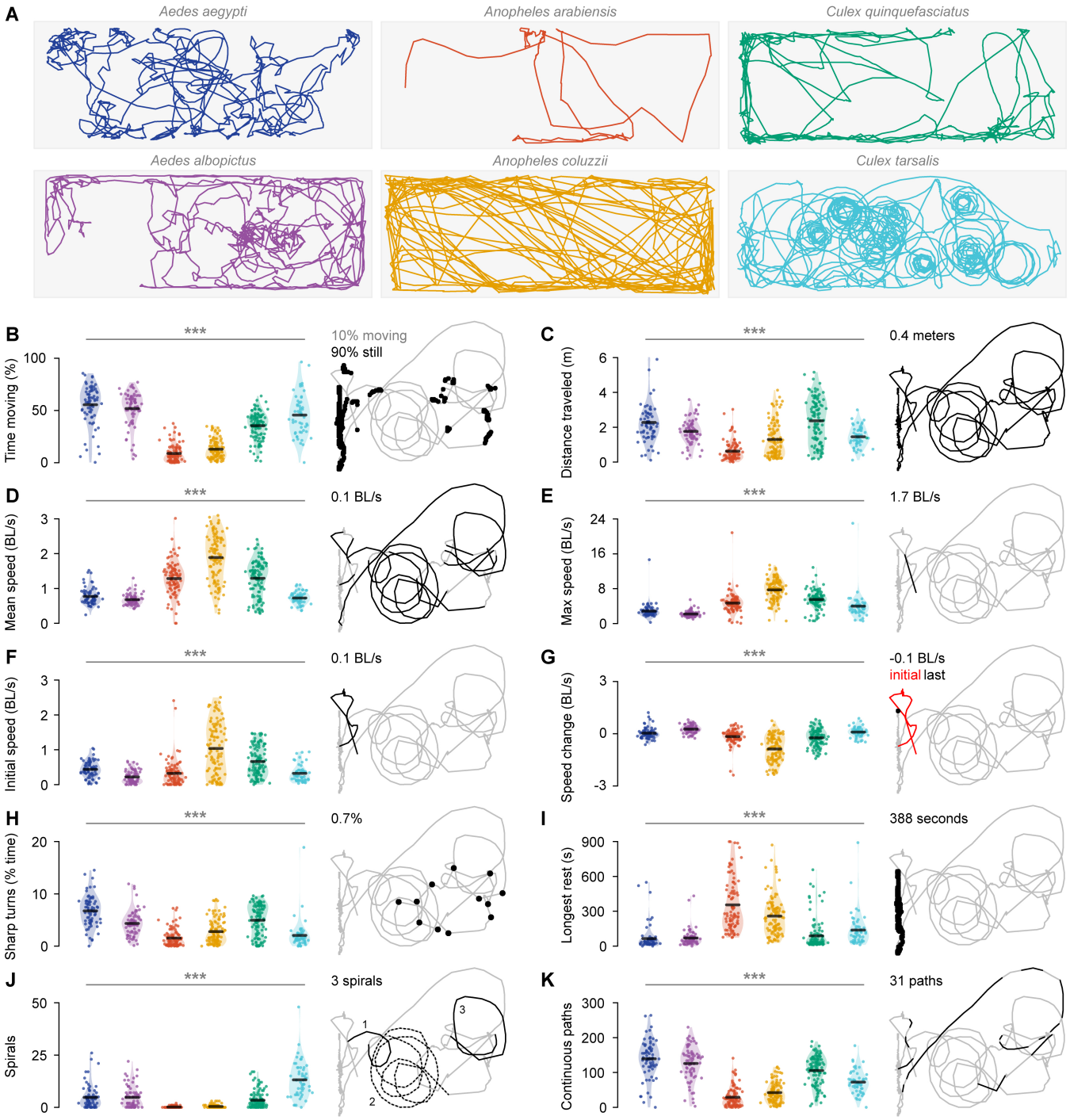

Figure 2: Larvae exhibit species-specific behavioral differences in the absence of chemosensory stimuli. A: Example trajectories visualizing one individual from each species, navigating in clean water. **B-K:** Species-specific distributions for each of ten navigation variables quantified from larval behavior in clean water. For each variable a violin plot visualizes the distribution for each species, with scatter points showing values for individual animals. A black bar marks the mean value for each species. Asterisks above each plot represents the significance of differences across species (Kruskal-Wallis test; ***: $p<0.001$). For all plots, a sample trajectory from a *C. quinquefasciatus* individual is shown on the right in gray, with red and black lines highlighting sections of the trajectory included in that variable. From left to right in all graphs: *Ae. aegypti* (navy); *Ae. albopictus* (purple); *An. arabiensis* (red); *An. coluzzii* (yellow); *C. quinquefasciatus* (green); *C. tarsalis* (aqua). **B:** Time spent moving (%) **C:** Total distance traveled (meters) **D:** Mean speed when moving (body lengths·s^{-1}) **E:** Maximum speed (body lengths·s^{-1}) **F:** Initial speed, or mean speed in first minute (body lengths·s^{-1}) **G:** Speed modification, or difference in mean speed between first and last minutes (body lengths·s^{-1}) **H:** Sharp turns (% total time spent turning >45°) **I:** Longest continuous rest period (s) **J:** Number of spirals **K:** Number of continuous paths that are not spirals.

climation phase is likely to elicit disturbance response to mechanical movement. Thus, we measured the mean speed of animals during the initial minute following introduction to the arena, as well as throughout the entire 15 minute acclimation period. We also calculated a metric subtracting the speed during the initial minute from the last (15th) minute, to quantify the change in larval behavior post-disturbance. Because we found significant differences in larval size across species (Fig S2), we normalized all speed measurements to each individual's body length (body lengths$\cdot s^{-1}$). Finally, some metrics were intended to measure the physiological capacity of the starved larvae, such as the longest rest period and maximum observed speed.

Exploration differences among species

We next investigated whether or not these observed differences were consistent with known phylogenetic relationships. In particular, do different species exhibit different trajectory patterns when all navigation variables are considered? To answer this question, we created a Euclidean distance matrix of larval trajectories by incorporating all ten navigation variables (Fig S1). We found significant differences among the six mosquito species (Fig 3, perMANOVA $p<0.001$, pseudo $F=70.7$). To visualize these results, we reduced the dimensionality of this data using Principal Component Analysis (PCA) based on the same Euclidean distance matrix (Fig 3A). PC1 and PC2 explained a significant proportion of variation in the data, but not subsequent PC axes (Monte Carlo permutation test, PC1 $p<0.001$; PC2 $p<0.001$; PC3-10: $p>0.05$). In brief, we found that larvae appeared to cluster in ordination space into four distinct categories: very fast animals (upper left); animals that traveled a long distance and conducted many sharp turns (upper right); animals that rested for long periods of time (lower left); and animals that traveled in spiral patterns and changed their behavior drastically during the 15 minute period (lower right).

We next asked if sister mosquito species display exploratory behavior that is more similar to each other than to other species. A post-hoc pairwise perMANOVA for each species-species pair showed that all species differed significantly in navigation from each other, including sister species (Table 1). We observed that both *Aedes* species were more similar to each other than to any other species (comparison of pseudo-F statistics across species-species pairs), and both *Anopheles* species were also closest to each other than to non-sister species. However, *C. quinquefasciatus* was most similar to *Ae. aegypti*, while *C. tarsalis* was most similar to *Ae. albopictus*. It is interesting to note that *C. quinquefasciatus* and *Ae. aegypti* both inhabit man-made containers, while *C. tarsalis* and *Ae. albopictus* can inhabit large vegetated areas such as rice fields and lakes. Although our study only compares six species and is not intended to draw phylogenetic conclusions, our limited panel of results suggest that both evolutionary history and ecological specialization may correlate with similar navigation behaviors in different species.

Larval response to attractive and aversive cues

Next, we examined the change in larval behavior after introduction of 0.5% food extract, 10mM quinine, or distilled water. These stimuli were chosen to investigate larval cue-finding behavior, because previous studies have shown that these cues elicit robust preferences in *Ae. aegypti* mosquito larvae [14, 27]. Corroborating a previous study [14], we found that *Ae. aegypti* significantly preferred 0.5% food extract. To quantify preference, we normalized the median concentration preferred by each larvae during the experiment phase, to the corresponding larval behavior during the acclimation phase. *Ae. aegypti* preferred a median food concentration of 20% more than would be expected from their pre-experiment behavior ($p=0.0002$, pairwise t-test). We observed similar attraction for all other species (Fig 4A): *Ae. albopictus* (+32%, $p<0.001$), *An. arabiensis* (+13%, $p=0.005$), *An. coluzzii* (+7%, $p=0.04$), *C. quinquefasciatus* (+14%, $p=0.006$), and *C. tarsalis* (+16%, $p=0.001$). Further, we investigated changes in larval behavior after introduction of 10mM quinine, an aversive tastant. Similar to our previous study [14], *Ae. aegypti* significantly avoided quinine, preferring a median concentration of 9% less than would be expected from their pre-experiment behavior ($p<0.001$). We observed similar aversion in *Ae. albopictus* (-11%, $p<0.001$), *An. arabiensis* (-7%, $p=0.002$), and *An. coluzzii* (-7%, $p=0.001$) (Fig 4A). Interestingly, neither *C. quinquefasciatus* nor *C. tarsalis* exhibited aversion to quinine (*C. quinquefasciatus* $p=0.42$; *C. tarsalis* $p=0.60$). In response to the addition of distilled water — a negative control for mechanical disturbance — all species exhibited no change in preference ($p>0.05$).

We next explored the mechanism of larval navigation to food sources. In our previous work, we found that *Ae. aegypti* explore their environment using a non-directional search strategy that results in random discovery of preferred cues [14]. In all species in this study, we found that larval preference also appeared to be consistent with random cue discovery. Discovery time did not significantly differ between water, food, and quinine for any species ($p>0.05$, Kruskal-Wallis test, Fig 4B), suggesting that larvae encounter environmental cues by random chance. In addition, we did not observe strong differences in orientation (Fig 4C) or turn frequency (Fig 4D) between different stimuli for any of the six species. Although surprising, these results are consistent with earlier literature using both video-tracking methods [14] and researcher observations [15, 16].

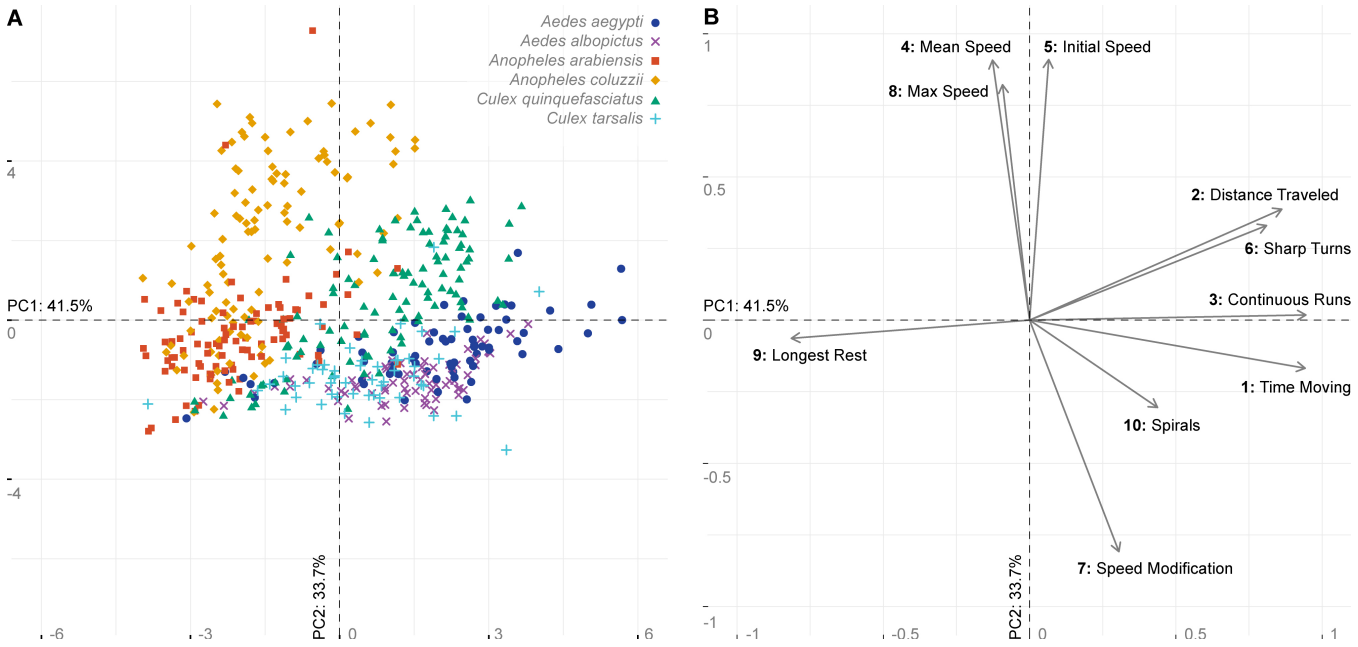

Figure 3: Larvae exhibit species-specific behavioral differences in the absence of chemosensory stimuli. A: PCA biplot of ten individual variables describing larval trajectories based on the Euclidean distance matrix visualized in Fig S1. PC1 and PC2 explain a significant proportion of variance in the original data (Monte Carlo test, PC1: 41.5%, $p<0.001$; PC2: 33.7%, $p<0.001$), while all other PC axes did not ($p>0.05$). Scatter points depict individual larvae in the ordination space, colored by species: *Ae. aegypti* (navy circles, n=67), *Ae. albopictus* (purple x markers, n=70), *An. arabiensis* (red squares, n=93), *An. coluzzii* (yellow diamonds, n=108), *C. quinquefasciatus* (green triangles, n=110), and *C. tarsalis* (aqua + markers, n=53). **B:** Vector arrows (**1-10**) indicate the direction of variable gradients in the ordination space. Ordered from highest to lowest contribution to PC1 and PC2, these variables include: **1:** Time spent moving (variable contribution to PC1: 21.4%; PC2: 0.8%); **2:** Distance traveled (PC1: 17.9%; PC2: 4.5%); **3:** Continuous paths (PC1: 21.5%; PC2: 0%); **4:** Mean speed (PC1: 0.4%; PC2: 24.5%); **5:** Initial speed in first minute (PC1: 0.1%; PC2: 24.6%); **6:** Sharp turns (PC1: 15.8%; PC2: 3.2%); **7:** Speed modification, or the difference in mean speed between first and last minutes (PC1: 2.2%; PC2: 19.4%); **8:** Maximum speed (PC1: 0.2%; PC2: 20.1%); **9:** Longest rest period (PC1: 16%; PC2: 0.1%); and **10:** Spirals (PC1: 4.6%; PC2: 2.8%)

In our previous study, we were able to conduct deep analyses and simulations into the mechanism of *Ae. aegypti* navigation, using a dataset of over 500 individual animals observed independently, with approximately 2 million total data points. In this current study, we did not have the necessary data to conduct the simulations or 3,000 experiments necessary for similar analyses across species. Nevertheless, we visualized some of the same behavioral changes as a reference for future experiments (Fig S3, Fig S4, Fig S5). We found several interesting patterns in these datasets. For example, in the vast majority of cases, animals did not appear to change their behavior — such as the number of looped searches or sharp turns — after addition of the stimulus. In cases where animals did change their behavior — such as *An. coluzzii*, which decreased initial speed in the post-stimulus period — animals seemed to exhibit the same behavioral changes for all experiments, independently of the stimulus added. Corroborating our previous results, we found that in our current work, *Ae. aegypti* also appear to aggregate near preferred cues by decreasing their movement speed near preferred areas (Fig S4). Interestingly, we observed the same pattern for *Ae. albopictus* but not for any other species (Fig S4). Similarities between closely related species was reflected in the PCA analyses: the exploration responses were often distinct between species (Figs. 3A, S4K). However, once food was added, all the species significantly slowed their swimming speeds, causing them to cluster in the PCA space (Fig. S4N). Although further experiments are necessary to understand these results, it is likely that the *Anopheles* and *Culex* species in our study use different kinematic changes to navigate with respect to chemosensory cues, such as adjusting their turning frequency.

Discussion

Our results raise several interesting questions for future research. In our experiments investigating larval cue-finding, we predicted that larvae may exhibit navigation strategies adapted to their environment, with species living in small containers displaying different strategies than those that breed in larger lakes or streams. However, our results showed that the six different species of mosquito larvae were strikingly homogeneous in their chemosensory responses to food: none of the species were able to change their behavior to find food cues faster in our experimental paradigm.

	Aedes aegypti	*Aedes albopictus*	*Anopheles arabiensis*	*Anopheles coluzzii*	*Culex quinquefasciatus*	*Culex tarsalis*
Aedes aegypti		11.12 ***	89.92 ***	115.66 ***	25.66 ***	20.13 ***
Aedes albopictus	5.54		99.66 ***	118.58 ***	38.73 ***	16.96 ***
Anopheles arabiensis	0.76	0.03		33.10 ***	71.41 ***	48.50 ***
Anopheles coluzzii	1.44	6.79	18.19 ***		69.04 ***	63.56 ***
Culex quinquefasciatus	4.90	18.77 ***	21.33 ***	0.06		29.69 ***
Culex tarsalis	0.02	4.84	0.22	3.15	3.21	

Table 1: Comparisons of navigation patterns among species. Values in upper right half of the matrix represent pseudo-F statistics from pairwise perMANOVA tests. Asterisks after each value indicate the significance of the corresponding p-value after Bonferroni correction: *: $p<0.05$; **: $p<0.01$; ***: $p<0.001$; no asterisk: not statistically significant. In the upper right, significant values with a high pseudo-F statistic represent species-species pairs that exhibit statistically significant differences in overall navigation behavior. Values in the lower left half of the matrix represent F statistics for a pairwise test of multivariate dispersion (ANOVA with Bonferroni correction). Significant values with a high F-statistic in the bottom half of the matrix represent species-species pairs with statistically significant differences in the intra-species variability of navigation behavior. These results suggest that some, but not all, of the observed differences between species-species pairs may be due to differences in behavioral diversity among individuals, rather than in differences in raw behavioral metrics.

Are there intrinsic physical properties to chemical diffusion in small, stagnant aquatic environments that makes more directed navigation particularly difficult? Although many of the species examined are naturally adapted to habitats of similar size to the experimental arena [9, 19], it is possible that larvae may exhibit different navigation strategies in larger environments where the chemical gradients may be shallower or influenced by turbulent kinetic motion. Additionally, are there physiological limitations to larval chemosensation, such as the sensitivity of receptors or complexity of neural processing circuits, that prevent larvae from utilizing more complex navigation processes?

Second, is there an evolutionary benefit to different navigation behaviors exhibited by each species in clean water? Interspecific larval competition significantly affects distribution of mosquito species in the wild and in laboratory experiments [3, 28, 29]. It is possible that this competitive environment drives larvae to exploit different foraging niches through different navigation strategies. Alternatively, it is possible that the different environmental conditions preferred by each species, such as lakes, streams, and containers, result in different navigation strategies consistent across habitats. Although our study did not examine enough species to quantitatively answer this question, it is interesting to note that *Aedes* and *Anopheles* mosquito larvae exhibited greater similarity to sister species even when the sister species inhabited vastly different natural larval habitats. By contrast, the two *Culex* species exhibited the greatest similarity toward non-sister species that inhabited similar ecological environments.

It is important to note that our investigative study may not address important characteristics of mosquitoes found in the wild. For example, although all larvae analyzed in this study successfully completed development under the same laboratory rearing conditions, it is likely that environmental variables including temperature, concentration of dissolved organic matter, and water depth were more optimal for some species than others. Indeed, species exhibited significantly different mortality rates post-experiment, suggesting that the 24-hour starvation period may have been more stressful for some species (Fig S2). In addition, our experimental trials only observed larvae for a total of 15 minutes after stimulus addition, and it is possible that larvae may exhibit different behaviors in longer time scales.

Nevertheless, we believe that this study reveals an important area of future research. To our knowledge, this is the first study to quantitatively compare exploration behavior among mosquito larvae using machine vision rather than researcher observations. Even among the small subset of species examined in this study, we saw immediate and clear differences in exploration, stimulus preference, and chemosensory navigation. Future studies incorporating additional mosquito species — especially outgroups that are not disease vectors — would add fascinating comparisons that may help clarify the evolutionary basis of exploration behavior in mosquitoes. Furthermore, with the advent of new tools to examine the sensory bases of behaviors, including binary expression systems for cell-type specific labeling and manipulation [30, 31], it may soon be possible to interrogate and functionally link different navigational behaviors with the sensory channels mediating those responses. Because laboratory arena sizes and rearing conditions are already within the natural range of many mosquito species, mosquito larvae may be a promising field for phylogenetic behavior questions from a practical perspective. Finally, our results underscore the importance of understanding disease vector behavior at all life history stages. We suggest that species-specific vector control research may be particularly important to improving disease prevention.

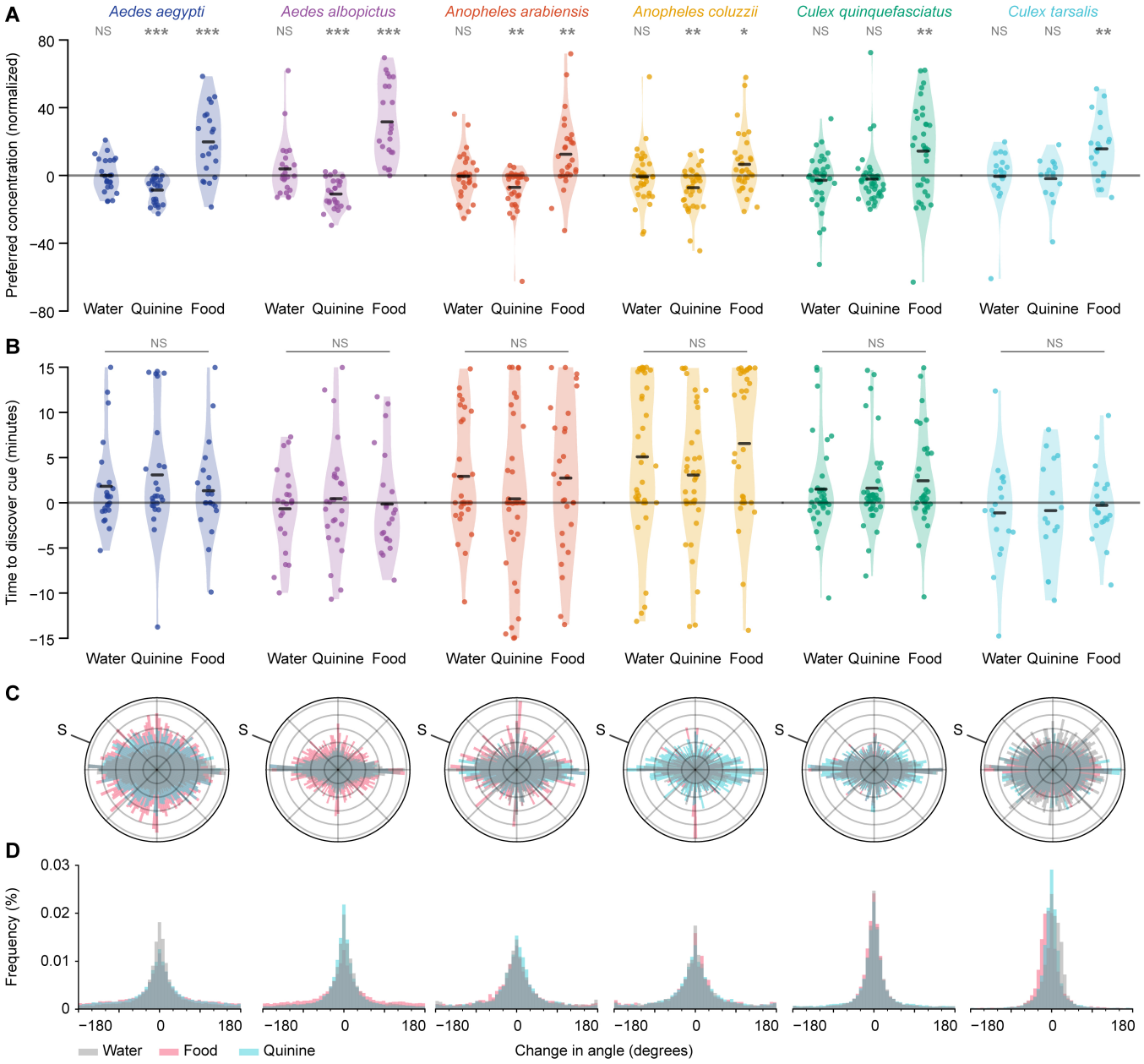

Figure 4: Larval gathering near preferred cues is more consistent with passive aggregation than active navigation. A: All larval species were significantly attracted to food extract. With the exception of the two *Culex* species, larvae were also significantly repelled by the aversive tastant quinine. **B:** However, none of the six larval species were able to change their navigation behavior to find food faster, or delay occupying high-concentration areas of quinine: *Ae. aegypti* (p=0.60, Kruskal-Wallis test); *Ae. albopictus* (p=0.71); *An. arabiensis* (p=0.52); *An. coluzzii* (p=0.22); *C. quinquefasciatus* (p=0.64); *C. tarsalis* (p=0.93). **C:** For all species, animals did not appear to change their behavior to move towards or away from any stimuli. Polar plots showing aggregated movement direction for all animals throughout the 15 minute experiment for water (grey), food (pink) or quinine (light blue). The label "S" marks the approximate direction of each stimulus. Each bar in the polar plot represents the proportion of time that animals moved in that specific direction. For visualization purposes, all polar plots are normalized to the maximum frequency for each stimulus. **D:** Turning frequency for each species did not appear to change depending on the added stimulus. Frequency histograms for aggregated larval turning frequency in response to the addition of water (grey), food (pink) or quinine (light blue). Y axis ranges are identical for all six plots. **C-D:** To reduce noise from passively drifting animals, plots only include data where larvae were moving at 1mm·s^{-1}. Although our experiments did not have sufficient power to statistically inspect these differences, animals do not appear to significantly change orientation across stimuli.

Materials and Methods

Mosquitoes

Six species of wild-type mosquitoes were obtained from BEI Resources (NIAID, NIH): *Ae. aegypti* (Strain COSTA RICA, MRA-726, contributed by William G. Brogdon), *Ae. albopictus* (Strain ATM-NJ95, Centers for Disease Control and Prevention for distribution by BEI, NR-48979), *An. arabiensis* (Strain DONGOLA, MRA-856, contributed by Mark Q. Benedict), *An. coluzzii* (Strain Ngousso, MRA-1279, contributed by Frédéric Simard), *C. quinquefasciatus* (Strain JHB, NR-43025), and *C. tarsalis* (Strain YOLO, NR-43026). All species were reared in milliQ water in a shallow tray (26×35×4cm) and fed with fish food (Petco; Hikari Tropic First Bites). Larvae were reared using the circadian cycle recommended by species-specific BEI rearing guidelines (16:8 light:dark for *C. tarsalis*; 12:12 for all other species). One day before the experiment, L3-stage larvae were isolated in Falcon^{TM} 50mL conical centrifuge tubes (Thermo Fischer Scientific, Waltham, MA, USA) containing ∼15mL milliQ water. Starved larvae were denied food for at least 24 hours before the experiment. Animals that died before eclosion or pupated during the experiment were omitted, and all animals were tested during the light phase of their circadian cycle.

Preparation of Odor Stimuli

Stimuli were used that elicited robust behavioral responses across species. Two stimuli were used: an attractive food solution and quinine, a compound that elicits aversion in *Ae. aegypti* larvae [14]. The food extract solution was made fresh daily by dissolving 0.5% food (Petco; Hikari Tropic First Bites) in milliQ water for one hour, then passing the mixture through a 0.2μm filter (VWR International 28145-477) to remove solid particulates. Quinine hydrochloride was prepared at 10mM in milliQ water (Aldrich Q1125). For all species, we saw no difference in mortality between the three treatments (p=1 for all species, Fig S2), suggesting that exposure to quinine or food extract did not significantly harm larvae physiologically.

Behavior Arena and Imaging

We computed the trajectories of individual larvae in a custom behavior arena as previously described [14, 27]. Briefly, individual larvae were introduced to a 8×3cm rectangular behavior arena containing 20mL of distilled milliQ water. Larvae were allowed to acclimate within the dark arena for 15 minutes, while being recorded by a Basler Scout Machine Vision GigE camera under infrared light. Subsequently, 100μL of one stimulus was pipetted gently into the upper left corner of the arena (Fig 1C), and larval behavior was recorded for an additional 15 minutes. In a separate experiment without larvae, we pipetted 100μL of fluorescein dye into an identically shaped arena, in order to map stimulus concentration within the arena throughout the 15 minute experiment [14] (Fig 1C). Trajectory paths were extracted from each video using Multitracker software by Floris van Breugel [32] and additional code developed previously [14]. We visually inspected each trajectory path and manually corrected errors and omissions introduced by the tracking software.

Trajectory Quantification

During foraging and swimming behaviors, mosquito larva can exhibit species-specific differences in their swimming kinematics and behaviors, including changing the duration of activity [33], increasing or decreasing their swim speeds, or exhibiting complex changes in locomotion [5]. We thus quantified ten aspects of larval navigation in clean water to represent many of these ecologically relevant behaviors. Time spent moving was quantified as a proportion (0-100%), with movement defined as >1mm·s^{-1}. Total distance traveled was measured in meters. To normalize for any size-specific differences across individuals or species (Fig S2), we converted larval speed measurements into body lengths per second. Experimenters were blind to larval species or sex when measuring body lengths. Thus, body lengths·s^{-1} were used for quantifying maximum speed, mean speed when moving, mean speed in first minute, and the difference in mean speed between first and last minutes. Spirals were defined as a distinct time period in which larvae engaged in >4 seconds of continuous spiraling movement. Sharp turns were defined as turns of >45° conducted at a speed of >4mm·s^{-1}. Continuous paths were defined as sustained movement at the same Δ angle, not including spirals. Rests were defined as periods of time >10 seconds of no movement.

Statistical Analyses

Statistical analyses were performed in R [34] and in Python [35]. We used a non-parametric Kruskal-Wallis test with Bonferroni correction to compare navigation characteristics across species for each of the ten aspects of larval navigation (Fig 2), because we found that not all variables followed a normal distribution (Shapiro-Wilk test, p>0.05). To create the Euclidean distance matrix for larval similarity analysis (Fig S1), we first standardized all variables to zero mean and unit variance. To compare larval trajectories across species, both as a group of six and in species-species pairs, we used a perMANOVA and test of multivariate dispersion ANOVA with a Bonferroni correction (Table 1). We used a Monte Carlo permutation test to select significant eigenvectors for visualization in our PCA ordination (Fig 3). We used a pairwise t-test to

compare larval preference for different stimuli for each species (Fig 4A). Preference was defined as the median concentration preferred by the larvae during the 15 minute experiment, normalized to the areas chosen by the same larva during the preceding 15 minute acclimation phase. This normalization was necessary to control for innate larval preference for corners or walls reported in some species [14]. Discovery time across different stimuli were compared for each species using a non-parametric Kruskal-Wallis test (Fig 4B). A non-parametric test was used because we found that discovery time data did not follow a normal distribution (Shapiro-Wilk test, $p>0.05$). Discovery time was defined as the time taken (in seconds) to first encounter a section of the behavioral arena $\geq$50% concentration, normalized to the time taken to first encounter the same area during the clean water acclimation period. We used a Fisher's Exact Test with Bonferroni correction to assess mortality differences among larval species, as well as among experimental treatments in larvae of the same species (Fig S2). We used a non-parametric Kruskal-Wallis test to compare body length between different species (Fig S2), because we found that body length data did not follow a normal distribution for all species (Shapiro-Wilk test, $p>0.05$).

Acknowledgements

We thank Floris van Breugel for assistance in developing methods for video data analysis, and Julian Olden for advice on statistical methods. We also thank Binh Nguyen and Kara Kiyokawa for maintaining the Riffell lab mosquito colony, and Dustin Miller for advice on rearing mosquitoes procured from the CDC. Finally, we thank two anonymous peer reviewers for their time and effort in suggesting helpful revisions to this manuscript.

Author Contributions

Conceptualization: E.K.L. and J.A.R.; Methodology: E.K.L. and J.A.R.; Software: E.K.L.; Investigation: K.T.H. and E.K.L.; Resources: E.K.L. and J.A.R.; Data Curation: E.K.L. and K.T.H.; Writing — Original Draft: E.K.L; Writing — Review and Editing: E.K.L, J.A.R, and K.T.H.; Visualization: E.K.L. and K.T.H.; Supervision: J.A.R.; Project Administration: J.A.R; Funding acquisition: J.A.R., E.K.L., and K.T.H.

Declaration of Interests

The authors declare no competing financial interests.

Funding

This work was supported in part by the National Institute of Health grants RO1DCO13693-04 and R21AI137947 to J.A.R.; National Science Foundation grant DGE-1256082 to E.K.L.; Air Force Office of Sponsored Research under grant FA9550-16-1-0167 to J.A.R.; CoMotion Innovations Scholarship to K.T.H.; Robin Mariko Harris Award to E.K.L.; and the Margo and Tom Wyckoff Award to E.K.L.

Additional Files

Code associated with this manuscript can be found at: `https://github.com/eleanorlutz/aedes-aegypti-2020`.

References

[1] E. N. Weeks, J. Baniszewski, S. A. Gezan, S. A. Allan, J. P. Cuda, and B. R. Stevens, "Methionine as a safe and effective novel biorational mosquito larvicide," *Pest Manag. Sci.*, vol. 75, pp. 346–355, Feb. 2019.

[2] L. Regis, S. B. da Silva, and M. A. Melo-Santos, "The use of bacterial larvicides in mosquito and black fly control programmes in Brazil," *Mem. Inst. Oswaldo Cruz*, vol. 95 Suppl 1, pp. 207–210, 2000.

[3] M. F. Hartman, "Malaria mosquito larvae in competition for limited resources," B.S. Thesis, 2016.

[4] W. A. Ramoska and T. L. Hopkins, "Effects of mosquito larval feeding behavior on *Bacillus sphaericus* efficacy," *J. Invertebr. Pathol.*, vol. 37, pp. 269–272, May 1981.

[5] R. W. Merritt, R. H. Dadd, and E. D. Walker, "Feeding behavior, natural food, and nutritional relationships of larval mosquitoes," *Annu. Rev. Entomol.*, vol. 37, pp. 349–376, 1992.

[6] S. N. Bevins, "Invasive mosquitoes, larval competition, and indirect effects on the vector competence of native mosquito species (*Diptera: Culicidae*)," *Biol. Invasions*, vol. 10, no. 7, pp. 1109–1117, 2008.

[7] B. W. Alto, L. P. Lounibos, S. Higgs, and S. A. Juliano, "Larval competition differentially affects arbovirus infection in *Aedes* mosquitoes," *Ecology*, vol. 86, pp. 3279–3288, Dec. 2005.

[8] D. A. Yee, B. Kesavaraju, and S. A. Juliano, "Larval feeding behavior of three co-occurring species of container mosquitoes," *J. Vector Ecol.*, vol. 29, no. 2, p. 315, 2004.

[9] J. J. Skiff and D. A. Yee, "Behavioral differences among four co-occurring species of container mosquito larvae: Effects of depth and resource environments," *J. Med. Entomol.*, vol. 51, pp. 375–381, Mar. 2014.

[10] M. H. Reiskind and M. Shawn Janairo, "Tracking *Aedes aegypti* (*Diptera: Culicidae*) larval behavior across development: Effects of temperature and nutrients on individuals' foraging behavior," *J. Med. Entomol.*, 2018.

[11] J. B. Z. Zahouli, B. G. Koudou, P. Müller, D. Malone, Y. Tano, and J. Utzinger, "Urbanization is a main driver for the larval ecology of *Aedes* mosquitoes in arbovirus-endemic settings in south-eastern Côte d'Ivoire," *PLoS Negl. Trop. Dis.*, vol. 11, p. e0005751, July 2017.

[12] S. A. Juliano, "Species interactions among larval mosquitoes: Context dependence across habitat gradients," *Annu. Rev. Entomol.*, vol. 54, pp. 37–56, 2009.

[13] P. D. Workman and W. E. Walton, "Larval behavior of four *Culex* (*Diptera: Culicidae*) associated with treatment wetlands in the southwestern United States," *J. Vector Ecol.*, vol. 28, pp. 213–228, Dec. 2003.

[14] E. K. Lutz, T. S. Grewal, and J. A. Riffell, "Computational and experimental insights into the chemosensory navigation of *Aedes aegypti* mosquito larvae." Mar. 2019.

[15] C. Aly and S. Mulla, "Orientation and ingestion rates of larval *Anopheles albimanus* in response to floating particles," *Entomol. Exp. Appl.*, vol. 42, pp. 83–90, Sept. 1986.

[16] C. Aly, "Feeding rate of larval *Aedes vexans* stimulated by food substances," *J. Am. Mosq. Control Assoc.*, vol. 1, pp. 506–510, Dec. 1985.

[17] W. Takken and B. G. J. Knols, *Olfaction in Vector-host Interactions*. Wageningen Academic Pub, 2010.

[18] L. Ruzzante, M. J. M. F. Reijnders, and R. M. Waterhouse, "Of genes and genomes: Mosquito evolution and diversity," *Trends Parasitol.*, vol. 35, pp. 32–51, Jan. 2019.

[19] S. Christophers, *Aedes aegypti (L.) the yellow fever mosquito: Its life history, bionomics and structure*. Cambridge University Press, 1960.

[20] L. Mousson, C. Dauga, T. Garrigues, F. Schaffner, M. Vazeille, and A.-B. Failloux, "Phylogeography of *Aedes* (*Stegomyia*) *aegypti* (l.) and *Aedes* (*Stegomyia*) *albopictus* (*Skuse*) (*Diptera: Culicidae*) based on mitochondrial DNA variations," *Genet. Res.*, vol. 86, pp. 1–11, Aug. 2005.

[21] N. Minakawa, J. C. Beier, J. I. Githure, C. M. Mutero, and G. Yan, "Spatial distribution and habitat characterization of *Anopheline* mosquito larvae in Western Kenya," *Am. J. Trop. Med. Hyg.*, vol. 61, no. 6, pp. 1010–1016, 1999.

[22] J. Etang, A. M. Mbida, P. N. Akono, J. Binyang, C. E. E. Moukoko, L. G. Lehman, P. Awono-Ambene, A. Talipouo, W. E. Eyisab, D. Tagne, R. Tchoffo, L. Manga, and R. Mimpfoundi, "*Anopheles coluzzii* larval habitat and insecticide resistance in the island area of Manoka, Cameroon," *BMC Infect. Dis.*, vol. 16, p. 217, May 2016.

[23] A. R. Van Dam and W. E. Walton, "The effect of predatory fish exudates on the ovipostional behaviour of three mosquito species: *Culex quinquefasciatus*, *Aedes aegypti* and *Culex tarsalis*," *Med. Vet. Entomol.*, vol. 22, no. 4, pp. 399–404, 2008.

[24] Y. C. Chan, B. C. Ho, and K. L. Chan, "*Aedes aegypti* (l.) and *Aedes albopictus* (*Skuse*) in Singapore City. 2. larval habitats," *Bull. World Health Organ.*, vol. 44, no. 5, pp. 629–633, 1971.

[25] N. Minakawa, G. Sonye, M. Mogi, and G. Yan, "Habitat characteristics of *Anopheles gambiae s.s.* larvae in a Kenyan highland," 2004.

[26] W. J. Bell, "Searching behavior patterns in insects," *Annu. Rev. Entomol.*, vol. 35, pp. 447–467, Jan. 1990.

[27] M. Bui, J. Shyong, E. K. Lutz, T. Yang, M. Li, K. Truong, R. Arvidson, A. Buchman, J. A. Riffell, and O. S. Akbari, "Live calcium imaging of *Aedes aegypti* neuronal tissues reveals differential importance of chemosensory systems for life-history-specific foraging strategies," *BMC Neurosci.*, vol. 20, no. 1, p. 27, 2019.

[28] S. A. Juliano, "Species introduction and replacement among mosquitoes: interspecific resource competition or apparent competition?," *Ecology*, vol. 79, pp. 255–268, Jan. 1998.

[29] M. A. H. Braks, N. A. Honório, L. P. Lounibos, R. Lourenço-De-Oliveira, and S. A. Juliano, "Interspecific competition between two invasive species of container mosquitoes, *Aedes aegypti* and *Aedes albopictus* (*Diptera: Culicidae*), in Brazil," *Ann. Entomol. Soc. Am.*, vol. 97, pp. 130–139, Jan. 2004.

[30] O. Riabinina, D. Task, E. Marr, C.-C. Lin, R. Alford, D. A. O'Brochta, and C. J. Potter, "Organization of olfactory centres in the malaria mosquito *Anopheles gambiae*," 2016.

[31] B. J. Matthews and L. B. Vosshall, "How to turn an organism into a model organism in 10 'easy' steps," 2020.

[32] F. van Breugel, A. Huda, and M. H. Dickinson, "Distinct activity-gated pathways mediate attraction and aversion to CO_2 in *Drosophila*," *Nature*, vol. 564, no. 7736, pp. 420–424, 2018.

[33] A. Sih, "Antipredator responses and the perception of danger by mosquito larvae," *Ecology*, vol. 67, pp. 434–441, Apr. 1986.

[34] R Foundation for Statistical Computing, "R: A language and environment for statistical computing," 2015.

[35] Python Core Team, "Python: A dynamic, open source programming language," 2015.

Supplementary Figures

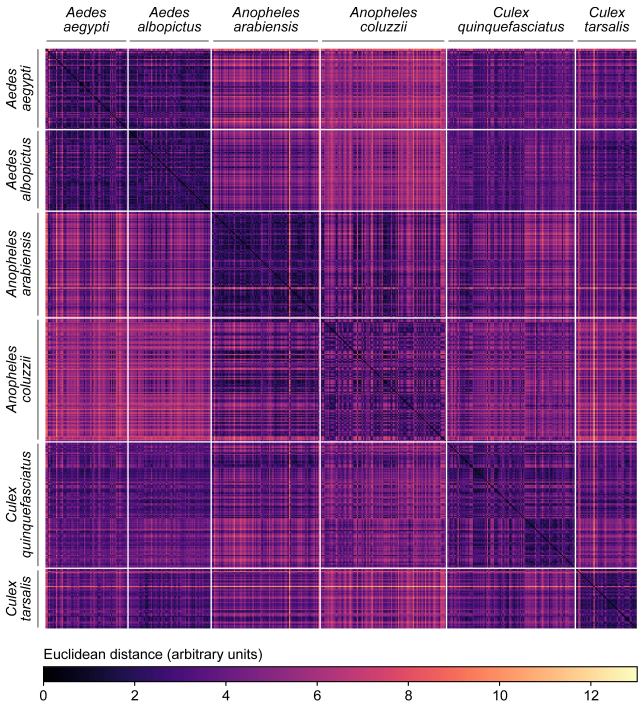

Figure S1: Euclidean distance matrix of individual differences between larvae. Euclidean distance matrix incorporating all ten navigation behavior variables in clean water. Each row or column visualizes one individual larvae, arranged in species groups and then in order of experiment date. White lines mark boundaries between different species. Higher Euclidean distances (arbitrary units) represent lower similarity between individuals. The diagonal of black cells (upper left corner to lower right corner) indicate self-self comparisons (distance = 0).

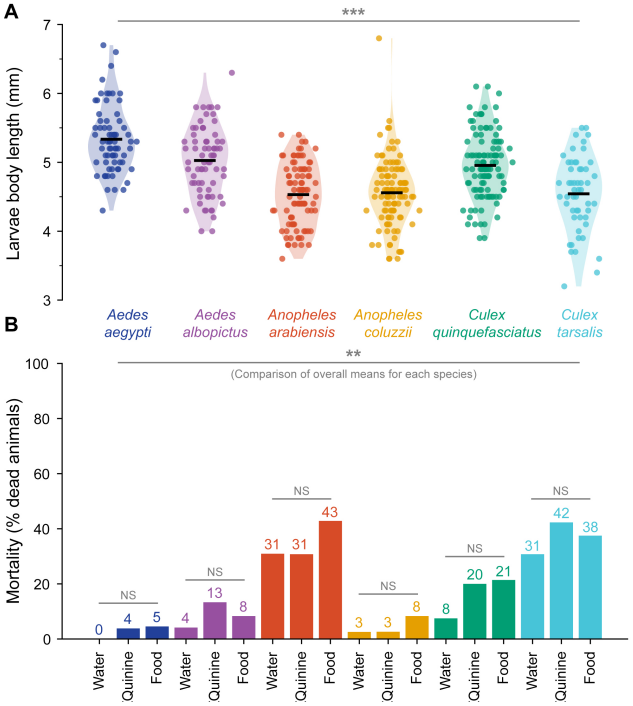

Figure S2: Larval size and mortality are significantly different across species. A: Size of starved L3 larvae differed significantly across species ($p<0.001$, Kruskal-Wallis test with Bonferroni correction). Scatter points depict individual larvae, colored by species from left to right: *Ae. aegypti* (navy, n=67, mean=5.33mm), *Ae. albopictus* (purple, n=70, mean=5.03mm), *An. arabiensis* (red, n=93, mean=4.53mm), *An. coluzzii* (yellow, n=108, mean=4.56mm), *C. quinquefasciatus* (green, n=110, mean=4.95mm), and *C. tarsalis* (aqua, n=53, mean=4.54mm). Horizontal black bars visualize the mean of each group. Due to these size differences across species, speed measurements were standardized to larval body size for each individual. **B:** Post-experiment mortality for each species and treatment. Numbers shown above each bar mark the percentage value for each treatment. Differences were statistically significant across species ($p=0.003$, Fisher's Exact Test with Holm-Bonferroni correction), but not across the three treatments for the same species ($p=1$ for all species). Asterisks indicate the significance of the corresponding p-value: *: $p<0.05$; **: $p<0.01$; ***: $p<0.001$; NS: not statistically significant. All animals that died before eclosion (shown here) were omitted from analyses.

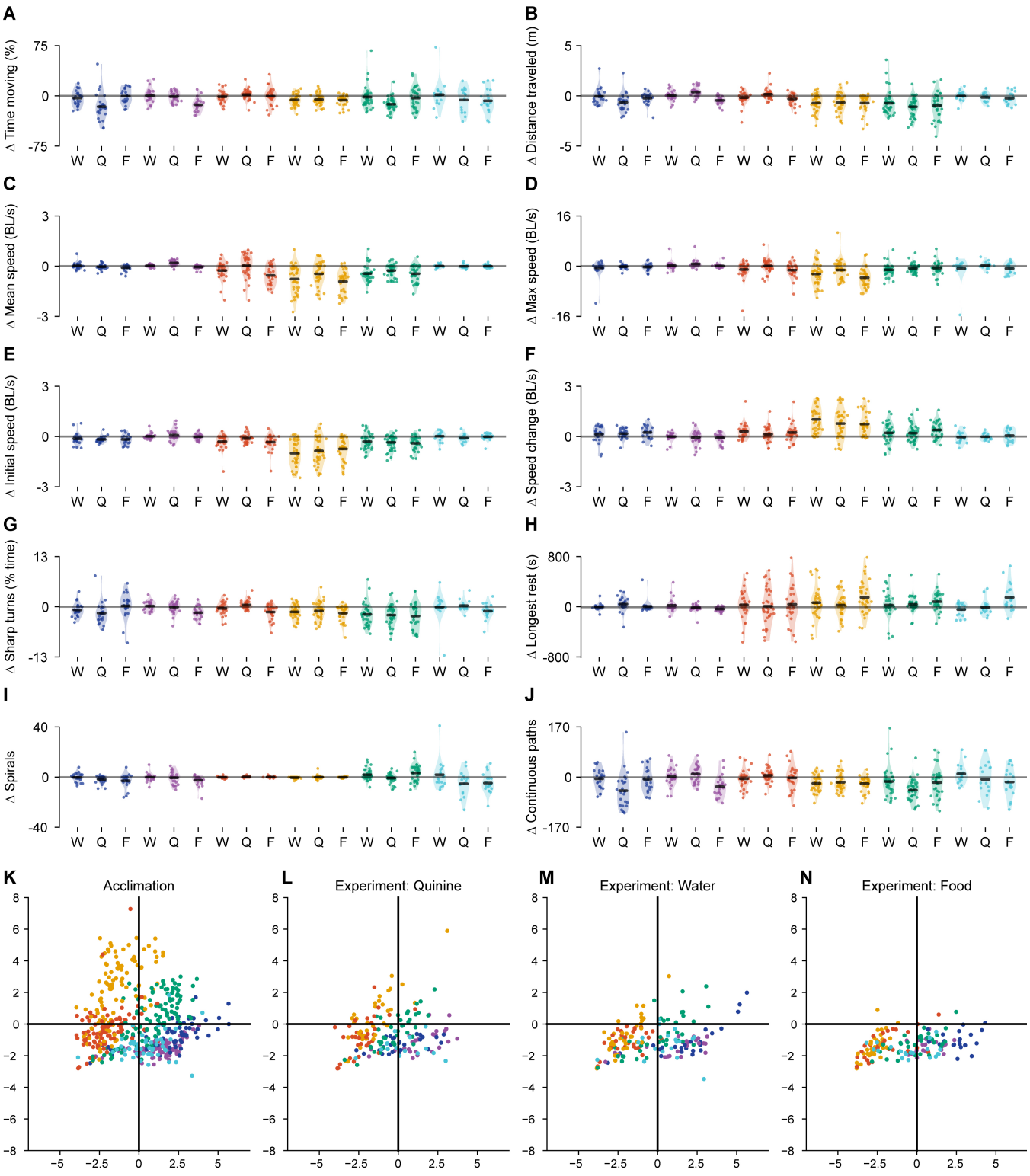

Figure S3: Changes in kinematic navigation behavior following stimulus addition. A-J: Changes in each of the ten navigational behavior measurements following the addition of water (W), quinine (Q), or food extract (F). From left to right in all plots: *Ae. aegypti* (navy); *Ae. albopictus* (purple); *An. arabiensis* (red); *An. coluzzii* (yellow); *C. quinquefasciatus* (green); and *C. tarsalis* (aqua). Each scatter point represents one individual, and the y axis shows the change in the navigational variable (experiment period - acclimation period). Thus, a point lying at 0 represents no change in behavior following addition of the stimulus. **A:** Time spent moving (%) **B:** Total distance traveled (meters) **C:** Mean speed when moving (body lengths·s^{-1}) **D:** Maximum speed (body lengths·s^{-1}) **E:** Initial speed, or mean speed in first minute (body lengths·s^{-1}) **F:** Speed modification, or difference in mean speed between first and last minutes (body lengths·s^{-1}) **G:** Sharp turns (% total time spent turning >45°) **H:** Longest continuous rest period (s) **I:** Number of spirals **J:** Number of continuous paths that are not spirals. **K-N:** Representation of the same ten variables as in A-J, in PCA space. **K:** Reproduction of acclimation data for all animals visualized in Fig 3A. **L:** Experiment data from all animals responding to quinine, reprojected into the same PC space as in K. **M:** Experiment data from all animals responding to water, reprojected into the same PC space as in K. **N:** Experiment data from all animals responding to food, reprojected into the same PC space as in K.

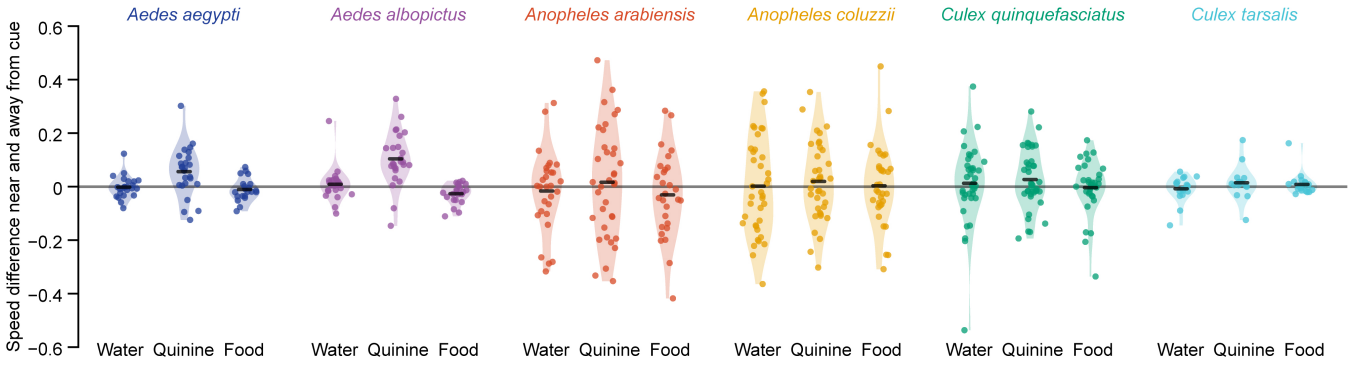

Figure S4: Species exhibit potential differences in navigation strategy toward preferred areas. In a previous study, we conducted deep analyses into the mechanism of *Ae. aegypti* navigation, using a dataset of over 500 individual animals observed independently. This study revealed that *Ae. aegypti* aggregate near preferred cues by decreasing their movement speed near preferred areas. In this current study, we did not have the reagent resources or manpower to conduct the 3,000 experiments necessary for a similar analysis. Nevertheless, we visualized the speed near and far from cues for each species and each stimulus. In this graph, each scatter point represents one individual, and the y axis shows the change in speed near the experimental cue (speed in areas >50% concentration - speed in areas <50% concentration), normalized to larval behavior in corresponding sections of the arena in the 15 minute acclimation period.

Figure S5 (following page): Larval distribution and trajectory maps for all species and experimental conditions. A-F: Distribution histograms across the x axis (above) and trajectory maps (below) of all starved animals during the experiment phase for water (left column), quinine (center column), and food (right column); *Ae. aegypti* (**A**), *Ae. albopictus* (**B**), *An. arabiensis* (**C**), *An. coluzzii* (**D**), *C. quinquefasciatus* (**E**), and *C. tarsalis* (**F**). Although trajectories are shown aggregated into one image for each panel, all animals were tested individually. Scatter points show the position of each animal at the end of the experiment. It is important to note that these histograms show the aggregated position data from all animals throughout the entire 15 minute experiment. Thus, a single animal exhibiting strong attraction or aversion may disproportionately influence this data visualization. For statistical tests reported in this paper, a single preference value was calculated for each animal (Fig 4A) to avoid such effects. Note that the distribution histograms for *An. arabiensis* and *An. coluzzii* appear particularly sparse, because these two *Anopheles* species spent the majority of the experiment at rest.

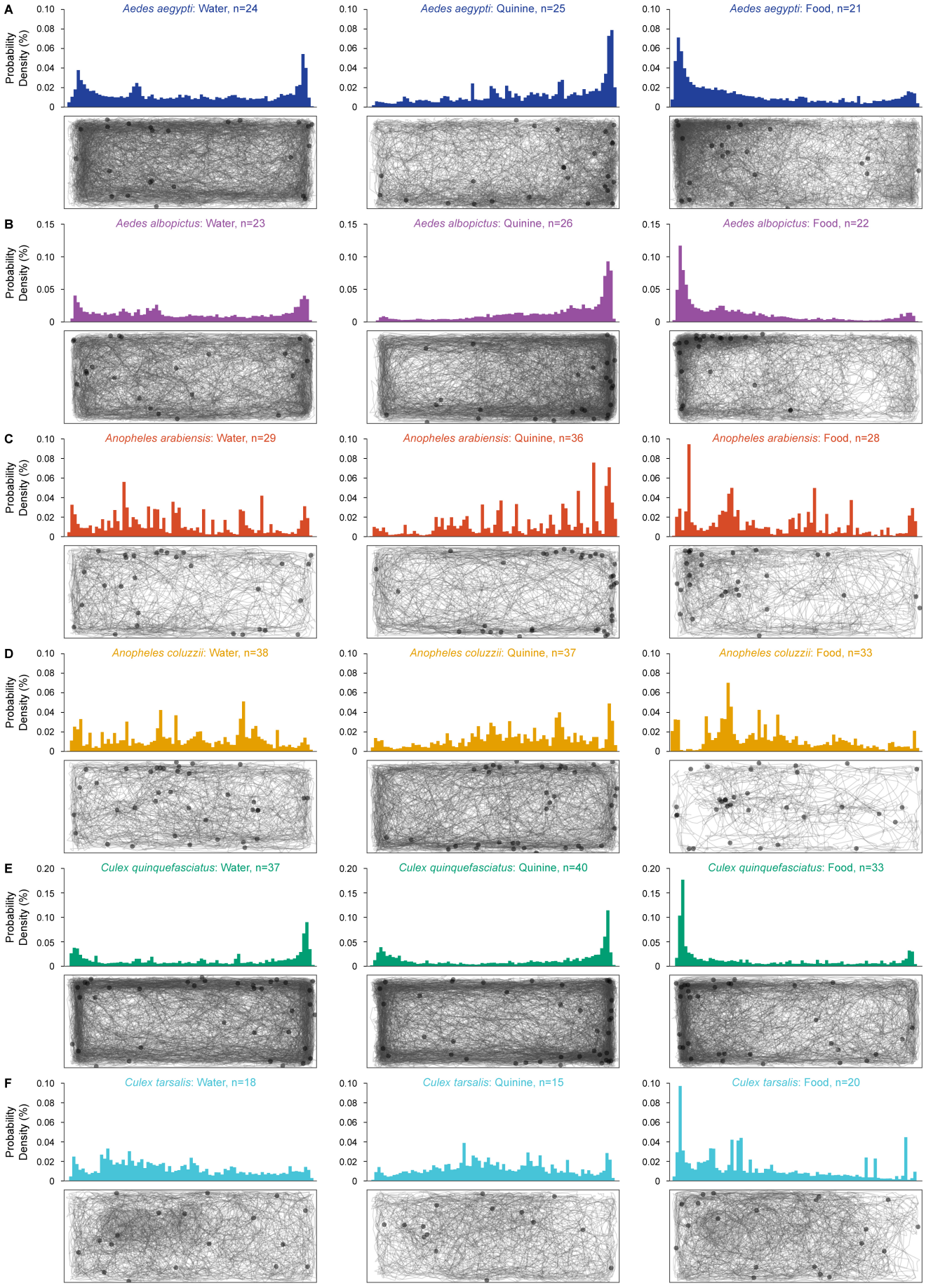
A
Aedes aegypti: Water, n=24
Aedes aegypti: Quinine, n=25
Aedes aegypti: Food, n=21
B
Aedes albopictus: Water, n=23
Aedes albopictus: Quinine, n=26
Aedes albopictus: Food, n=22
C
Anopheles arabiensis: Water, n=29
Anopheles arabiensis: Quinine, n=36
Anopheles arabiensis: Food, n=28
D
Anopheles coluzzii: Water, n=38
Anopheles coluzzii: Quinine, n=37
Anopheles coluzzii: Food, n=33
E
Culex quinquefasciatus: Water, n=37
Culex quinquefasciatus: Quinine, n=40
Culex quinquefasciatus: Food, n=33
F
Culex tarsalis: Water, n=18
Culex tarsalis: Quinine, n=15
Culex tarsalis: Food, n=20
Probability Density (%)

In this dissertation we provide new insights into species-specific larval mosquito behavior.

Taken together, our results highlight several important questions and areas of future research in the field.

First, the development of a GCaMP6 genetically modified line of *Aedes aegypti* facilitates future research into chemosensory neurobiology in mosquitoes. What is the neural basis of mosquito behaviors such as multimodal integration of heat and odors? How are different host odor profiles encoded in the mosquito brain? Two-photon imaging in adult GCaMP6 *Ae. aegypti* may lend insight into these questions. Nevertheless, we were unable to develop a working method for two-photon live calcium imaging in *Ae. aegypti* larvae [1]. We are also not aware of other studies that successfully collected neural recordings from the brain of intact, behaving mosquito larvae. The future development of such methods could open the door to understanding the neural mechanism of the unusual larval foraging behaviors observed in our experiments.

Second, we identify an unusual foraging strategy in *Ae. aegypti* larvae that results in random food discovery under experimental conditions [2]. What might be the evolutionary history leading to this unusual foraging strategy? Neural tissue is metabolically expensive, and it is possible that mosquito larvae have evolved to maximize fast development over complex neurcal circuits as young larvae. Alternatively, *Ae. aegypti* adults may rely on a scattered oviposition strategy in which they lay a large number of eggs under the assumption that most larvae will die. Importantly, our experiments only analyzed larval behavior in small containers typical of natural *Ae. aegypti* habitats. Recording and analyzing the behavior of mosquito larvae in larger containers or even natural environments like lakes and ponds - particularly in species adapted to larger environments - may add insight into the possible evolutionary history of this unusual foraging strategy.

Third, our findings show that significant differences exist in the innate exploration behavior of disease vector mosquito species. Why did this broad range of behaviors develop even among closely related species? Are large differences in exploration behavior correlated with an evolutionary history of competition between species? Alternatively, are these behavioral differences adaptations to different habitats inhabited by each species? It is important to note that our exploration of species-specific mosquito behavior [3] was limited by the number of species available as commercial research resources. Thus, our study was biased toward species that are easy to rear in captivity and of interest to the broader vector biology community. A more comprehensive study including species not associated with humans would be extremely interesting for developing a thorough understanding of cross-species mosquito search behavior.

Finally, our results suggest that larval behavior, which varies significantly among species, may call for different larval control techniques for different species. Applied research developing new larvicide application recommendations based on cross-species differences may be of great use to global public health.

Almost half of the human population live in areas that sustain disease vector mosquitoes [4]. As climate change continues, the habitat range of these tropical insects is only expected to increase. Investigating mosquito behavior at all life stages is essential to understanding these important disease vector species, and may help inform global public health programs.

References

[1] M. Bui, J. Shyong, E. K. Lutz, T. Yang, M. Li, K. Truong, R. Arvidson, A. Buchman, J. A. Riffell, and O. S. Akbari, "Live calcium imaging of *Aedes aegypti* neuronal tissues reveals differential importance of chemosensory systems for life-history-specific foraging strategies," *BMC Neurosci.*, vol. 20, June 2019.

[2] E. K. Lutz, T. S. Grewal, and J. A. Riffell, "Computational and experimental insights into the chemosensory navigation of *Aedes aegypti* mosquito larvae," *Proc. Biol. Sci*, 2019.

[3] E. K. Lutz, K. T. Ha, and J. A. Riffell, "Chemosensory navigation in six species of disease vector mosquito larvae," *BioRxiv*, 2020.

[4] WHO, "Mosquito-borne diseases," 2019.